Defense Documentation Center

Defense Logistics Agency

Cameron Station • Alexandria, Virginia

AMRL-TR-70-35

A FOUR-DEGREE-OF-FREEDOM LUMPED PARAMETER MODEL OF THE SEATED HUMAN BODY

PETER R. PAYNE
EDWARD G. U. BAND

WYLE LABORATORIES — PAYNE DIVISION

JANUARY 1971

AEROSPACE MEDICAL RESEARCH LABORATORY
AEROSPACE MEDICAL DIVISION
AIR FORCE SYSTEMS COMMAND
WRIGHT-PATTERSON AIR FORCE BASE, OHIO

121

NOTICES

When US Government drawings, specifications, or other data are used for any purpose other than a definitely related Government procurement operation, the Government thereby incurs no responsibility nor any obligation whatsoever, and the fact that the Government may have formulated, furnished, or in any way supplied the said drawings, specifications, or other data, is not to be regarded by implication or otherwise, as in any manner licensing the holder or any other person or corporation, or conveying any rights or permission to manufacture, use, or sell any patented invention that may in any way be related thereto.

Federal Government agencies and their contractors registered with Defense Documentation Center (DDC) should direct requests for copies of this report to:

DDC
Cameron Station
Alexandria, Virginia 22314

Non-DDC users may purchase copies of this report from:

Chief, Storage and Dissemenation Section
Clearinghouse for Federal Scientific & Technical Information (CFSTI)
Sills Building
5285 Port Royal Road
Springfield, Virginia 22151

Organizations and individuals receiving announcements or reports via the Aerospace Medical Research Laboratory automatic mailing lists should submit the addressograph plate stamp on the report envelope or refer to the code number when corresponding about change of address or cancellation.

Do not return this copy. Retain or destroy.

100 - MARCH 1971 - CO105 - 29-71-473

BLANK PAGE

FOREWORD

The research covered in this report was performed under Air Force Contract F33615-67-C-1807. This contract was originally awarded to Peter R. Payne, Inc., on June 15, 1967, and was transferred to the Payne Division of Wyle Laboratories upon the acquisition of Peter R. Payne, Inc., by Wyle Laboratories in April 1968. The contract end date was June 15, 1970.

The Air Force Program Monitor for this contract was Mr. James W. Brinkley of the Vibration and Impact Branch, Biodynamics and Bionics Division of the Aerospace Medical Research Laboratory, Aerospace Medical Division of Air Force Systems Command, Wright-Patterson Air Force Base, Ohio.

This technical report has been reviewed and is approved.

CLINTON L. HOLT, Colonel, USAF, MC
Commander
Aerospace Medical Research Laboratory

CONTENTS

CONTENTS (continued)

LIST OF SYMBOLS

a_i	Coefficients of δ_3^i in spinal spring force equation (lb/ft^i) $F_{\delta_3} = \sum_{i=1,2,3} a_i \delta_3^i$
b_i	Coefficients of δ_1^i in buttock spring force equation (lb/ft^i) $F_{\delta_1} = \sum_{i=1,2,3} b_i \delta_1^i$
C	Constant of integration
C_n	Capacitance of component n in electric analog (farads)
c_{A_n}	Apparent damping coefficient of damper n
c_n	Damping constant of damper n (1/sec) ($c_n = K_n / m_n$)
$\bar{c}_{A_n}$	Apparent damping ratio of damper n (-)
$\bar{c}_n$	Damping ratio of damper n (-) ($\bar{c}_n = c_n/\omega_n$)
$\bar{c}_{n_E}$	Effective damping ratio in equivalent single degree of freedom system (-)
DRI	Dynamic response index
F_c	Driving force (lb) ($F_c = F_o \sin \Omega t$)
F_o	Driving force amplitude (lb)
F_{D_n}	Force generated in damper n (lb) ($F_{D_n} = 2K_n \dot{\delta}_n$)
F_{δ_n}	Force generated in spring n (lb) ($F_{\delta_n} = k_n \delta_n$)
F_n	Combined acceleration term (ft/sec^2) [$F_n = (2c_n \dot{\delta}_n + \omega_n^2 \delta_n)$]
f	Amplitude ratio function, defined by $f = \sqrt{1+\zeta^2 p^2} / \sqrt{(1-p^2)+\zeta^2 p^2}$ $= \ddot{y}_o / \ddot{y}_s$

g	Acceleration due to gravity (ft/sec^2)
$I(\ )$	Imaginary part of function ( )
K_n	Linear damping constant of damper n (lb sec/ft) ($F_{D_n} = 2K_n \dot{\delta}_n$)
$\bar{k}_m$	Average stiffness of vertebra m (lb/ft)
k_n	Stiffness of spring n (lb/ft)
L_n	Inductance of component n in electric analog (henry)
m_n	Mass of lumped mass n (lb sec^2/ft)
m_T	Total mass (lb sec^2/ft)
N	Imposed gravitational acceleration (g)
n	Lumped parameter index (-)
p	Defined by $p = \frac{\Omega}{\omega_n}$ (Appendix I) (-)
q	Defined as $q = 2\bar{c}_n$ (Appendix I) (-)
q_n	Defined as $q_n = 1 \Big/ \sqrt{[1 - (\frac{\Omega}{\omega_{A_4}})^2]^2 + 4\bar{C}_{A_4}{}^2 (\frac{\Omega}{\omega_{A_4}})^2}$
$R(\ )$	Real part of function ( )
R_n	Resistance of component n in electric analog (ohms)
t	Time (secs)
u	Defined by $u = \sqrt{1 + q^2 p^2}$ (Appendix I) (-)
v	Defined by $v = \sqrt{1 - (2 - q^2) p^2 + p^4}$ Appendix I) (-)
$W_{1,2}$	Work done in compressing a vertebra from δ_{m_1} to δ_{m_2} (ft/lb)
W_n	Weight of body component n (lb)
y_n	Vertical displacement of mass n above ground reference (ft)
$\dot{y}_n$	Vertical velocity of mass n (ft/sec)
$\ddot{y}_n$	Vertical acceleration of mass n (ft/sec^2)

$\ddot{y}_T$	Vertical acceleration of whole system under steady load (ft/sec^2)
Z	Impedance (lb sec/ft)
$\|Z\|$	Magnitude (Amplitude of impedance) (lb sec/ft)
$\|Z\|_{max}$	Maximum value of impedance magnitude (lb sec/ft)
α	Coefficient of δ in force/deflection curve (lb/ft^1 or lb/in^1)
β	Coefficient of δ^2 in force/deflection curve (lb/ft^2 or lb/in^2)
γ	Coefficient of δ^3 in force/deflection curve (lb/ft^3 or lb/in^3)
Δ_n	Visceral overshoot function defined as $\Delta_n = \pi\bar{c} \Big/ \sqrt{1 - \bar{C}_n^2}$
δ_m	Deflection in vertebra m (ft or in)
δ_n	Deflection in spring n and/or damper n (ft)
$\dot{\delta}_n$	Deflection rate of spring n and/or damper n (ft/sec)
$\ddot{\delta}_n$	Deflection acceleration of spring n and/or damper n (ft/sec^2)
η	Defined by $\eta_n = \sqrt{1 - \bar{C}_n^2}$ (-)
λ_n	Unloaded length of spring n (ft)
ϕ	Mass ratio for 2 mass system (-) $\left(\phi = \frac{m_2}{m_1}\right)$
$\phi\left(\frac{p}{q}\right)$	Mass ratio for multi-mass system (-) $\left(\phi\left(\frac{p}{q}\right) = \frac{m_p}{m_q}\right)$
ψ_n	Deflection phase angle for spring n (rads) [See equations (8) and (11)]
Ω	Frequency of forcing function (rads/sec)
Ω_o	Forcing function frequency for maximum impedance (rads/sec)
Ω_{res}	System resonant frequency for maximum amplitude ratio (rads/sec)
ω_{A_n}	Apparent frequency of spring n (rads/sec)
ω_E	Effective frequency of spring n in equivalent single-degree-of-freedom system (rads/sec)
ω_n	Undamped natural frequency of spring n (rads/sec) $\left(\omega_n = \sqrt{k_n/m_n}\right)$

SECTION I

INTRODUCTION

The human body can always be damaged by sufficiently high acceleration levels. Even the gravitational acceleration of 32.2 ft/sec (ref. 1) can cause injuries (damage to the circulatory system, for example) in some individuals, after a sufficient period of time has elapsed. The higher acceleration levels associated with re-entry of a space vehicle, which are maintained for only a few minutes, give rise to "hydraulic problems," caused by the displacement of blood and other fluids from their normal location in the body. In contrast, "brief acceleration" or "short period" acceleration which endures for a period of less than a second, can cause structural damage, if the level is high enough, but cannot significantly distort fluid flow patterns. It is this short period category of accelerations, such as those that occur in aircraft escape systems, and the body's response to it, which is the subject of this report.

The precise nature of the structural injury caused by short period acceleration depends upon the orientation of the acceleration vector with respect to the human body, the restraint of the human body, the magnitude of the acceleration and the way in which the magnitude varies with time. This last aspect is sometimes referrred to as the "frequency content" of the input acceleration, but such terminology can be misleading. A reference to "frequency content" implies that such descriptors as the power spectral density of an input acceleration pulse can be correlated with injury mode, and at the present time this is not proven; indeed, quite cogent arguments can be made for the contention that power spectral density is not correlatable with injury, at least in a simple way.

The basic problem to be studied can be summarized as follows. Given an acceleration time history, such as that associated with the initial trajectory of an escape system, will it cause injury when applied to a human subject, and what will be the nature of the injury? Of course, there is a simple and direct way of determining the answer to this question by experiment, but we are prevented from using it because of obvious moral, legal, humanitarian and other prohibitions. Yet we cannot avoid answering the question because we could then be condemning some of our fighting men to death or injury in the future, either because they will have to use escape systems with excessively dangerous acceleration characteristics, or because their escape envelope is unnecessarily restricted in relation to the total envelope of their vehicle. And in a broader context, we must also find an answer to the question because of the thousands of people who unnecessarily lose their lives in automobile accidents and other crash environments; deaths which might often be avoided, given adequate restraint and protection.

It is generally agreed that the best line of attack is to develop an accurate description of the human body, including both its dynamic characteristics and the static load bearing capability of its many complex components, so that we can accurately calculate the effect of a given input acceleration time history, and also that we may be able to design a restraint or support system which optimumly couples it to the driving force associated with the acceleration. The construction of such a "dynamic model" is a task routinely undertaken in the aerospace industry (among others) for structures which are built from well

understood materials. A simple example is an aircraft, for which the strength of each element is accurately calculated, in order to ensure that it can perform its function without failure. We also determine the deformation of the aircraft's structure, and construct dynamic models which tell us how it will behave in response to gusts, how aeroelastic deformation influences its stability and handling characteristics, and to assure that flutter and divergence cannot occur with the flight envelope. But such a task is very much harder in the case of the human body, firstly because it is so much more complex than an aircraft, and secondly because many of its constituent materials are not "simple" linear materials obeying Hooke's law and having small damping. Additionally, the dynamic characteristics can be varied by tensing or relaxing the muscles which make up so much of the body. Other variations occur because the various body materials tend to change their characteristics with age, environment, and the degree of physical fitness of the subject, and because people are not manufactured to the same close tolerances as aircraft.

At first sight one might suppose that an adequate description of the human body could be built up by measuring the various quantities of interest from cadaver material. Information of this type is certainly helpful, and indeed the pioneer of biodynamics, Sigmund Ruff (ref. 2), obtained a remarkably accurate estimate of the ability of the human spine to withstand ejection seat acceleration in this way. It does have severe limitations, however, because cadaver material is hard to obtain for the age groups of primary interest, and its dynamic and even static properties are thought to be substantially different from the in vivo case. Additionally, the important contributions of the muscle structure and fluids are almost entirely absent in the cadaver.

It is therefore necessary to devise experiments with live human subjects from which meaningful data can be obtained. Since it is essential to avoid injury to the subjects, the acceleration levels used in such tests must be substantially lower than those which would cause injury, and the results have to be extrapolated in some way in order to predict the level at which injury would occur. It is also necessary to devise tests which will enable us to determine the damping in the various elements of the system, and the primary dynamic characteristics, such as resonant frequencies. One gross way of doing this is to excite the subject, either by a steady state sinusoidal vibration, or by an impact, and to measure the relative motions of various parts of his anatomy. This is a valuable technique in the positive spinal case (for example) where relatively large and rigid masses, such as the head and upper torso, are moving on the neck and spine respectively. Such measurements have been attempted both optically and by means of accelerometers mounted on the subject's body. Such "external" observations cannot tell us much about the movements of the various organs inside the body, of course. Also, while it is quite easy to attach a transducer to the hip or the upper shoulder, it is more difficult to ensure that this instrument accurately tracks the motion of the component to which it is attached. *

One particularly simple method of studying the apparent dynamic response of the human body is to measure its driving point impedance under steady state sinusoidal excitation. Because no instrumentation is attached to the body, this technique was at one time regarded as nearly ideal. In fact, from a purely experimental point of view it is very elegant, and were it not for the fact that impedance measurements taken in this way vary by

* See Goldman and Von Gierke in reference 1, for example.

as much as 100% from subject to subject, and even vary for a given subject in successive tests, the experimenter would be well satisfied with it. But such data turns out to have rather limited value to the theoretical biodynamicist in his construction of a dynamic model. As will be shown in this report, impedance data is of little value because it is only meaningful when the system is composed of linear springs and dampers. Additionally, impedance turns out to have very "limited visibility" in a series coupled system with finite damping elements. Putting this another way, we might regard an impedance measurement as a "ray of light" which permits us to "look into" the human body. But we then find that we are looking into a rather opaque medium. The ray of light shone up from the buttocks (as in the measurement of driving point impedance for a seated subject) tells us a considerable amount about the first-degree-of-freedom, namely the pelvic mass moving on the spring of the buttocks. However, it gives us very little illumination into the dynamic system immediately above the pelvic girdle, and for practical purposes, none for any of the systems above that.

One object of this report is to examine critically the impedance techniques as a means of obtaining dynamic information about the human body by simulating the same measurements on a mathematical model, the coefficients of which are known. We then put ourselves in the position of an experimenter who is trying to determine the nature of the model from his external measurements alone, on order to see whether he would meet with any success. In general, we conclude that he would not, unless all the dynamic elements in the body were linear, and the damping was very low.

If there is an overall conclusion to this work, it is this; there is no "right way" to discover the "right model" for the human body. We must laboriously build a model piece-by-piece, sometimes relying upon intuition, sometimes on the biologist, and sometimes relying on the results of a fortuitous experimental observation, but constantly comparing the apparent external behavior of our model with experimental observations such as those obtained on the AMRL drop test facility in order to make sure that it is not straying from the reality of physical measurements. It will be a long time before we can feel that we have a completely adequate model, and many hundreds of workers will then have contributed to its construction, just as in any other discipline. In the present report we have developed a four-degree-of-freedom model of a seated man subjected to vertical accelerations. The characteristic parameters of the model are selected by making use of relevant available data and by matching calculated driving point impedance characteristics with measured values. It is realized that a number of multidegree-of-freedom models have been developed previously, but it is believed that development of the model in this way allows some important conclusions to be reached concerning the dynamics of the body.

SECTION II

THE CONCEPT OF MECHANICAL IMPEDANCE

In structural engineering the concept of the linear dynamic system is widely used. Since many structures are made up of metal components, each of which obeys Hooke's law (the linear relationship between stress and strain) the dynamic response of the whole is quite accurately described by a matrix of second order, linear differential equations, of the type used to describe linear electrical circuits. In the most simple example, the motion of a single-degree-of-freedom mass/spring/dash pot mechanical system driven by a forcing function applied to the mass (see figure 1a) can be described by the equation

$$m\ddot{y} + 2K\dot{y} + ky = F(t)$$

or

$$m\dot{v} + 2Kv + k\int v\,dt = F(t)$$

This is analogous to a simple electric circuit in which a resistance, a condenser, and an inductance are connected in series, in which the relationship between current and input voltage is given by:

$$L\dot{I} + RI + \frac{1}{C}\int I\,dt = E(t)$$

Thus for any consistent sets of units there is a direct correspondence between the following quantities:

mass m	-	Inductance L
spring constant k	-	reciprocal of capacitance $\frac{1}{C}$
damping constant ZK	-	resistance R
velocity $v=\dot{y}$	-	current I
driving force F(t)	-	input voltage E(t)
time t	-	time t

It is therefore natural to take advantage of the powerful analytical techniques developed by electrical engineers over the last eighty years. The concept of impedance is one of these techniques, which for the simple case shown in figure 1a translates into mechanical system technology as

$$\text{Electrical Impedance} = Z = \frac{\text{Voltage}}{\text{Current}} = \frac{E}{I} = R + i\left(\Omega L + \frac{1}{\Omega C}\right)$$

and

$$\text{Mechanical Impedance} = Z = \frac{\text{Force}}{\text{Velocity}} = \frac{F_c}{\dot{y}_c} = 2K + i(\Omega m - k/\Omega)$$

so that, in this case, the real and complex parts of Z are given by:

$$R(Z) = 2K \qquad \text{and} \qquad I(Z) = \Omega m - k/\Omega$$

The complex notation is the most convenient way of expressing the impedance in terms of both its magnitude and phase relationship. Figure 1 shows diagramatically how the impedance characteristics of a number of mechanical systems will depend on the characteristics of the system. It should be observed that the characteristics of those parts of the system closest to the driving point are fairly readily discernible from the impedance characteristic, but that the further from the driving point they are the less influence they have on the impedance characteristic. Mechanical impedance of a system may be calculated from direct measurements of the driving force magnitude and velocity. Dynamically similar systems have equal impedance/frequency characteristics so that, inversely, if the impedance of two systems are equal then there is good reason to suppose that they are dynamically similar.

At first sight, this technique seems attractive as a means of studying the dynamic response of the human body. Alternative methods, such as attaching accelerometers to various parts of the test subject's anatomy have well known shortcomings; in particular, it is difficult to mount them "rigidly," so that they move with the skeletal structure, because they are necessarily attached to the relatively soft flesh covering the structure. It is, therefore, easy to understand the attraction of a test procedure which requires no instrumentation of the subject, but merely an unambiguous measurement of input force and velocity.

Unfortunately, as indicated in figure 1 and as will be shown later in this report, the driving point impedance of a series connected lumped parameter model only gives useful information for those few systems which are closest to the driving point.

For the series system illustrated in figure 1d for example, measurement of the driving point impedance will show a large peak corresponding to the resonance of spring and damping k, K, in which all the other masses tend to move with mass m. The larger the damping ratios, the less effect systems further from the driving point have on the impedance characteristic and the more the features of the characteristics will be obscured (see fig. 16). An apparent frequency and damping can be deduced for this mode, but it bears little resemblance to the actual values of system (1), or indeed to any simply identifiable characteristic of the model. Thus, the procedure sometimes used of comparing experimental impedance measurements with a single-degree-of-freedom, lumped parameter mode, may be very misleading. Much more sophisticated methods of data analysis are required to recover any useful information from impedance data, starting with computer techniques of smoothing the experimental data in a mathematically meaningful way. Even when this is done, however, only the first system in the series is clearly visible, when the damping is as high as that of the human body.

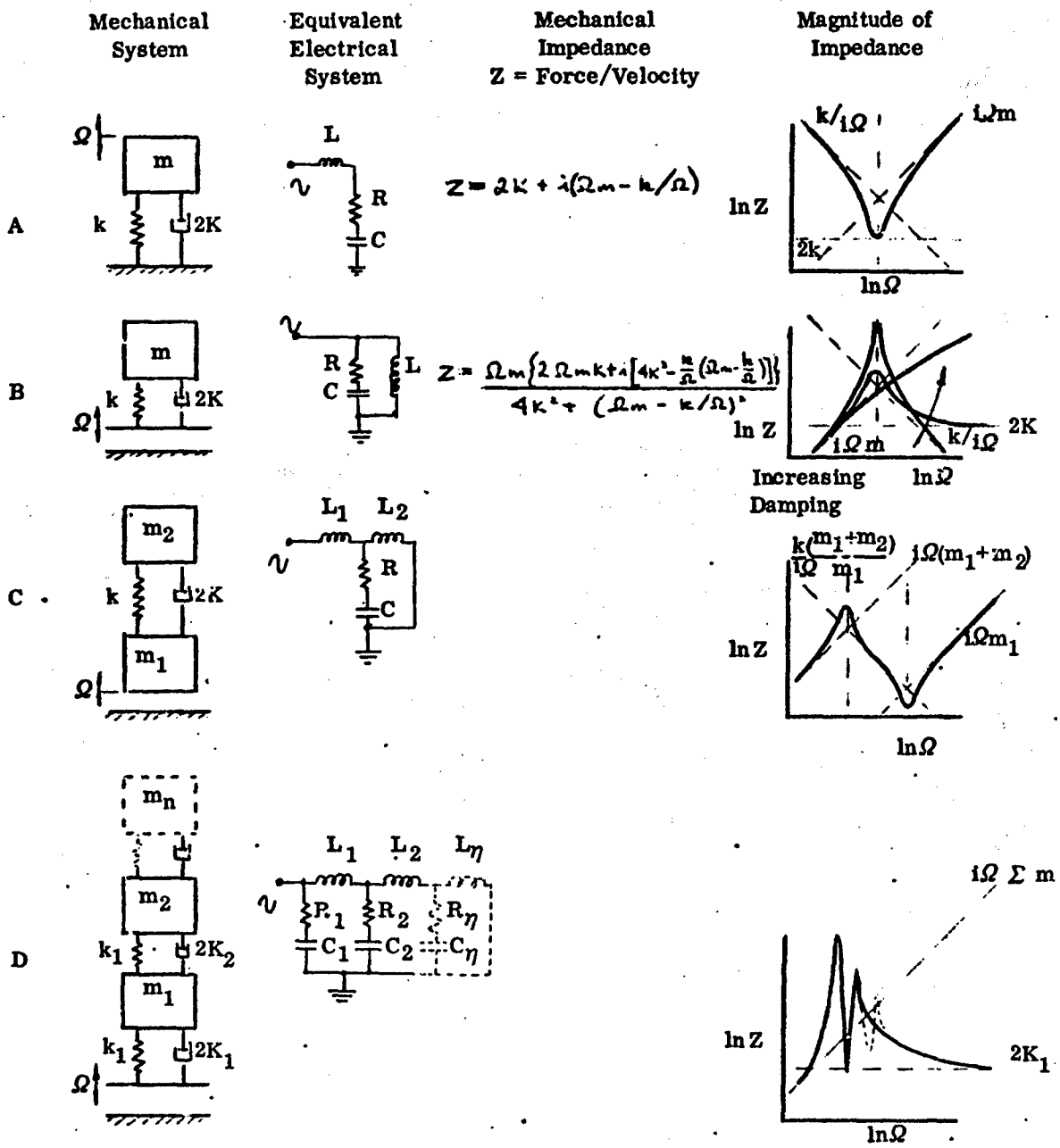

Figure 1. Impedance Characteristics of Simple Mechanical Systems (ref. 3)

A TWO-DEGREE-OF-FREEDOM SYSTEM

Figure 2 shows the variation of impedance modulus with frequency for an arbitrarily selected two-degree-of-freedom model. Four different values are used for the lower spring and damper. It is remarkable that, when the lower system is soft such as in the cases shown where $\omega_1 = 10$ or 20, the impedance curve appears to be that of a single-degree-of-freedom system and gives no indication of the presence of the second peak attributable to the second-degree-of-freedom. It is also notable that, at high frequencies

$$|Z| \rightarrow 2K_1 \quad \text{as} \quad \Omega \rightarrow \infty$$

This result, and those indicated in figure 1, can be generalized for any number of degrees of freedom. It implies:

(a) that the lowest mass tends to become stationary at high frequency, so that all the work is absorbed in the lowest damper, and

(b) that the lowest damper therefore masks the effect of high frequency resonances further up in the system.

In a similar way it can be shown that when the model is terminated by a mass (m_n) at the driving point (as in figure 1c)

$$|Z| \rightarrow m_n\Omega \quad \text{as} \quad \Omega \rightarrow \infty$$

At the low frequency end of the impedance characteristic, the whole system mass tends to move as a single body so that

$$|Z| \rightarrow m_T\Omega \quad \text{as} \quad \Omega \rightarrow o$$

where m_T is the total mass. This result is true, whatever type of element terminates the model at the driving point.

Let us now pretend that we do not know that the impedance curves in figure 2 were developed by a two-degree-of-freedom system. Lacking this knowledge, it would be reasonable to assume that the system generating the curves of figure 2 could be approximated by a single-degree-of-freedom, particularly for the lower values of ω_1. Such an assumption would lead to the results shown in table 1.

It is interesting to note that this calculation gives a reasonable figure for the apparent stiffness (k_A) of the lower spring, the maximum error being a 20% under-estimate. The apparent damping constant ($2K_A$) of the equivalent single-degree-of-freedom model agrees very closely with the actual value for the lower system (k_1), based on both Z_{max} and the asymptotic value of Z as $\Omega \rightarrow \infty$. For practical purposes, then, the apparent damping ratio ($\bar{c}_A$) of the single-degree-of-freedom approximation is, however, considerably less than the actual damping ratio ($\bar{c}_1$) of the actual system. Thus, the single-degree-of-freedom assumption gives a satisfactory indication of the characteristics of the lower members of the multi-degree system.

The relative amplitudes of the two masses are shown in figure 3. It is clear that the Z max corresponds to both masses moving more or less together on the lower spring and damper. A second resonance occurs at a frequency of about 8 Hz, and may be regarded as being due to the upper mass moving on its own spring and damper, rather like a vibration absorber, so that the lower mass is relatively quiescent. It will now be shown that this second resonance is independent of the lower spring and damper values.

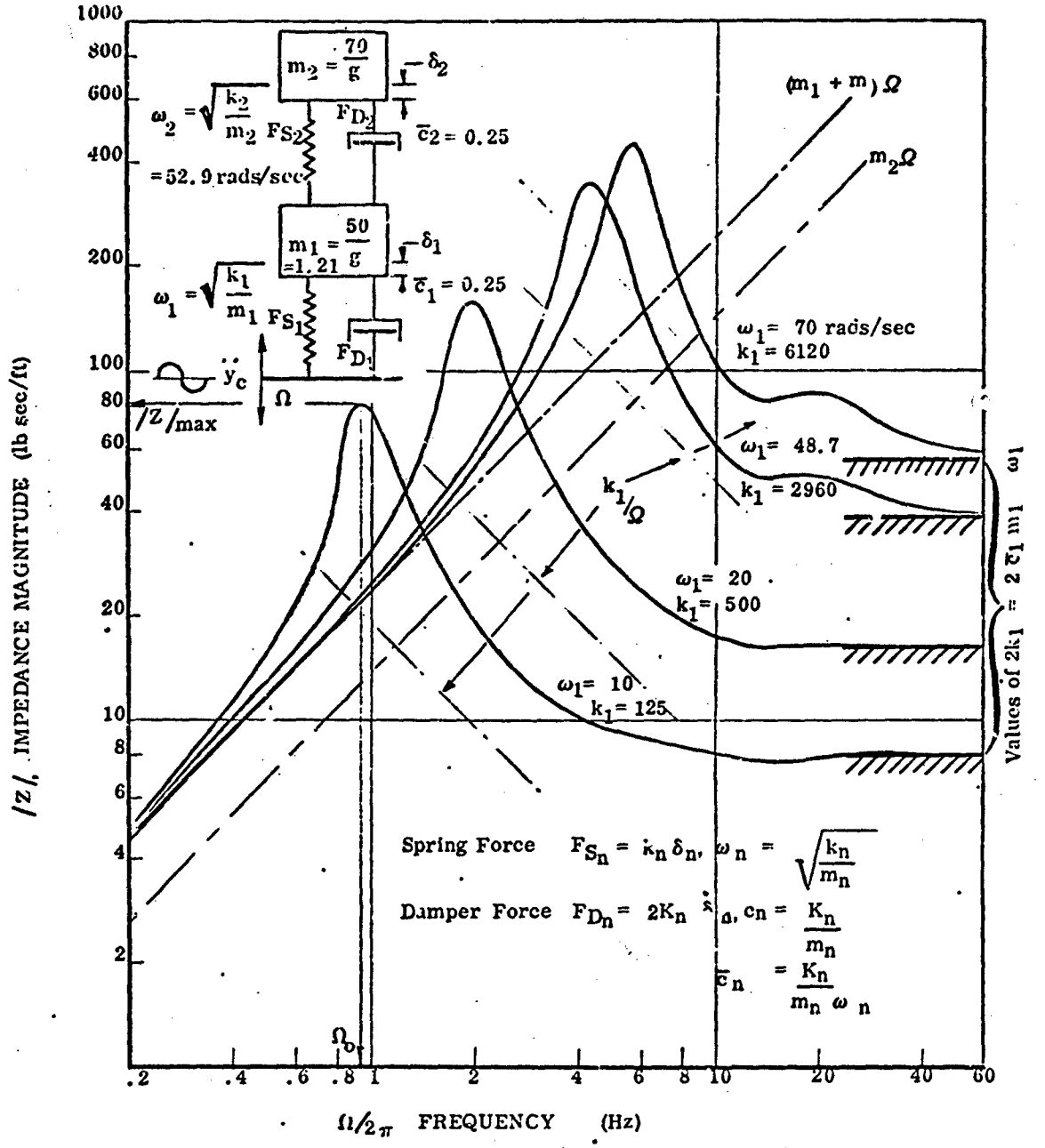

Figure 2. Impedance of a Two-Degree-of-Freedom System

TABLE I

Equivalence of One- and Two-Degree-of-Freedom Systems

	ω_1 (rads/sec)	10	20	48.7	70
Values for 2-Degree-of-Freedom System from figure 2	k_1 (lb/ft)	125.0	500.0	29.60	6.20
	$\bar{c}_1$ (-)	.25	.25	.25	.25
	m_1 (lb sec^2/ft)	1.25	1.25	1.25	1.25
	m_T (lb sec^2/ft)	3.73	3.73	3.73	3.73
	$2K_1 = 2\bar{c}\, m_1 \omega_1$ (lb sec/ft)	6.25	1.25	30.4	43.8
	$\lvert Z\rvert_{max}$ (lb sec/ft)	80.0	158.0	340.0	400.0
	Frequency for $\lvert Z\rvert_{max}$, Ω_o (rad/sec)	5.98	12.58	27.65	36.5
Apparent Equivalent 1-Degree-of-Freedom System	$\lvert Z\rvert_{max} / \Omega_o m_T$ (-)	3.58	3.37	3.295	3.24
	*Apparent $\bar{c}_A$ (-)	1.48	.155	.16	.163
	$(\bar{c}_A/\bar{c}_1)$	(.592)	(.62)	(.64)	(.652)
	Apparent ω_A (rad/sec)	5.98	12.58	27.65	36.5
	(ω_A/ω_1)	(.598)	(.629)	(.568)	(.521)
	Apparent $k = \omega_A^2 m_T$	133.0	469.0	28.40	49.60
	(k_A/k_1)	(1.06)	(.939)	(.960)	(.81)
	Apparent $2K_A = 2\bar{c}_A m_T \omega_A$ (lb sec/ft)	6.6	14.5	33.0	44.4
	$(2K_A/2K_1)$	(1.05)	(1.06)	(1.085)	(1.01)

* Those values of $\bar{c}_A$ are read from figure 24 of reference 7, for the appropriate values of $\lvert Z\rvert_{max} / \Omega_o m_T$.

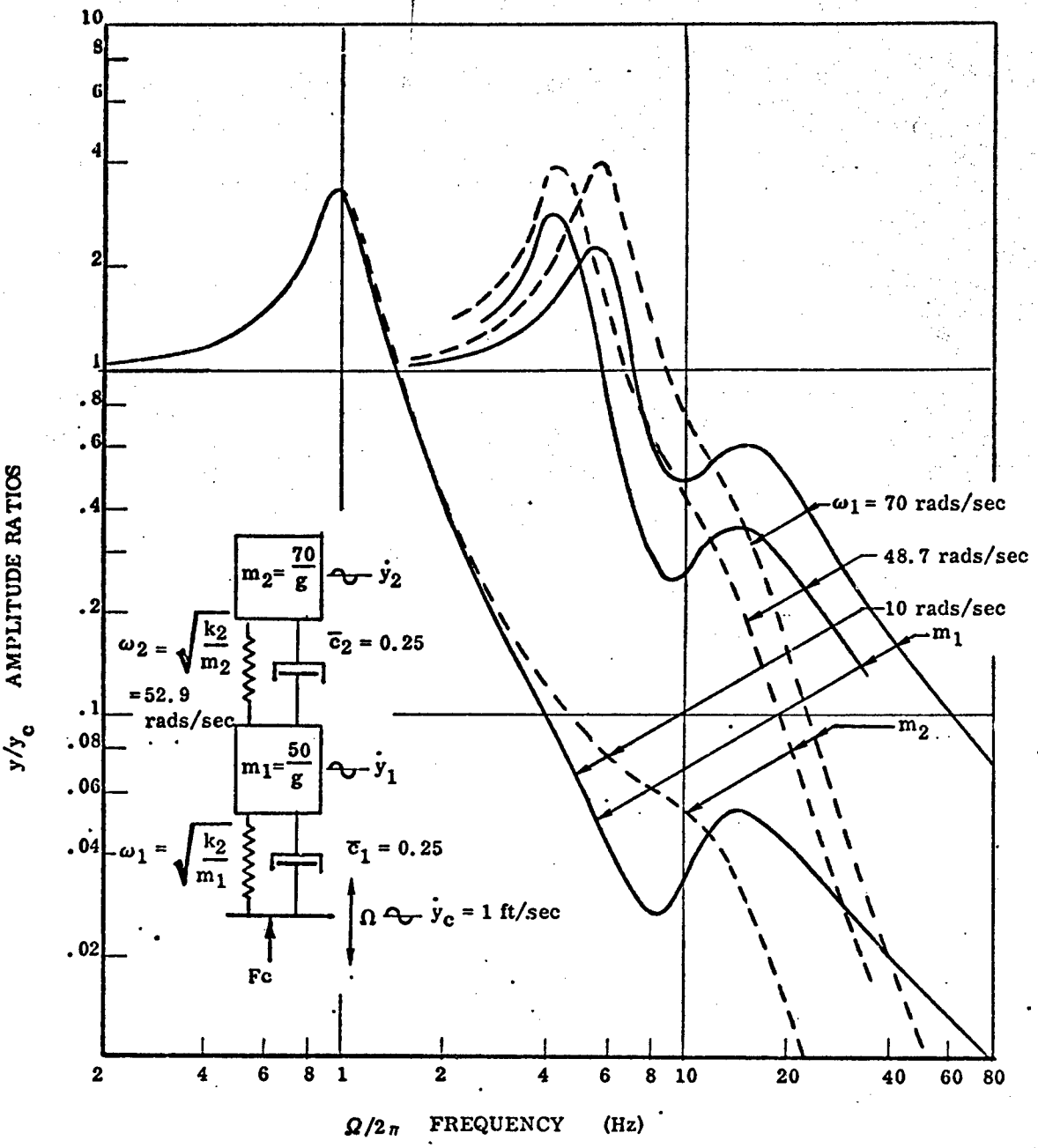

Figure 3. Amplitudes of Two Degree of Freedom System

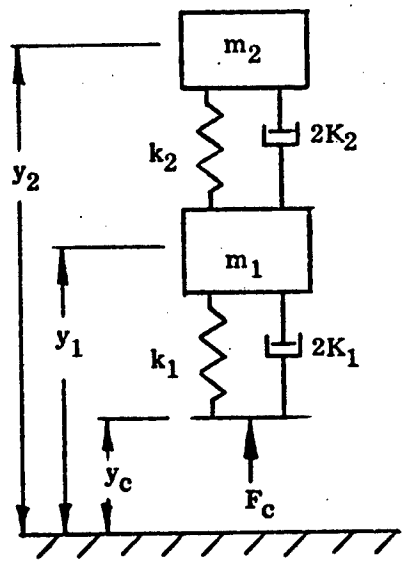

δ_n = compression of spring n

= $\lambda_n - (y_n - y_{n-1})$

λ_n = unstretched length of spring n

Figure 4. Notation for a Two-Degree-of-Freedom System.

The equations of motion for the two-degree-of-freedom system shown in figure 4 may be written as follows:

$$\left.\begin{aligned} m_1 \ddot{y}_1 &= (2K_1\dot{\delta}_1 + k_1\delta_1) + (2K_2\dot{\delta}_2 + k_2\delta_2) \\ m_2 \ddot{y}_2 &= (2K_2\dot{\delta}_2 + k_2\delta_2) \end{aligned}\right\} \quad (1)$$

Now $\ddot{y}_1 = \ddot{y}_c - \ddot{\delta}_1$

$\ddot{y}_2 = \ddot{y}_c - \ddot{\delta}_1 - \ddot{\delta}_2$

$\therefore \ddot{y}_c = (2c_1\dot{\delta}_1 + \omega_1^2\delta_1) - \phi(2c_2\dot{\delta}_2 + \omega_2^2\delta_2) + \ddot{\delta}_1$

$\ddot{y}_c = (2c_2\dot{\delta}_2 + \omega_2^2\delta_2) + \ddot{\delta}_1 + \ddot{\delta}_2 \quad (2)$

where $\phi = m_2/m_1$, $\omega_n^2 = k_n/m_n$, $c_n = K_n/m_n = \omega_n \bar{c}$

Behavior of the Lower System

The force in the lower spring and damper must be equal to the applied force

i.e., $$2c_1\dot{\delta}_1 + \omega_1^2\delta_1 = \frac{F_c}{m_1} \tag{3}$$

or $$\dot{\delta}_1 + \left(\frac{\omega_1}{2c_1}\right)\delta_1 = \frac{\bar{F}_c}{2c_1 m_1} = \frac{F_c}{2K_1}$$

$$\therefore \quad \delta_1 = e^{-\int\frac{\omega_1}{2c_1}dt}\left[\int e^{\int\frac{\omega_1}{2c_1}dt}\frac{F_c}{2K_1}dt + C\right]$$

$$= e^{\frac{-\omega_1 t}{2c_1}}\left[\int e^{\frac{\omega_1 t}{2c_1}}\frac{F_c}{2K_1}dt + C\right] \tag{4}$$

For the case when $F_c = F_0 \sin \Omega t$. the integral becomes

$$\int e^{\frac{\omega_1 t}{2c_1}} F_c\, dt = \frac{F_0}{2K_1}\int e^{\frac{\omega_1 t}{2c_1}}\sin\Omega t\, dt$$

$$= \frac{F_0 e^{\frac{\omega_1 t}{2c_1}}}{2K_1\Omega}\;\frac{\left[\frac{\omega_1}{\Omega}\frac{1}{2c_1}\sin\Omega t - \cos\Omega t\right]}{\left[1 + \left(\frac{1}{2c_1}\frac{\omega_1}{\Omega}\right)^2\right]}$$

$$\therefore \quad \delta_1 = \frac{F_0}{2K_1\Omega}\frac{\left[\frac{\omega_1}{2c_1\Omega}\sin\Omega t - \cos\Omega t\right]}{\left[1 + \left(\frac{\omega_1}{2c_1\Omega}\right)^2\right]} + C e^{-\frac{\omega_1 t}{2c_1}} \tag{5}$$

The term containing the integration constant C is a transient function of the initial conditions, and can be ignored when considering steady state sinusoidal excitation, because

the steady state condition can be written as

$$\delta_1 = \frac{F_0}{\omega_1 m_1} \quad \frac{\omega_1 \sin\Omega t - 2\bar{C}_1 \Omega \cos\Omega t}{\left[(2\bar{C}_1\Omega)^2 + \omega_1^2\right]} \tag{6}$$

Note that as $\Omega \rightarrow 0$

$$\delta_1 \rightarrow \frac{F_0}{\omega_1^2 m_1} \sin\Omega t = \frac{F_0}{R_1} \sin\Omega t$$

and $y_1 = y_2 = y_c$

This is the static displacement result, $|\delta_1| = \frac{F_0}{R_1}$, where the force is transmitted by the spring and the whole system moves as a solid body, in phase with the applied force. When $\Omega \rightarrow \infty$

$$\delta_1 \rightarrow -\frac{F_0 \cos\Omega t}{2\bar{C}_1 m_1 \Omega} \rightarrow 0$$

but

$$\dot{\delta}_1 \rightarrow \frac{F_0}{2\bar{C}_1 m} \sin\Omega t \not\rightarrow 0$$

Thus the motion lags the applied force by $\pi/2$, and all the force is absorbed in the damper.

The maximum value of δ_1 is obtained by re-writing equation (6) as

$$\delta_1 = \frac{F_0 \sin(\Omega t + \psi_1)}{\omega_1^2 m_1 \sqrt{1 + (2\bar{C}\frac{\Omega}{\omega_1})^2}} \tag{7}$$

where

$$\sin\psi_1 = \frac{-2\bar{C}_1 \frac{\Omega}{\omega_1}}{\sqrt{1 + \left(2C_1 \frac{\Omega}{\omega_1}\right)^2}} \tag{8}$$

The maximum deflection amplitude occurs in the limit case ($\Omega \rightarrow 0$) when all the force is absorbed by the spring but the motion amplitudes are so large when $\Omega \rightarrow 0$ that the displacement amplitude ratios y_1/y_c and y_2/y_c tend to unity, masking the fact that the spring deflection is maximum at this point (see fig. 3).

Behavior of the Upper System

Equating equations (2)

$$(2c_1\dot{\delta}_1 + \omega_1^2\delta_1) = (1+\phi)(2c_2\dot{\delta}_2 + \omega^2\delta_2) + \ddot{\delta}_2 \qquad (9)$$

But $$(2c_1\dot{\delta}_1 + \omega_1^2\delta_1) = \frac{F_e}{m_1}$$

Thus the response of the second system is obtained directly from the equation

$$\ddot{\delta}_2 + 2c_2(1+\phi)\dot{\delta}_2 + \omega_2^2(1+\phi)\delta_2 = \frac{F_e}{m_1} \qquad (10)$$

It will therefore respond to the excitation as if it had an apparent damping coefficient of $c_2(1+\phi)$ and an apparent undamped natural frequency of $\omega_2\sqrt{1+\phi}$.

Since ω_1 and c_1 do not appear in equation (10), they can have no influence on δ_2; whatever their values. This is illustrated empirically in figure 5 by plotting y_2/y_1, for the cases illustrated in figure 3, where all the amplitude ratics y_m/y_e collapse on the single line of y_2/y_1.

When $F_e = F_0 \sin\Omega t$, the steady state response of the upper mass may be derived from equation (10) in a manner similar to the derivation of equation (6) from equation (3)

$$\delta_2 = \frac{\frac{\phi F_0}{m_2\omega_2^2}\sin(\Omega t + \psi_2)}{\sqrt{\left[(1+\phi) - \left(\frac{\Omega}{\omega_2}\right)^2\right]^2 + 4\bar{c}_2^2(1+\phi)^2\left(\frac{\Omega}{\omega_2}\right)^2}} \qquad (11)$$

where $$\tan\psi_2 = \frac{2\bar{c}_2(1+\phi)\frac{\Omega}{\omega_2}}{\left(\frac{\Omega}{\omega_2}\right)^2 - (1+\phi)}$$

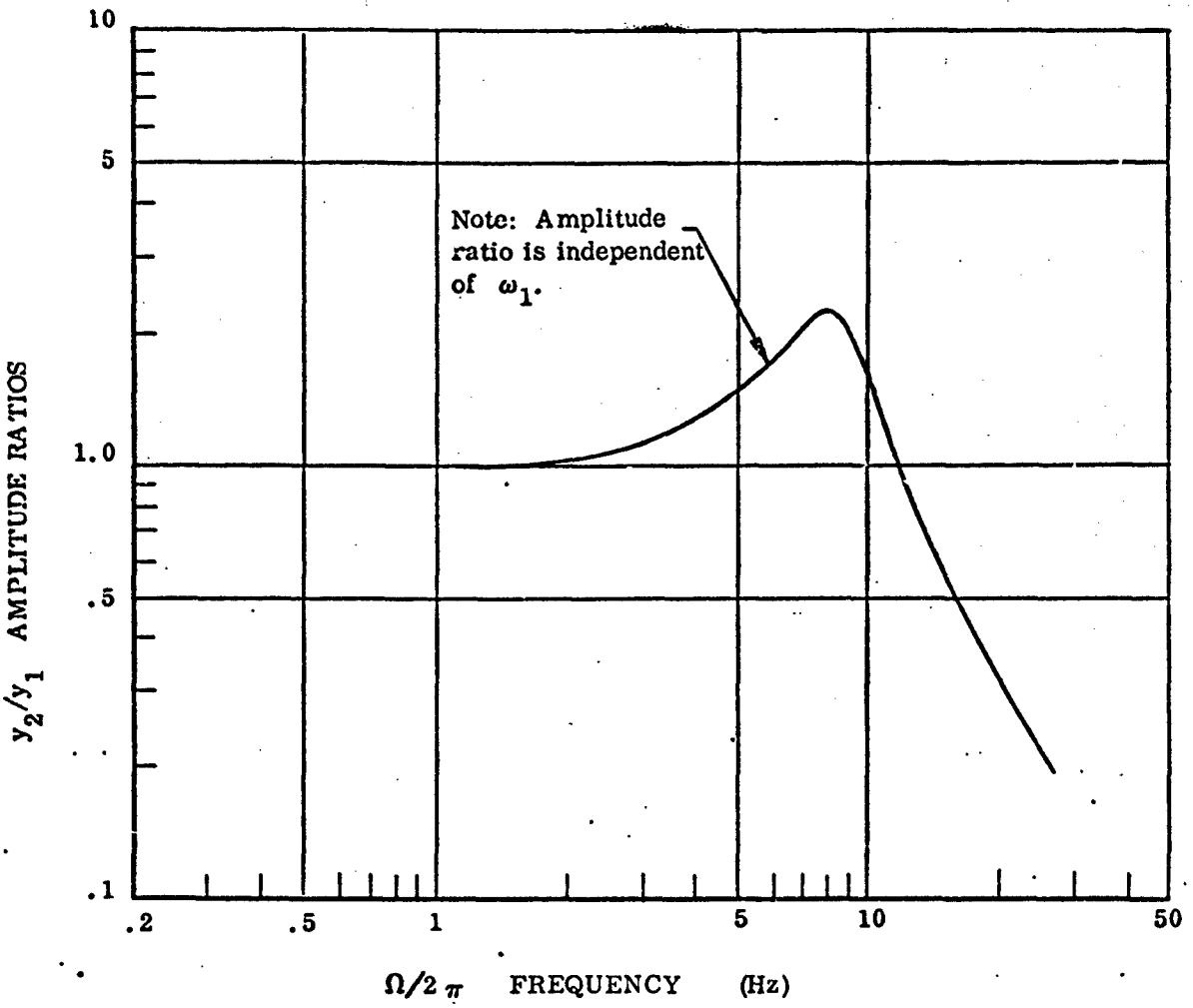

Figure 5. Amplitude Ratios of Two Degree of Freedom System of Figure 3

We note that the static displacement amplitude ($\Omega \rightarrow 0$) is

$$|\delta|_2 \rightarrow \frac{F_o}{k_2} \quad \frac{\phi}{(1+\phi)} \qquad \text{or} \qquad k\,|\delta|_2 \rightarrow \frac{F_o}{1 + \frac{m_1}{m_2}} \tag{12}$$

If F_c is a steady force, the entire system is accelerating at

$$\ddot{y}_T = \ddot{y}_1 = \ddot{y}_2 = \frac{F_c}{m_1 + m_2}$$

and the force in the upper spring is therefore

$$k_2 \delta_2 = m_2 \ddot{y}_T = \frac{F_c}{1 + \frac{m_1}{m_2}}$$

which is the result given by equation (12).

HIGHER-DEGREE-OF-FREEDOM SYSTEMS

Figure 6 shows the impedance of several multi-degree-of-freedom systems with a low damping coefficient of $\bar{c} = .03$. Despite this low damping, visibility of the higher modes is very poor, the corresponding peaks being orders of magnitude less than the first peak, and therefore virtually undiscoverable under real experimental conditions.

When the damping ratio is increased to the value of $\bar{c} = 0.3$, more typical of biodynamic structures, (fig. 7) it is found that only the first two or three peaks are visible, further compounding the problem.

The corresponding complex impedance plot for the ten-degree-of-freedom system with $\bar{c} = 0.3$ is given in figure 8 and the relative amplitudes of three of the ten masses in figure 9.

IMPEDANCE OF A NONLINEAR SYSTEM

So far we have considered only linear systems. Even so, only the first mode can be seen clearly in the impedance plot when the damping is appreciable, as in the human body. Phillips (ref. 4) found that force deflection measurements on a seated subject obeyed an approximately cubic deflection law. He, therefore, developed a single-degree-of-freedom model mounted on a damped cubic spring. The cubic spring has different stiffnesses at different values of mean loadings (or "bias") which conforms with the observed change in impedance characteristics measured in centrifuge experiments (refs. 5, 7). In figure 10 the apparent impedance of the Phillips model is presented with "coulomb," linear and hydraulic damping, at three different bias levels.

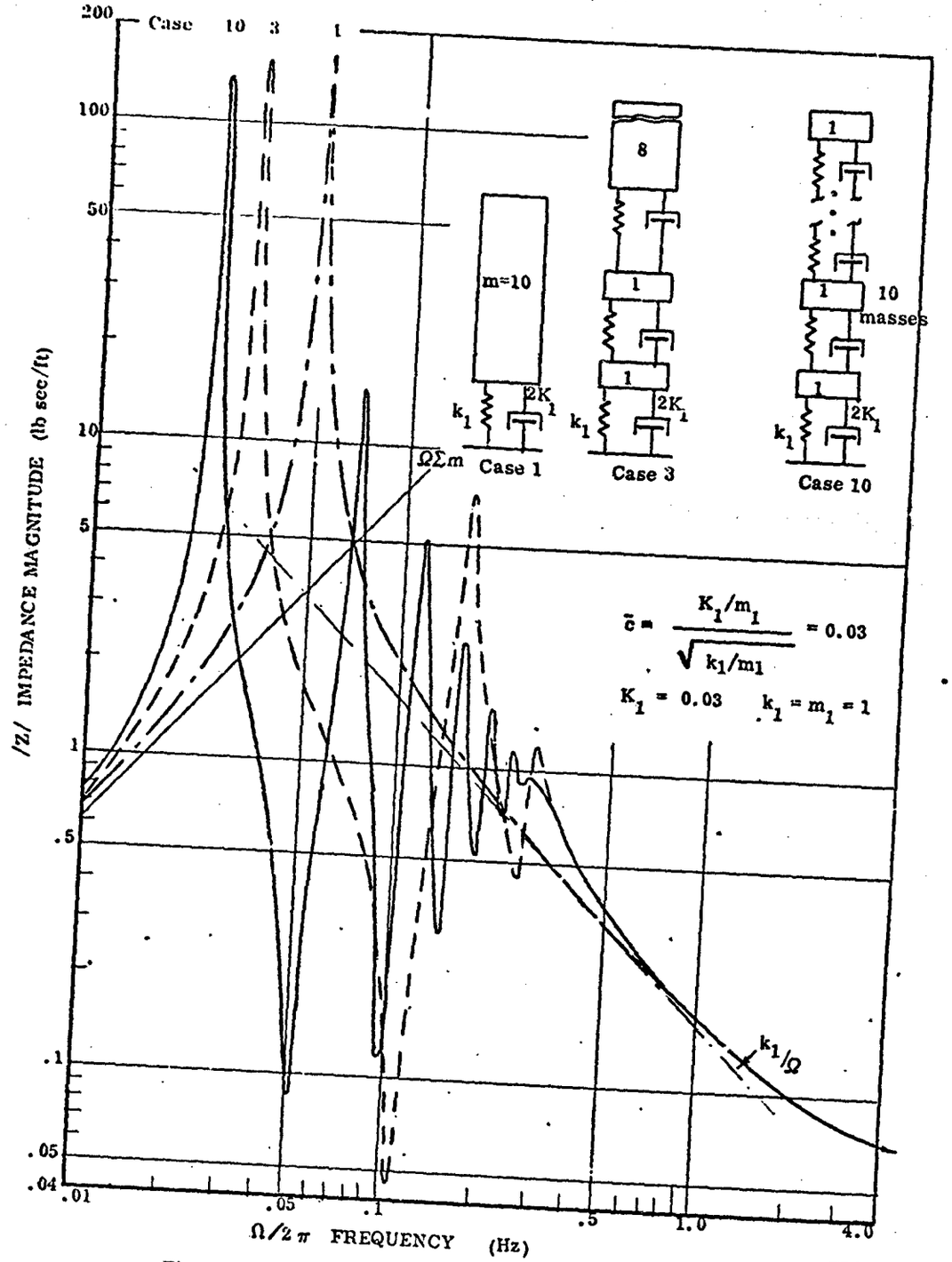

Figure 6. Comparison of 1 to 10 Degrees of Freedom Models
Damping Ratio $\bar{c} = .03$

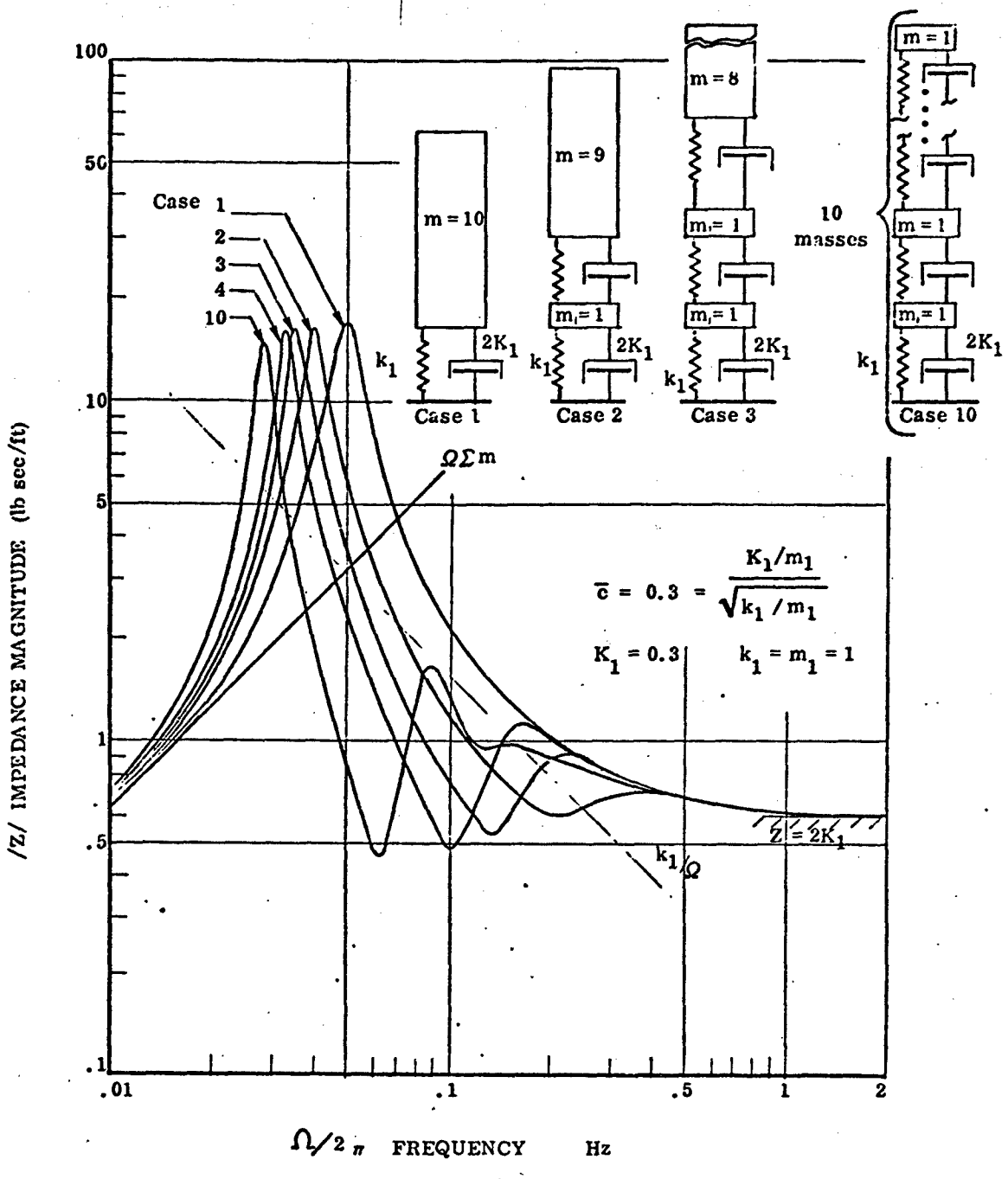

Figure 7. Comparison of 1 to 10 Degrees of Freedom Models
Damping Ratio $\bar{c} = .3$

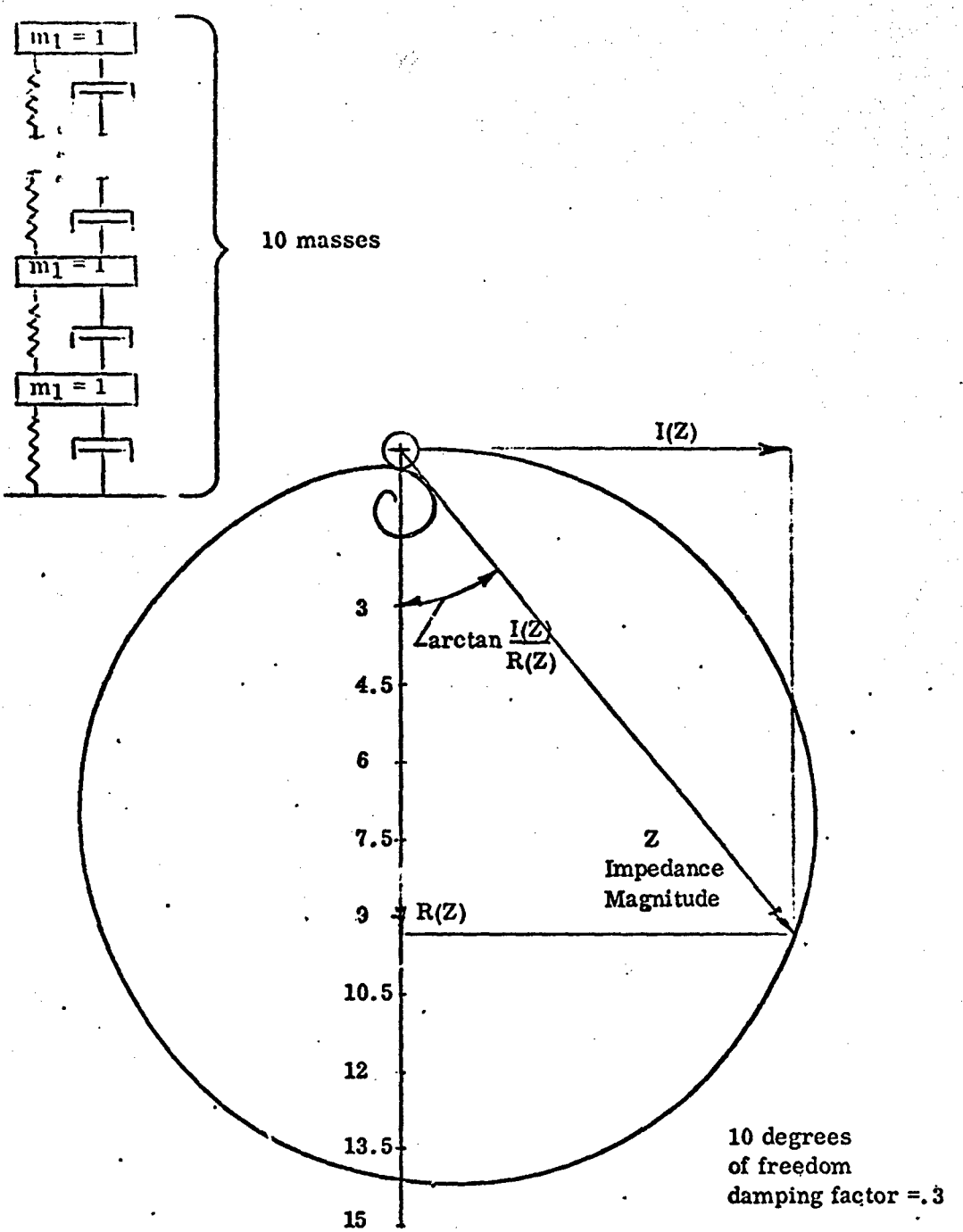

Figure 8. Complete Representations of Impedance vs. Phase Angle for Frequencies From .01 to 100 (ζ = .3) for the Ten Degrees of Freedom Model of Figure 7.

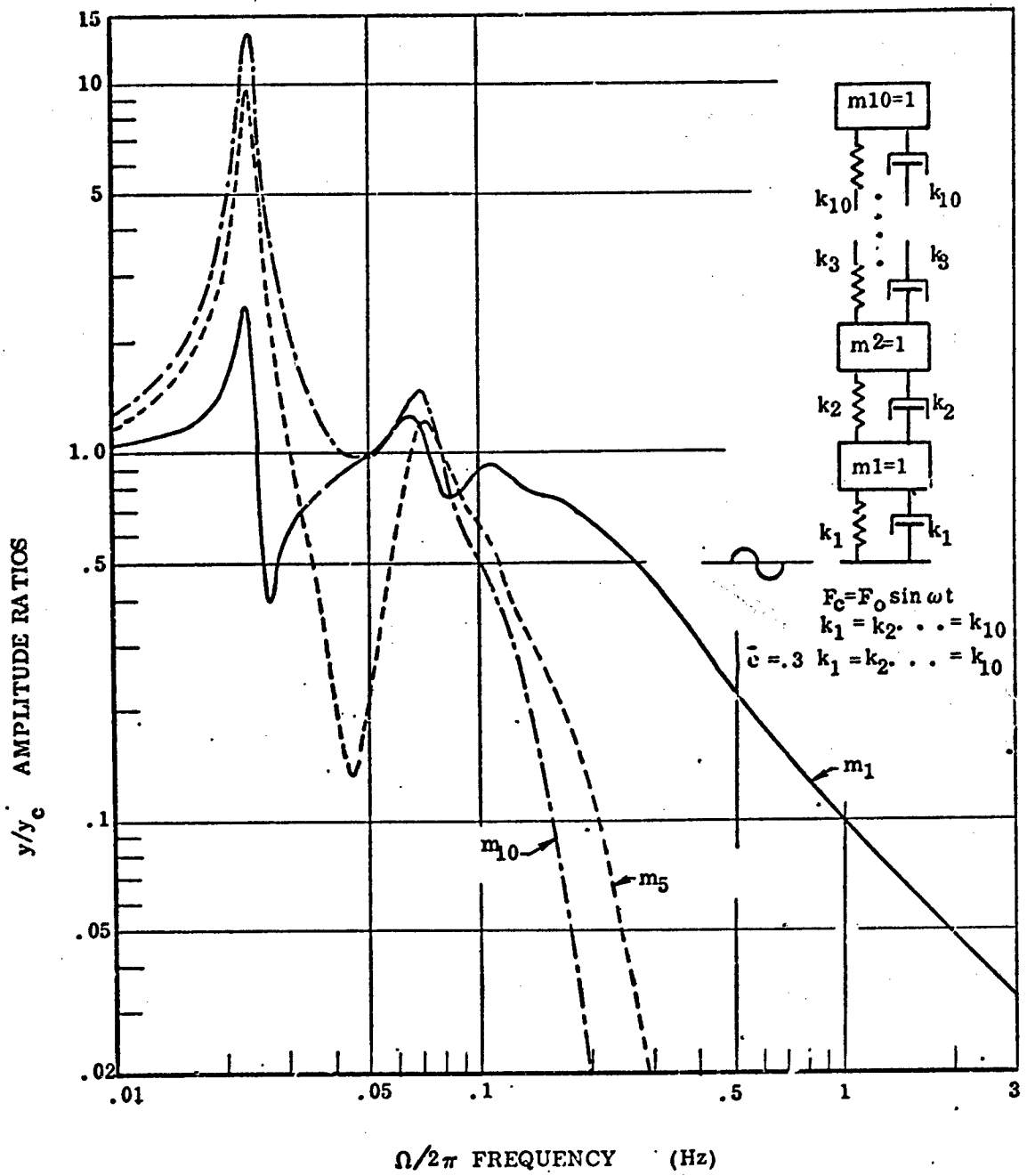

Figure 9. Amplitude Ratios for the Ten-Degree-of-Freedom Model of Figure 7.

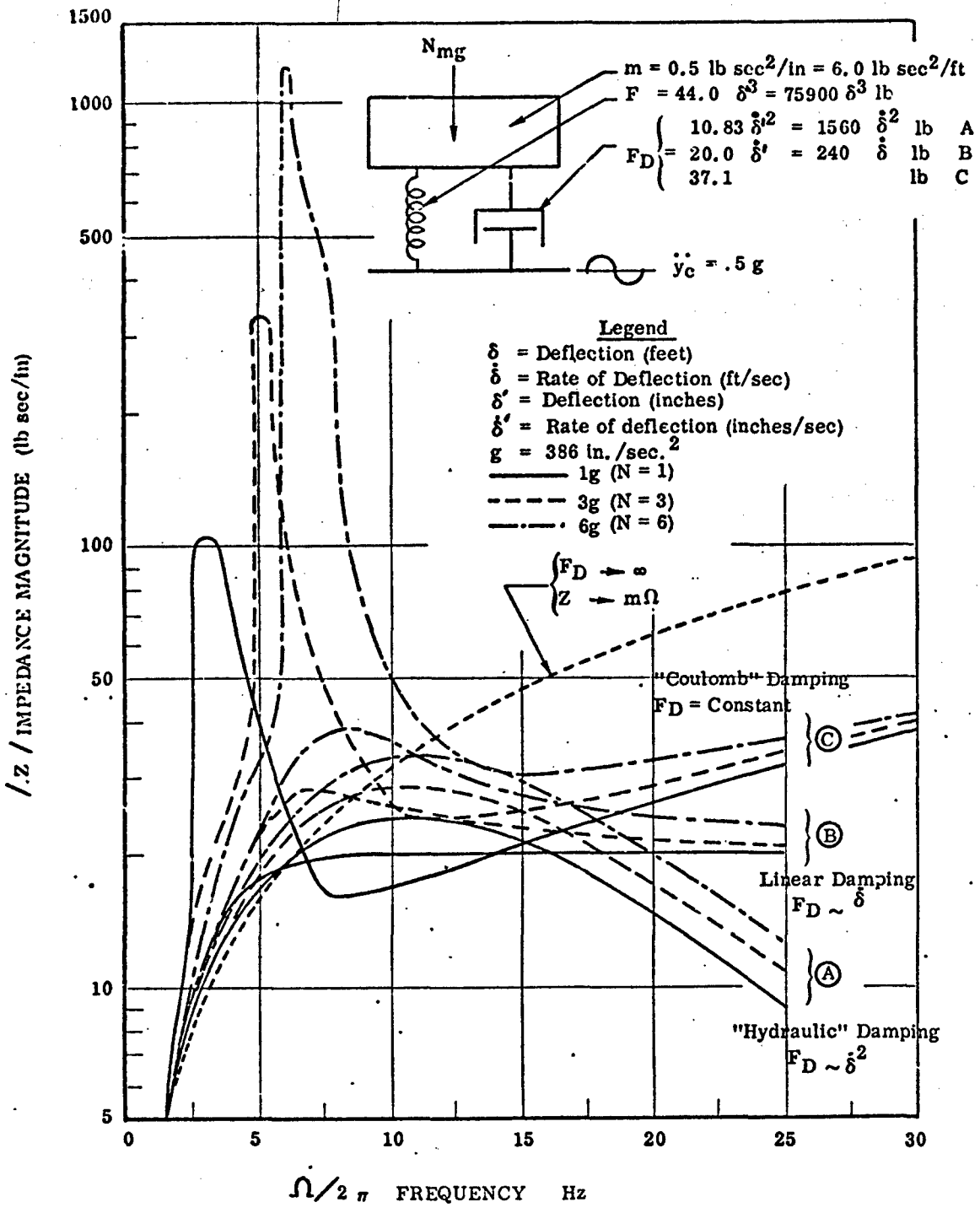

Figure 10. Apparent impedance of a non-linear model with different classes of damping and loading bias.

It is noteworthy that coulomb damping can result in an apparent impedance an order of magnitude greater than that of the same system with linear damping and that a change in loading bias of the cubic spring can change the impedance very considerably. This figure clearly indicates that, unless the type of damping is known, i.e., viscous, coulomb, etc., and the spring deflection characteristics, impedance data tells us almost nothing about the nature of the system.

THE DEFECTS OF EXISTING IMPEDANCE DATA FOR HUMAN SUBJECTS

Impedance measurements of live human subjects have been so far obtained in two ways - analysis of abrupt deceleration, and "steady state" sinusoidal excitation. The most recent "steady state" measurements, and in many ways the most interesting, are due to Vogt, Coermann and Fust (ref. 5), (seated position) and Vykukal (ref. 6), for a semisupine position. In both cases a centrifuge was used to bias the steady state acceleration and both investigators noted changes in impedance with increasing acceleration. Some of this data is reproduced in figures 11 and 12 for 1, 2, and 3 g bias conditions.

In both investigations the experimental scatter appears to be quite large, even though the experimental points are (most unfortunately) not given in the papers, and can only be inferred from the plots. This scatter is not too surprising when it is noted that in an earlier study Coermann (ref. 7) obtained for a 1 g loading:

$|Z|_{max}$ = 6.65×10^6 dyne/cm/sec, subject sitting erect = 455.5 lb sec/ft

$|Z|_{max}$ = 5.08×10^6 dyne/cm/sec, subject sitting relaxed = 347.5 lb sec/ft

At the low force levels associated with shake table measurements, muscle tension evidently plays a major role in the dynamics of the body. For large loadings, where the failure mode is generally vertebral fracture, one would not expect muscles to play so significant a role.

The most recent impedance measurement (ref. 5) under 1 g conditions ("slightly erect" posture) resulted in an impedance peak of only 267.5 lb sec/ft, possibly indicating an even larger inherent scatter than the two results mentioned above. A spread of nearly 2:1 in $|Z|_{max}$ is not very encouraging, especially when dynamic model analysis of ejection injuries (for example) indicates that the large deflection dynamic characteristics of the human body are rather surprisingly consistent.

In this connection, it is suggested that the Vogt, Coermann and Fust (ref. 5) data is more meaningfully presented as shown in figure 12, rather than by connecting up the data points with straight lines, and inferring that the resulting peaks and valleys have some physical meaning.

In a later section of this paper, it will be suggested that the first and largest peak in the impedance modulus for a seated human is due to the whole body resonating on the buttocks. This statement is only approximately correct, of course, because other resiliences in the

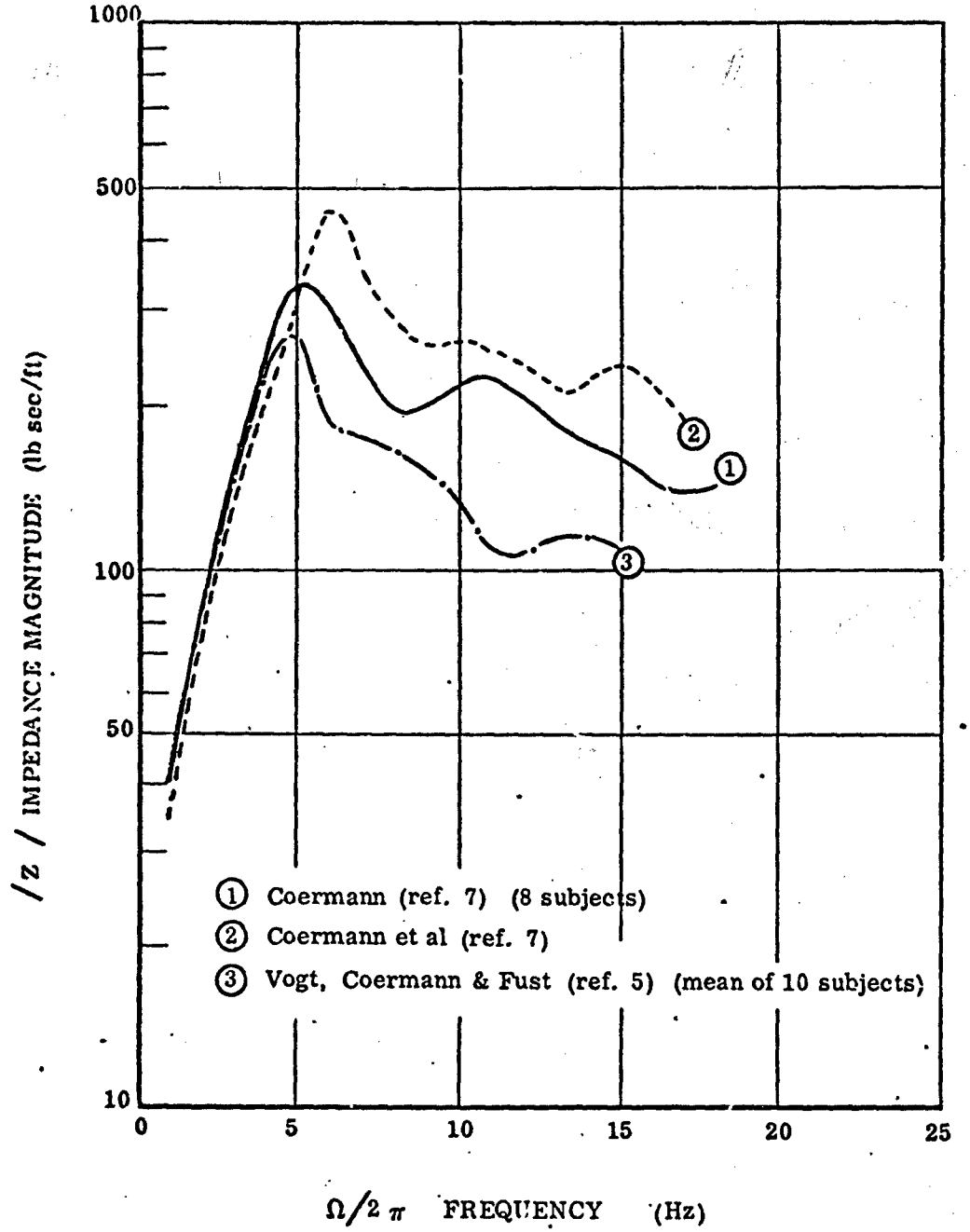

Figure 11. Average Experimentally Measured Impedance of Seated Human Subject Under 1 g Conditions

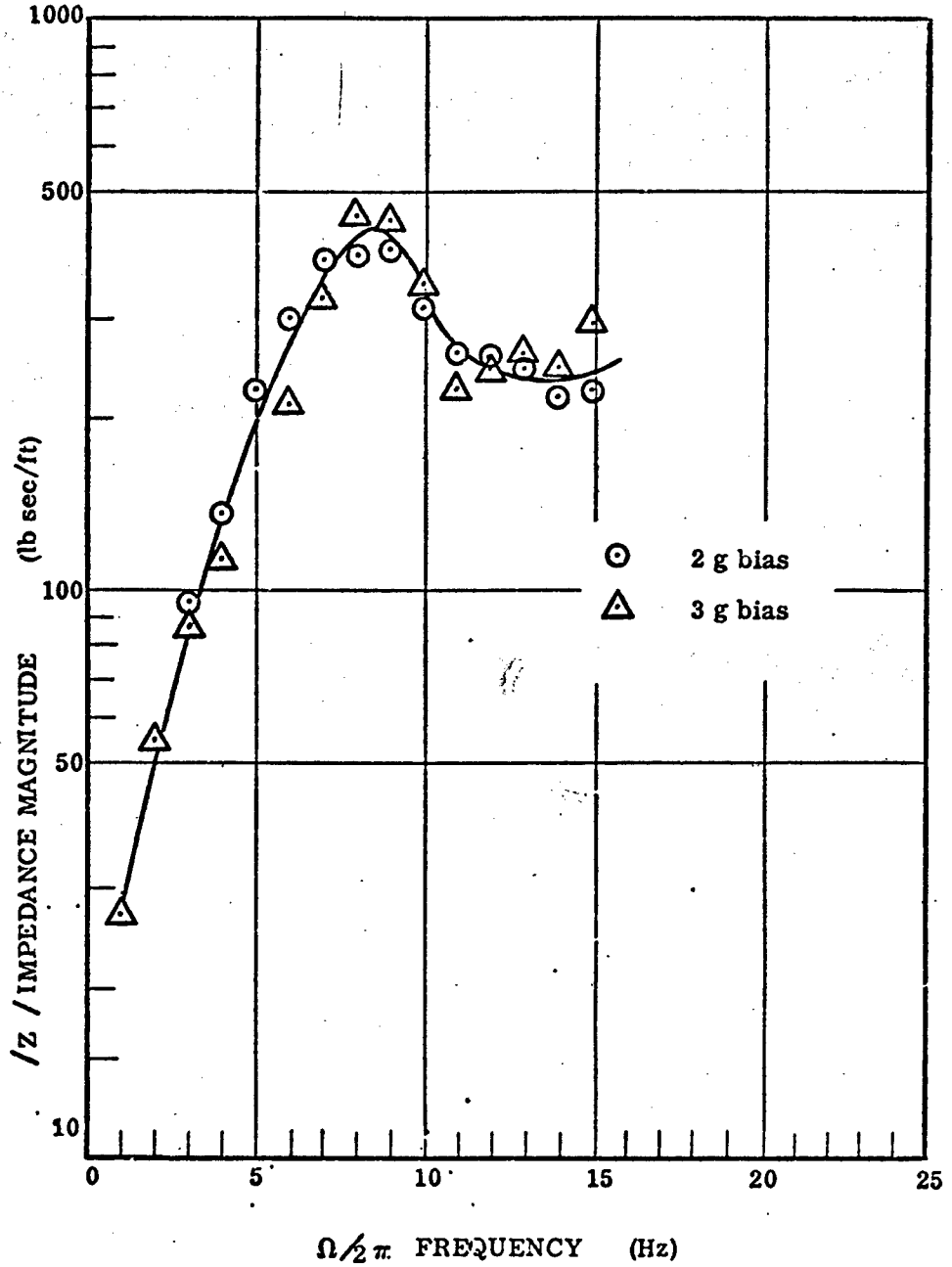

Figure 12. Inferred experimental data points for the impedance measurements of Vogt, Coermann and Fust (ref. 5) under 2 g and 3 g bias.

body are also deforming, but to a lesser extent. Since the variability in the size and muscle tone of the buttocks is greater than for most other portions of the (male) human body, it is not surprising that impedance measurements dominated by the buttock mode should be very variable, from subject to subject.

The available data on $|Z|_{max}$ is given in table 2, together with the characteristics of approximately equivalent single-degree-of-freedom lumped parameter systems which would give the same value of $|Z|_{max}$ at the same frequency. The two values of $|Z|_{max}$ for the "sitting erect" case are plotted in figure 13 and compared with the results given by the simple two-degree-of-freedom model shown in figure 2, using the ratios of the undamped natural frequencies calculated in table 2 (rather than their absolute values). The trend is seen to be in the right direction, at least, lending support to the hypothesis that Coermann's (ref. 7) buttocks in the 1963 experiments were significantly stiffer than the average of the ten subjects used in the 1968 report (ref. 5).

An attempt to reproduce these measured impedance data by using a four-degree-of-freedom lumped parameter model is described in the next section.

TABLE II

Equivalent Single-Degree-of-Freedom Model
for "Steady State" Impedance Measurements at 1 g

		Sitting Relaxed (ref. 7)	Sitting Erect (ref. 7)	Sitting "Slightly Erect" (ref. 5)
Experimental Values	$\|Z\|_{max}$ (dyne/cm/sec)	5.08×10^6	6.65×10^6	3.9×10^6
	$\|Z\|_{max}$ (lb sec/ft)	347.5	455.5	267.5
	Frequency for $\|Z\|_{max}$ $\Omega_o/2\pi$ (Hz)	5.3	6.3	5.0
	Frequency for $\|Z\|_{max}$ Ω_o (rads/sec)	33.30	39.6	31.42
	Subject Weight (lb)	185.0	185.0	176.0
	Effective Weight* mg (lb)	161.0	161.0	153.0
	Effective Mass* m (slugs)	5.01	5.01	4.76
Equivalent One-Degree-of-Freedom System	$\|Z\|_{max}/\Omega_o m$ (-)	2.083	2.30	1.7884
	$\bar{c}$ ** (-)	0.27	0.24	0.33
	Ω_o/ω ** (-)	1.018	1.012	1.037
	$\omega/2\pi$ (Hz)	5.21	6.22	4.82
	ω (rads/sec)	32.8	39.1	30.3
	Ω_o/Ω_{res} ** (-)	1.105	1.078	1.175
	$\Omega_{res}/2\pi$ (Hz)	4.8	5.84	4.25

Where Ω_{res} is the resonant frequency of the system at which the amplitude magnification is maximum.

---

* Effective weight is taken as 87% of the total weight on the assumption that the lower legs and feet are not excited.

** From Payne, reference 8.

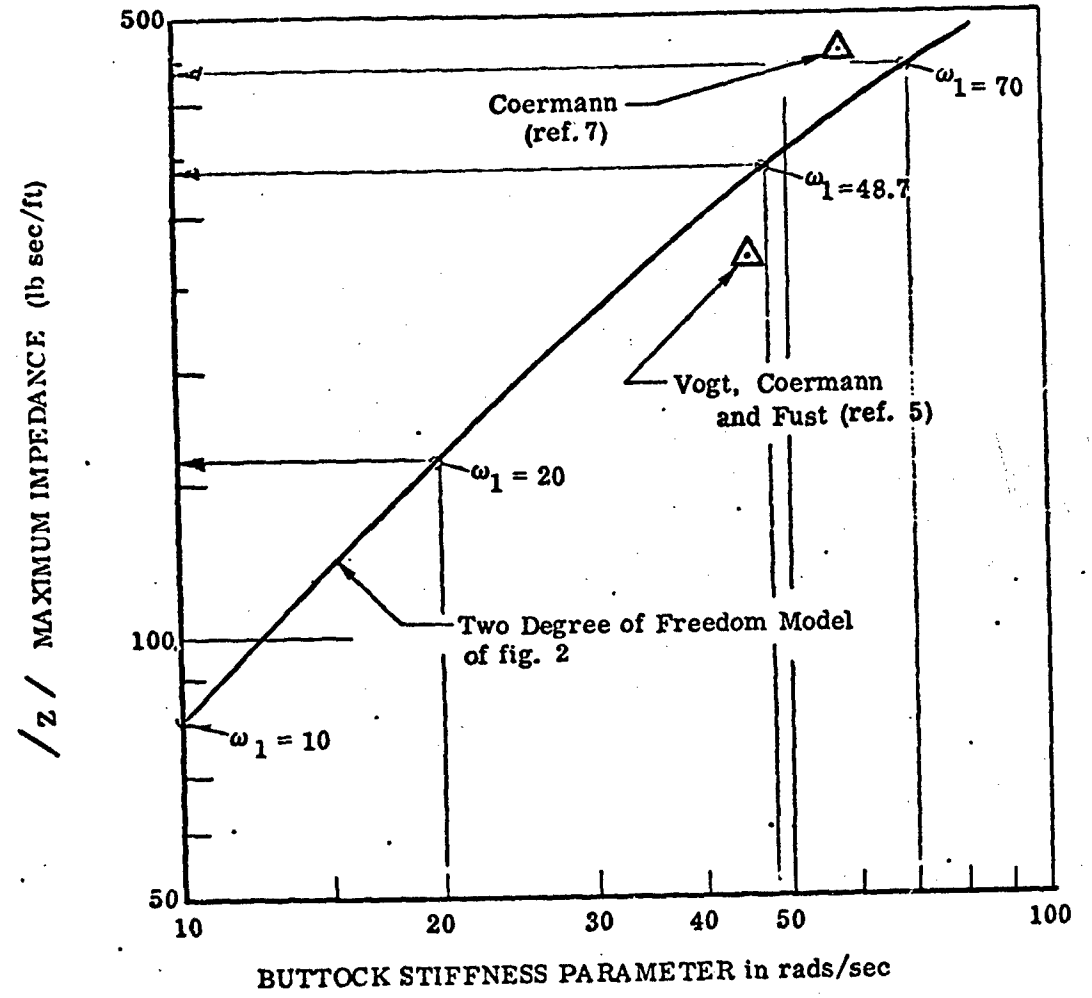

Figure 13. Apparent Variation of First Impedance Peak with Buttock Stiffness

SECTION III

A LINEAR FOUR-DEGREE-OF-FREEDOM SPINAL MODEL FOR THE SEATED MAN

The linear single-degree-of-freedom "spinal" model currently used to calculate Dynamic Response Index (DRI) is, of course, only the starting point for the development of a more sophisticated model. The first step is to add a "pelvic mass" at the bottom of the "spine spring" and a buttock resiliency underneath the pelvic mass. The pelvic mass and buttock spring represent the "buttock mode," and for the reasons discussed earlier, it seems likely that this mode has the greatest influence on impedance measurements of seated subjects.

The next logical addition to the model is a degree of freedom representing the viscera, since many studies have shown that this has a marked resonance between 3.0 and 3.5 Hz (see, for example, ref. 1 and the quoted exerpt on p.45). As shown in figure 14, this is most simple shown as being supported from the upper torso mass, although a case could obviously be made for an additional spring-damper connection to the pelvic mass, shown dotted in the figure. In view of the relatively greater significance of the links closest to the shake table, it would appear that the connection 5 will have a far greater influence on the impedance than 3. However, this concept (5) has not been pursued further.

Finally, since shake table measurements have shown marked head resonance with respect to the upper torso at around 30 Hz, it is desirable to add the degree of freedom on top of the upper torso.

These four degrees of freedom give the model shown in figure 14. In the next section we first derive the linear equations for this model, and then a more general relationship which permits the inclusion of nonlinear terms. The coefficients of these equations are then determined by an examination of experimental data, using various techniques.

EQUATIONS FOR THE FOUR-DEGREE-OF-FREEDOM MODEL

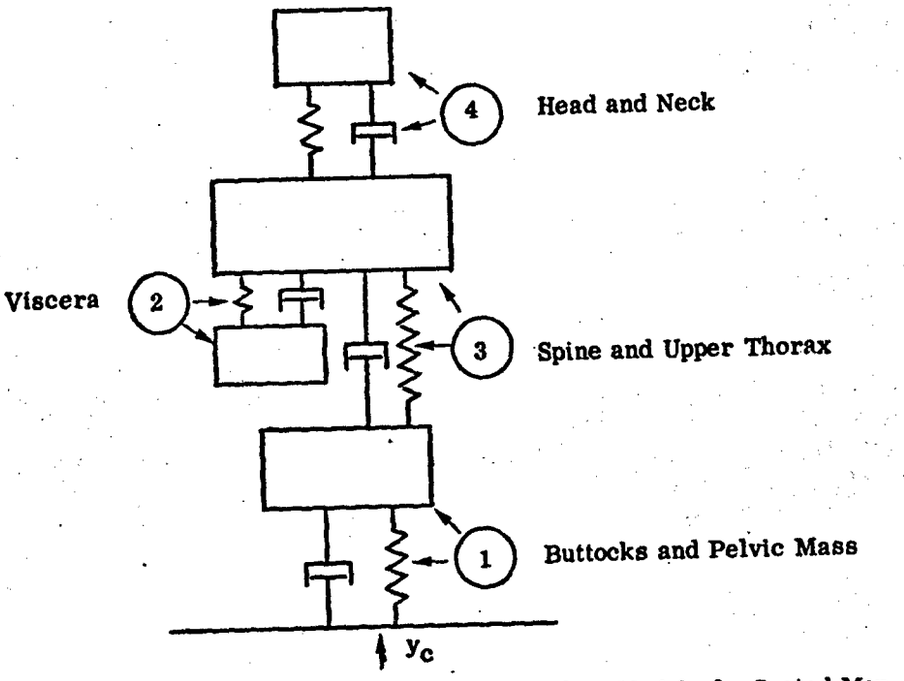

Figure 14. The Four-Degree-of-Freedom Model of a Seated Man

Let λ_n = unstretched length of spring n

δ_n = n^{th} spring deflection (+ ve in compression)

Then

$$\left.\begin{aligned} m_1\ddot{y}_1 &= (2K_1\dot{\delta}_1 + k_1\delta_1) - (2K_3\dot{\delta}_3 + k_3\delta_3) \\ m_3\ddot{y}_3 &= (2K_3\dot{\delta}_3 + k_3\delta_3) + (2K_2\dot{\delta}_2 + k_2\delta_2) - (2K_4\dot{\delta}_4 + k_4\delta_4) \\ m_4\ddot{y}_4 &= (2K_4\dot{\delta}_4 + k_4\delta_4) \\ m_2\ddot{y}_2 &= -(2K_2\dot{\delta}_2 + k_2\delta_2) \end{aligned}\right\} \quad (13)$$

Let $\omega_n^2 = k_i/m_n \qquad 2c_n = 2K_n/m_n$

$$\phi\left(\frac{p}{q}\right) = \frac{m_p}{m_q}$$

The equations (13) become

$$\left.\begin{aligned}
\ddot{y}_1 &= (2c_1\dot{\delta}_1 + \omega_1^2\delta_1) - \phi(\tfrac{2}{1})(2c_2\dot{\delta}_2 + \omega_2^2\delta_2) \\
\ddot{y}_3 &= (2c_3\dot{\delta}_3 + \omega_3^2\delta_3) + \phi(\tfrac{2}{3})(2c_2\dot{\delta}_2 + \omega_2^2\delta_2) - \phi(\tfrac{4}{3})(2c_4\dot{\delta}_4 + \omega_4^2\delta_4) \\
\ddot{y}_4 &= (2c_4\dot{\delta}_4 + \omega_4^2\delta_4) \\
\ddot{y}_2 &= -(2c_2\dot{\delta}_2 + \omega_2^2\delta_2)
\end{aligned}\right\} \quad (14)$$

Also $\delta_1 = \lambda_1 - (y_1 - y_c)$

$$\therefore y_1 = \lambda_1 + y_c - \delta_1$$

$$\therefore \ddot{y}_1 = \ddot{y}_c - \ddot{\delta}_1$$

Similarly $\ddot{y}_3 = \ddot{y}_c - \ddot{\delta}_1 - \ddot{\delta}_3$

and $\ddot{y}_4 = \ddot{y}_c - \ddot{\delta}_1 - \ddot{\delta}_3 - \ddot{\delta}_4$

$$\delta_2 = \lambda_2 - (y_2 - y_2)$$

$$\therefore \ddot{\delta}_2 = \ddot{y}_2 - \ddot{y}_2$$

$$\therefore \ddot{y}_2 = \ddot{y}_2 + \ddot{\delta}_2 = \ddot{y}_c - \ddot{\delta}_1 + \ddot{\delta}_2 - \ddot{\delta}_3$$

Making these substitutions, the equations of motion (14) become

$$\ddot{y}_c = (\ddot{\delta}_1 + 2c_1\dot{\delta}_1 + \omega_1^2\delta_1) - \phi(\tfrac{3}{1})(2c_3\dot{\delta}_3 + \omega_3^2\delta_3) \tag{15}$$

$$\ddot{y}_c = (\ddot{\delta}_3 + 2c_3\dot{\delta}_3 + \omega_3^2\delta_3) + \phi(\tfrac{2}{3})(2c_2\dot{\delta}_2 + \omega_2^2\delta_2) - \phi(\tfrac{4}{3})(2c_4\dot{\delta}_4 + \omega_4^2\delta_4) + \ddot{\delta}_1 \tag{16}$$

$$\ddot{y}_c = (\ddot{\delta}_4 + 2c_4\dot{\delta}_4 + \omega_4^2\delta_4) + \ddot{\delta}_1 + \ddot{\delta}_3 \tag{17}$$

$$\ddot{y}_c = -(\ddot{\delta}_2 + 2c_2\dot{\delta}_2 + \omega_2^2\delta_2) + \ddot{\delta}_1 + \ddot{\delta}_3 \tag{18}$$

Note from (17) and (18) that

$$(\ddot{\delta}_4 + 2c_4\dot{\delta}_4 + \omega_4^2\delta_4) + (\ddot{\delta}_2 + 2c_2\dot{\delta}_2 + \omega_2^2\delta_2) = 0$$

THE NONLINEAR EQUATIONS

If the damping and spring forces are nonlinear, we replace the terms,

$(2c_n\dot{\delta}_n + \omega_n^2\delta_n)$ by F_n, for simplicity, so that the equations become

$$\ddot{y}_c = \ddot{\delta}_1 + F_1 - \phi(\tfrac{3}{1})F_3 \tag{19}$$

$$\ddot{y}_c = \ddot{\delta}_1 + \ddot{\delta}_3 + F_3 + \phi(\tfrac{2}{3})F_2 - \phi(\tfrac{4}{3})F_4 \tag{20}$$

$$\ddot{y}_c = \ddot{\delta}_1 + \ddot{\delta}_3 + \ddot{\delta}_4 + F_4 \tag{21}$$

$$\ddot{y}_c = \ddot{\delta}_1 - \ddot{\delta}_2 + \ddot{\delta}_3 - F_2 \tag{22}$$

Equations (15) through (22) show how the response of one degree of freedom is modified by the other degrees of freedom. For example, suppose m_2 and m_4 are zero so that $\emptyset$ (2/3) and $\emptyset$ (4/3) are both equal to zero and the equation (20) becomes:

$$\ddot{y}_c = \ddot{\delta}_1 + \ddot{\delta}_3 + F_3$$

or for a linear system [from equation (17)]

$$\ddot{y}_c = (\ddot{\delta}_3 + 2c_3\dot{\delta}_3 + \omega_3^2\,\delta_3) + \ddot{\delta}_1$$

This is the "cushion theory" equation of reference 6.

THE BUTTOCK MODE IN THE LINEAR MODEL

It has already been established that the closer an element of a multi-mass model is to the driving point the more effect it has on the impedance characteristics. This is illustrated in figures 6 and 7. Thus, it is clear that probably the most important components of the seated human body in influencing the impedance are the buttocks. It is also rather obvious, upon consideration of this subject, that the spring rates, and possibly the damping rates of the buttocks may be highly nonlinear. Under high g loads, for example, the buttocks will "bottom out" and cease to influence the behavior of the body. The very markedly different effects of various types of nonlinearity are shown in figure 10. In order, however, to operate the linear four-degree-of-freedom model of the seated human body, it is necessary to assign linear values to the buttock spring stiffness and damping rate terms. The values used were as follows (the subscript 1 refers to the buttock/pelvic mass system):

Pelvic mass	m_1	=	64/32.2	(lb-sec^2/ft)
Undamped natural frequency	ω_1	=	39.55 to 198	(rad/sec)
Damping ratio	$\bar{c}_1$	=	.5 to .05	

The subject of a more realistic nonlinear representation of the buttocks mode will be treated in a later chapter (see p. 88).

THE SPINAL MODE AND ITS APPROXIMATE LINEAR MODEL

A method of computing the stiffness of the human spine has been given by Stech and Payne (ref. 9). This method is based upon Yorra's (ref. 11) stiffness measurement for a single L4 vertebra (fig. 15) extrapolated for all vertebrae between L5 and T1 inclusive by means of Ruff's (ref. 2) breaking load measurements shown in table 3. In the following analysis the subscript 3 refers to the total spinal loads and deflections and to the upper thorax mass, and the subscript m refers to those parameters that are particular to one vertebra (m = L4, etc.). Subscript 1 and 2 will be used to indicate the deflection of a particular vertebra from deflection S_{m_1} to S_{m_2}.

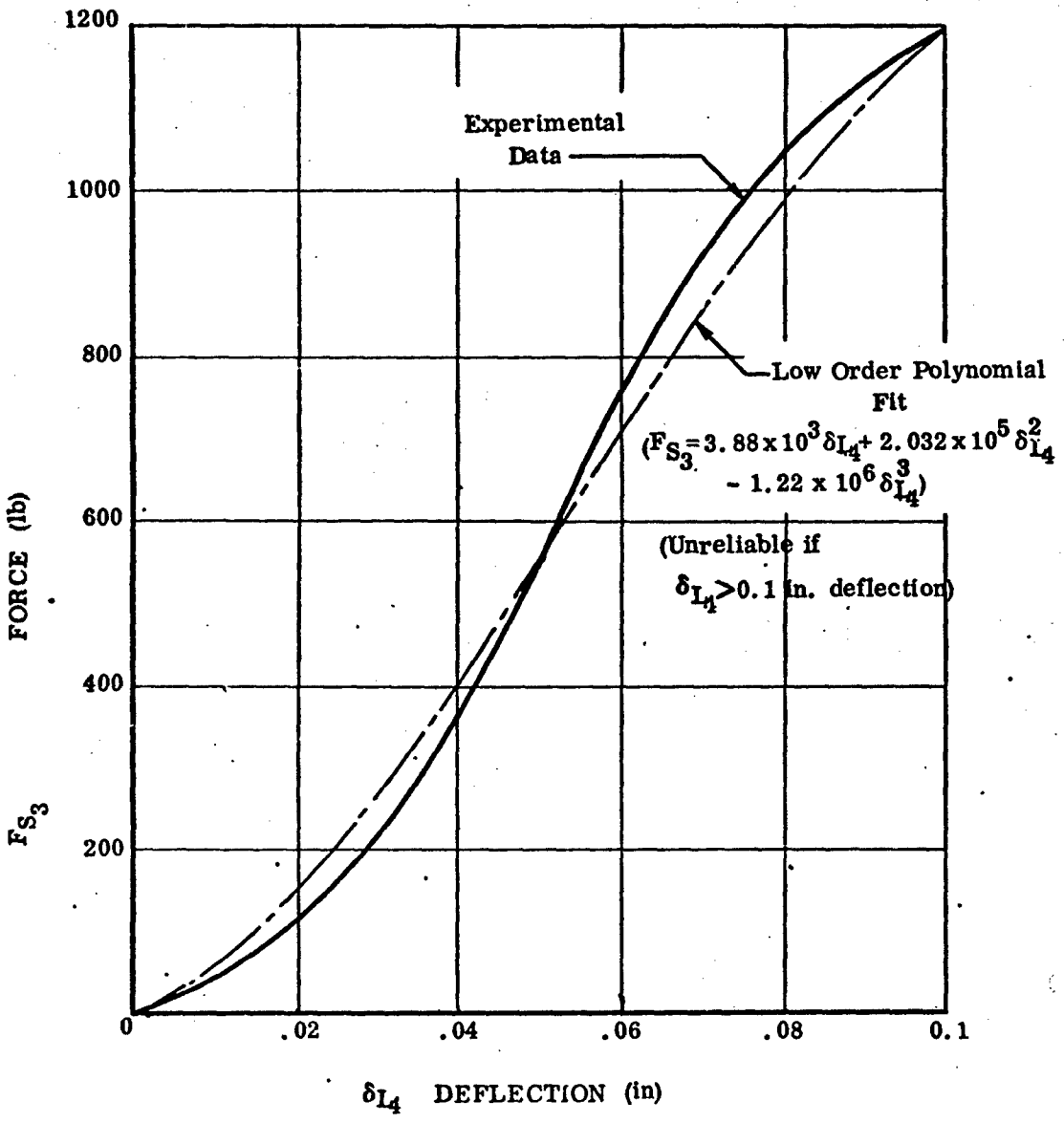

Figure 15. Yorra's Measurement of Load-Deflection for L-4 Vertebra, Age 57.5 Years (ref. 11)

TABLE III

Calculation of Vertebral Stiffness

Vertebra	% of Body Weight Carried	Weight Carried: 160 lb. Man	Breaking Strength in lbs.	Breaking Load in g	% of L4 Breaking Strength
T1	9	14.4	360	25.0**	16.6
T2	12	19.2	480	25.0**	22.1
T3	15	24.0	600	25.0**	27.7
T4	18	28.9	720	25.0**	33.2
T5	21*	33.8	840	25.0**	38.7
T6	25*	40.0	1000	25.0**	46.1
T7	29*	48.4	1160	25.0**	53.5
T8	33*	52.8	1315*	24.9	60.7
T9	37*	59.2	1493*	25.2	68.9
T10	40*	64.0	1632*	25.5	75.3
T11	44*	70.4	1700*	24.2	78.4
T12	47*	75.2	1757*	23.4	81.0
L1	50*	80.0	1790*	22.4	82.6
L2	53*	84.8	1925*	22.7	88.8
L3	56*	89.6	2161*	24.1	99.6
L4	58*	92.8	2168*	23.4	100.0
L5	60*	96.0	2366*	24.6	109.1

NOTES:

* Represents data collected experimentally by Geertz and reported by Ruff (ref. 2)

** Represents value assumed by Stech and Payne (ref. 10)

The errors inherent in the method are such that it is pointless to strive after extreme accuracy. Thus, a low order polynomial fit to Yorra's force-deflection curve, as shown in figure 15, is probably satisfactory for deflections less than one-tenth of an inch. This fit given by an expression of the following form is assumed to be similar for each of the individual vertebrae with appropriately scaled coefficients:

$$F_{s_3} = \alpha \delta_m + \beta \delta_m^2 - \gamma \delta_m^3 \tag{23}$$

Where δ_m is the deflection of the m vertebra. In the case of the L4 vertebra shown in figure 15, the coeffients used were as follows:

when δ_{2_4} is in inches		when δ_{2_4} is in feet	
α	$= 3.88 \times 10^3$	α	$= 4.66 \times 10^4$
β	$= 2.032 \times 10^5$	β	$= 2.925 \times 10^7$
γ	$= 1.22 \times 10^6$	γ	$= 2.11 \times 10^9$

The local stiffness is

$$\frac{dF_{s_3}}{d\delta_m} = \alpha + 2\beta \delta_m - 3\gamma \delta_m^2 \tag{24}$$

An "average stiffness" of a nonuniform spring may be defined by equating the work required to compress a spring with the characteristics given in equation (23) (from deflection δ_{m_1} to deflection δ_{m_2} in the case of the nth vertebra), with that required to compress an equivalent uniform spring of stiffness $\bar{k}_{m_{12}}$. The work done $W_{1,2}$ to compress each of these springs is given by:

Thus, for the spring represented by equation (23):

$$W_{1,2} = \int_1^2 (\alpha \delta_m + \beta \delta_m^2 - \gamma \delta_m^3)\, d\delta_m$$

$$= \frac{\alpha}{2}(\delta_{m_2}^2 - \delta_{m_1}^2) + \frac{\beta}{3}(\delta_{m_2}^3 - \delta_{m_1}^3) - \frac{\gamma}{4}(\delta_{m_2}^4 - \delta_{m_1}^4)$$

and for the equivalent uniform spring (defined by the equation $F_{s_3} = \bar{k}_{m_{12}} \delta_m$):

$$W_{1,2} = \int_1^2 \bar{k}_{m_{12}} \delta_m\, d\delta_m = \frac{\bar{k}_{m_{12}}}{2}(\delta_{m_2}^2 - \delta_{m_1}^2)$$

Equating these two values for $k_{m_{12}}$ and making the simplifying assumption that $\delta_{m_1} = 0$ which can be done with little loss of accuracy then the average stiffness is given by:

$$k_{m_{12}} = \alpha + \frac{2}{3}\beta \delta_{m_2} - \frac{1}{2}\gamma \delta_{m_2}^2 \tag{25}$$

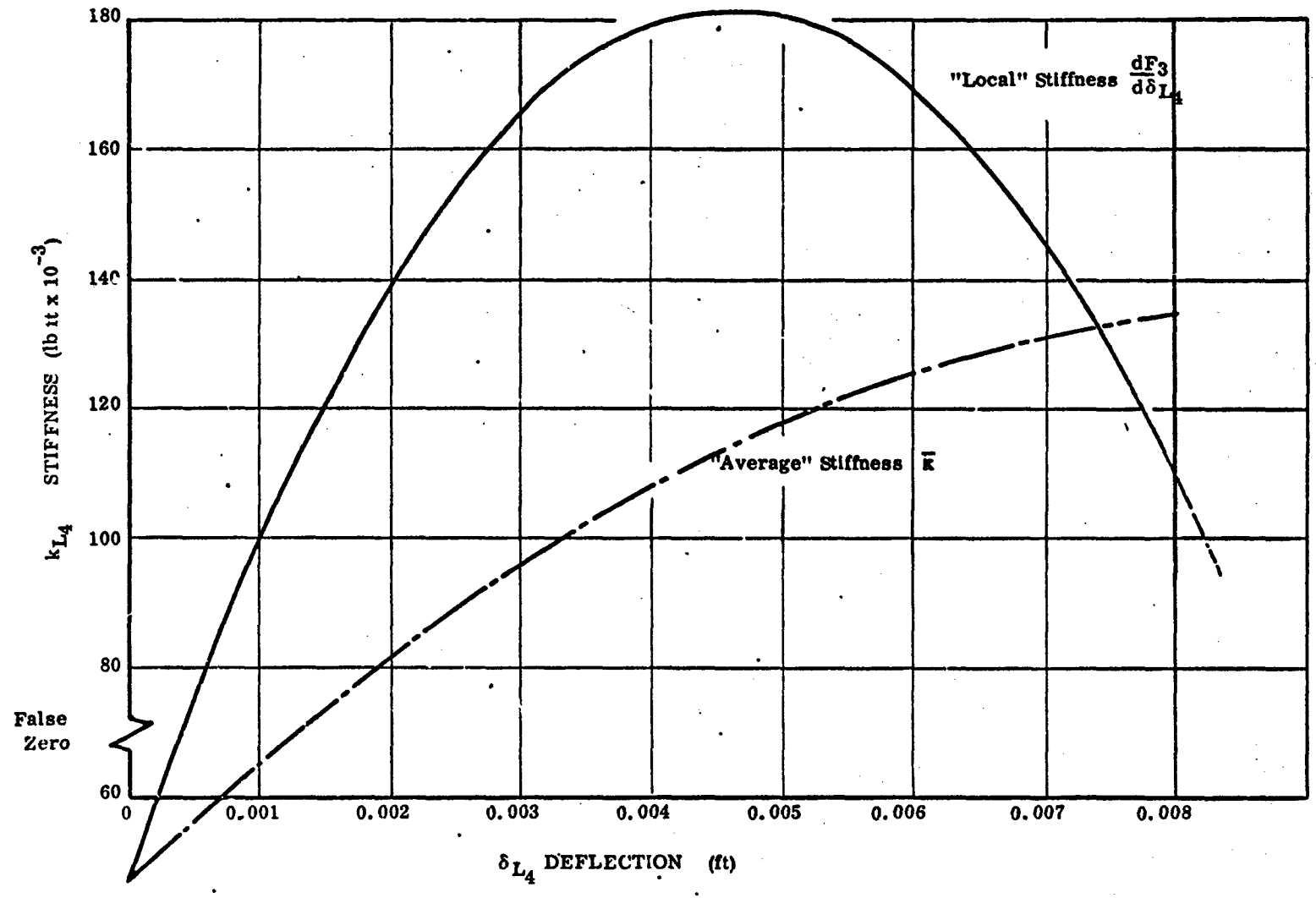

Figure 16. Stiffness of Vertebra L-4, from the Polynomial Approximation to Yorra's Data

Following the Stech and Payne procedure, the stiffness between each vertebra and the base of L5 at 1 g loading (table 4) can now be computed, with the results illustrated in figure 17. Stiffness multipliers for different g values (from figure 15) and age (from Stech and Payne) are given in figures 18 and 19.

In the original Stech and Payne analysis, the spine was taken to extend from T1 to L5 inclusive. A more detailed examination of the human anatomy has suggested that termination a the top of T4 would be more logical as little of the upper thorax is supported by vertebrae above this point. Thus, from figure 17 the total stiffnesses from L5 to T4 are, for a male subject age 57.5 years

$$\text{LOCAL} \qquad 1 \text{ g stiffness} = 4.97 \times 10^3 \text{ lb/ft}$$

$$\text{AVERAGE} \qquad 1 \text{ g stiffness} = 3.15 \times 10^3 \text{ lb/ft}$$

Corrected to age 27.9 years by means of a multiplier of 1.52 read from figure 19, these give

$$\text{LOCAL} \qquad 1 \text{ g stiffness} = 7.56 \times 10^3 \text{ lb/ft}$$

$$\text{AVERAGE} \qquad 1 \text{ g stiffness} = 4.79 \times 10^3 \text{ lb/ft} \tag{26}$$

For small amplitude excitation, assuming an upper thoracic mass $m_3 = 1.49$ lb sec^2/ft, the local 1 g stiffness gives

$$\omega_3 = \sqrt{\frac{7.56 \times 10^3}{1.49}} = 71.1 \text{ rads/sec (1 g)}$$

For small amplitude excitation about 2 g and 3 g we have, from figure 18

$$\text{LOCAL} \qquad 2 \text{ g stiffness} = 7.56 \times 1.255 \times 10^3 = 9.50 \times 10^3 \text{ lb/ft}$$
$$3 \text{ g stiffness} = 7.56 \times 1.43 \times 10^3 = 10.80 \times 10^3 \text{ lb/ft}$$

and $$\omega_3 = 71.1 \times \sqrt{1.255} = 79.6 \text{ rads/sec (2 g)} \tag{27}$$

$$= 71.1 \times \sqrt{1.43} = 85.0 \text{ rads/sec (3 g)} \tag{28}$$

These stiffnesses and frequencies are substantially greater than the figures previously deduced by Payne. At 10 g the average stiffness is given by

$$\text{Average} \qquad 10 \text{ g stiffness} = 4.79 \times 1.855 \times 10^3 = 8.9 \times 10^3 \text{ lb/ft}$$

$$\omega_3 = \sqrt{\frac{8.9 \times 10^3}{1.49}} = 77.4 \text{ rads/sec (10 g)} \tag{29}$$

Corrected to the single-degree-of-freedom spinal model, where the head (12 lb) and upper torso (48 lb) masses are lumped together, we obtain

$$\omega_3 = 77.4 \times \sqrt{\frac{48.0}{60.0}} = 69.3 \text{ rads/sec (10 g)} \tag{30}$$

$$= 11.05 \text{ Hz (10 g)}$$

TABLE IV

1g Stiffness Calculations (lb/ft units)

(for 57.5 Year Old Male Subject)

%	Vertebra	Stiffness of Each Vertebra		Total from L5 to Each Vertebra	
		Local Stiffness	Average Stiffness (from 0 to 1g)	Local	Average
.166	T1	18.02×10^3	11.4×10^3	3.016×10^3	1.910×10^3
.221	T2	24.0	15.2	3.623	2.295
.277	T3	30.1	19.05	4.27	2.703
.332	T4	36.0	22.8	4.972	3.149
.387	T5	42.0	26.6	5.768	3.654
.461	T6	50.0	31.7	6.69	4.236
.535	T7	58.1	36.8	7.72	4.89
.607	T8	65.9	41.7	8.90	5.64
.689	T9	74.8	47.4	10.29	6.52
.753	T10	81.7	51.8	11.93	7.56
.784	T11	85.1	53.9	13.97	8.85
.910	T12	87.9	55.7	16.72	10.59
.826	L1	89.6	56.8	20.65	13.08
.888	L2	96.4	61.0	26.83	16.99
.996	L3	108.2	68.5	37.18	23.55
1.0	L4	108.5	68.7	56.64	35.88
1.091	L5	118.5	75.1	118.5	75.1

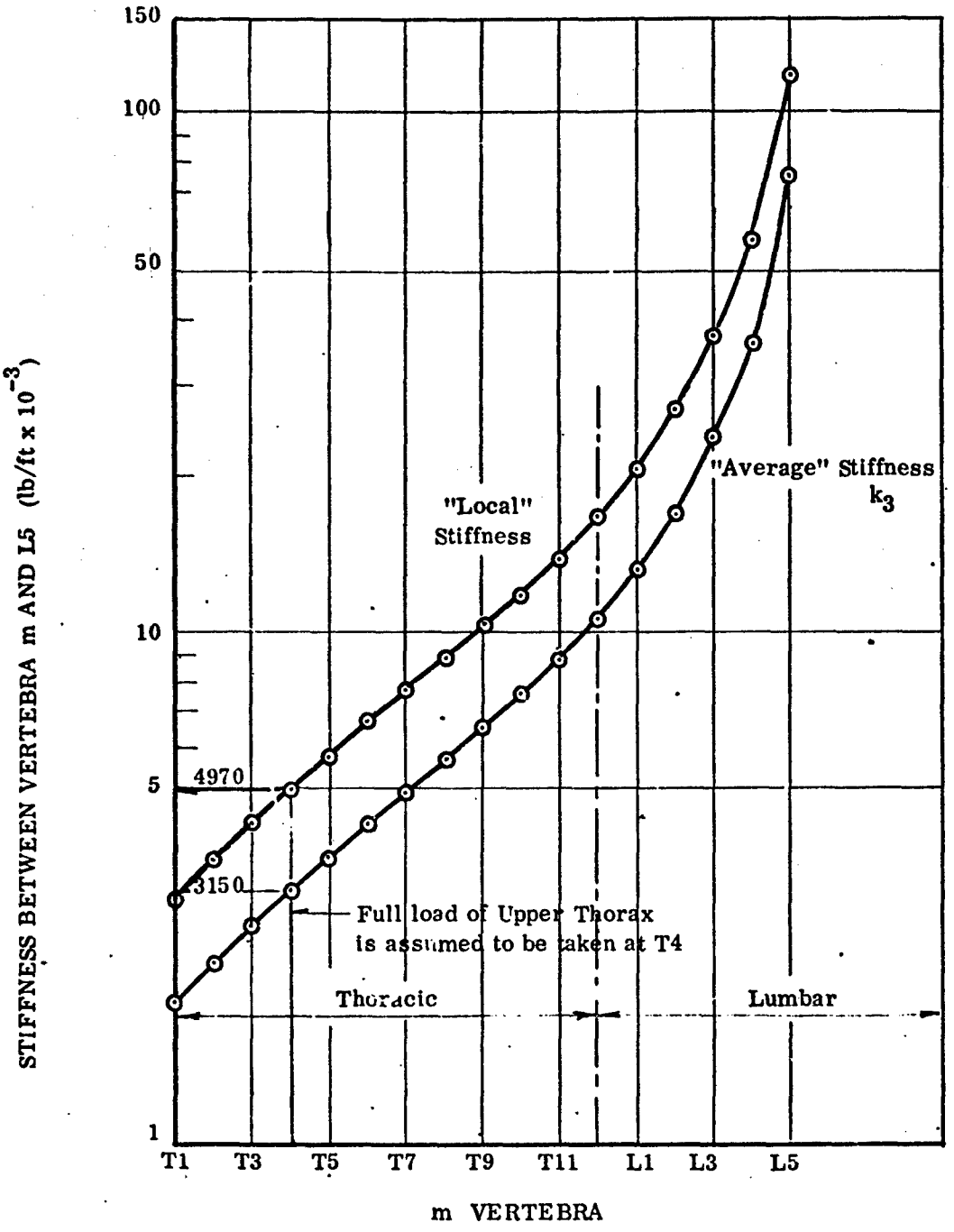

Figure 17. Spinal Stiffness at 1 g for 57.5 Year Old Male

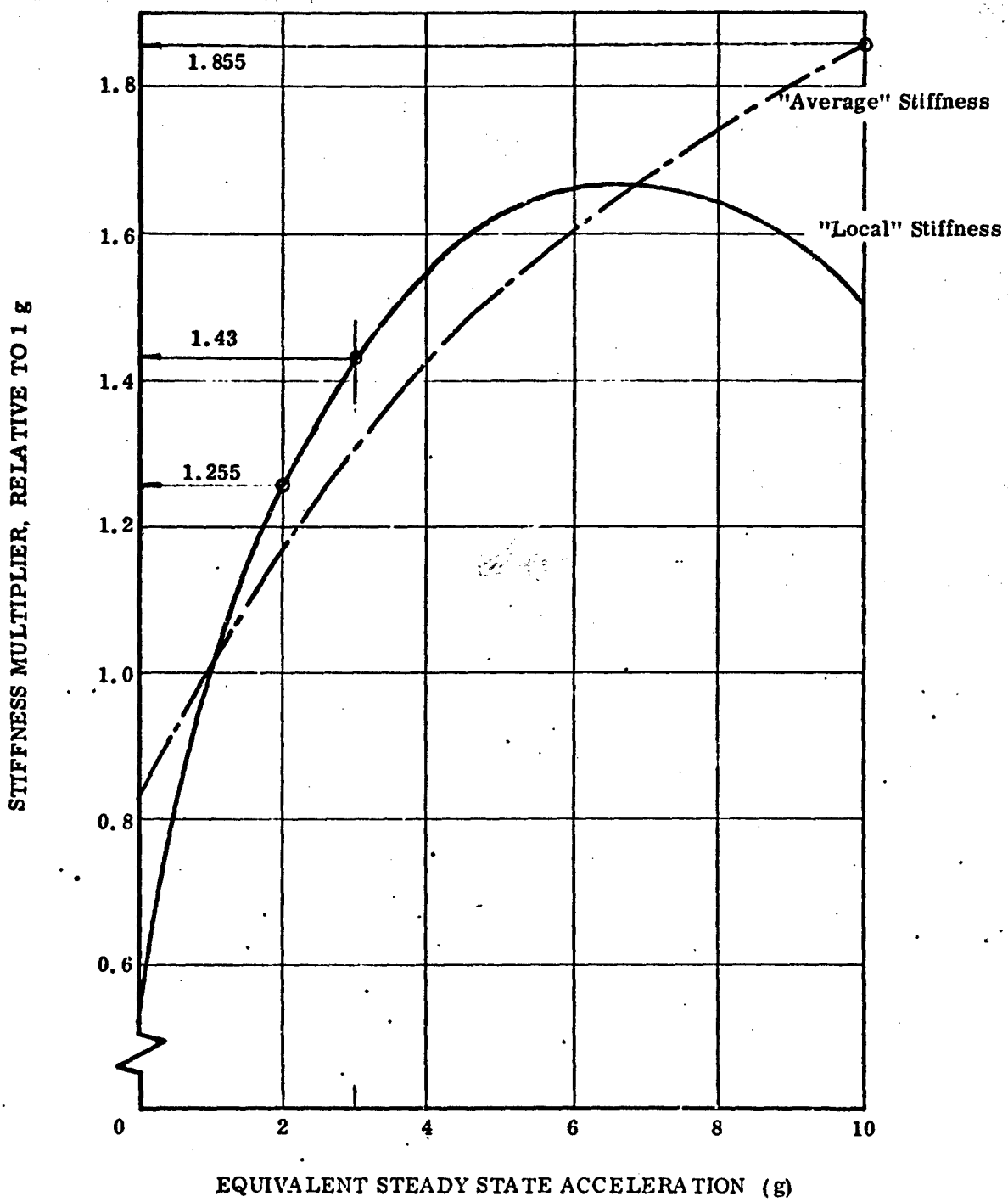

Figure 18. Average and Local Stiffness Between L5 and T4 Inclusive (Age 57.5 Years) as a Function of Loading

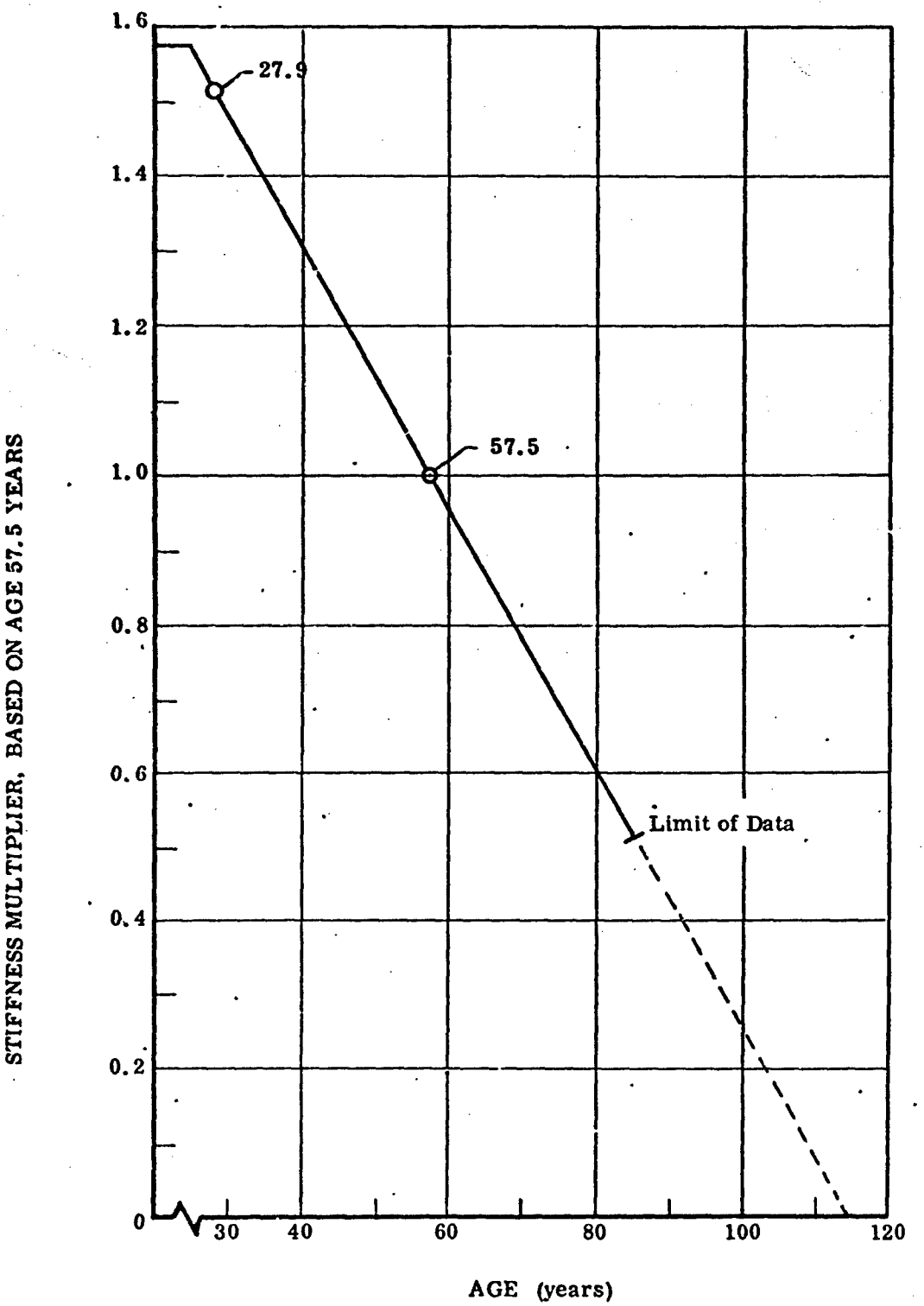

Figure 19. Correction Factor for the Effect of Age on Spinal Stiffness

The equivalent values using the T1 vertebra instead of the T4 vertebra would be:

AVERAGE 10 g stiffness (T1) = $1.91 \times 10^3 \times 1.52 \times 1.855 = 5.39 \times 10^3$ lb/ft

and

$$\omega_3(T1) = \sqrt{\frac{5.39 \times 10^3 \times 32.2}{60}} = 54 \text{ rad/sec (10 g)}$$

$$\omega_3(T1)/2\pi = 8.58 \text{ Hz}$$

This is very close to the value of 8.45 Hz deduced for the original Payne injury model. However, it is now assumed to be more realistic to use the T4 values for k_3 and ω_3.

In the linear four-degree-of-freedom model described in the next chapter of this report, the following ranges of values were chosen for a parametric study of the impedance of spinal/upper torso mode:

Upper Torso Mass:	m_3	=	48/32.2 lb sec^2/ft
		=	1.49 lb sec^2/ft
Spring Rates:	k_3	=	2400 to 6300 lb/ft
Undamped Natural Frequencies:	ω_3	=	40 to 65 rads/sec
Damping Ratio:	$\bar{c}_3$	=	.075 to .3 (-)
Damping Rates:	2K	=	13.2 to 52.8 lb sec/ft

These values were varied in the ranges given in an attempt to match measured impedance curves such as those shown in figures 11 and 12. The mass was fairly readily definable and so was not varied. The spring rate k_3 was varied across a range representing the spread of observed data. The damping was varied over a much wider range both to observe the effect of the change and because experimental measurements vary widely.

THE VISCERAL MODE

Goldman and Von Gierke (ref. 1) have pointed out that "one of the most important subsystems of the body, which is excited in the standing and sitting position as well as in the lying position, is the thorax-abdomen system. The abdominal viscera have a high mobility due to the very low stiffness of the diaphragm and the air volume of the lungs and the chest wall behind it. Under the influence of both longitudinal and transverse vibration of the torso, the abdominal mass vibrates in and out of the thoracic cage. Vibrations take place in other than the (longitudinal) direction of excitation; during the phase of the cycle when the abdominal contents swing toward the hips, the abdominal wall is stretched outward and the abdomen appears larger in volume; at the same time, the downward deflection of the diaphragm causes a decrease of the chest circumference. At the other end of the cycle the abdominal wall is pressed inward, the diaphragm upward and the chest wall is expanded. This periodic displacement of the abdominal viscera has a sharp resonance between 3 and 3.5 Hz. The oscillations of the abdominal mass are coupled with the air oscillations of the mouth-chest system."

Weis and Mohr (ref. 12) have used cineradiographic analysis to record the dynamic deflection of visceral components during and after a positive spinal impact in the seated position. They show the deflection time history of the diaphragm as a typical example. If this is regarded (for the moment) as a single-degree-of-freedom system, then the apparent damping and frequency can be determined from the overshoot above the statically deflected position or datum, measured from the maximum downward deflection position, using the equation

$$\text{Overshoot Ratio, OR} = \frac{\text{overshoot above datum}}{\text{datum}} = 1 + e^{-\pi \bar{c}_2 / \eta_2} \qquad (31)$$

where $\eta_2 = \sqrt{1 - \xi_2^2}$ and subscript 2 refers to the visceral system.

$\pi \bar{c}_2 / \eta_2 =$

(The relationship between $\bar{c}_2$ and $\pi \bar{c}_2 / \eta_2$ is plotted in figure 20.)

When this is done, the following results are obtained:

	Subject Tense	Subject Relaxed
Overshoot Ratio, OR (-)	1.063 } from ref. 12	1.212 } from ref. 12
Apparent frequency $\lambda/2\pi$ (Hz)	9.68 }	6.37 }
$\pi \bar{c}_2 / \eta_2 =$	2.77	1.554
$\bar{c}_2$ (from fig. 20) (-)	0.66	0.44
Undamped natural frequency $\omega_2/2\pi = f\,(2\pi, \bar{c}_2)$ (Hz)*	12.0	7.1

The apparent stiffness is therefore much greater than is indicated by the shake table measurements of Coermann et al (ref. 7), indicating, at first sight, considerable nonlinearity in the visceral springs. On the other hand, the apparent frequencies are of the same order

*See figure 22 of ref. 8

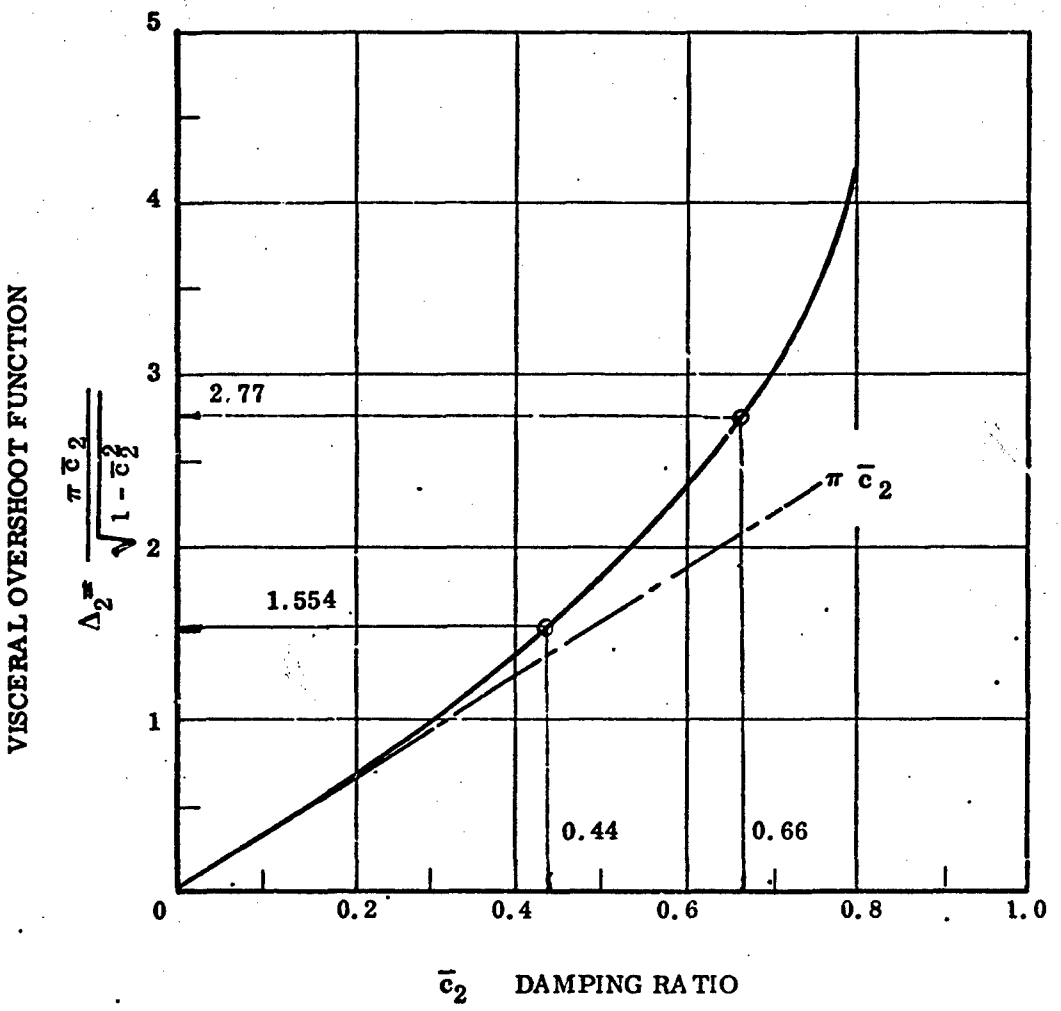

Figure 20. The Visceral Overshoot Function $\frac{\pi \bar{c}_2}{\eta_2} = \frac{\pi \bar{c}_2}{\sqrt{1-\bar{c}_2^2}}$.

as the spinal mode, so that the Weis and Mohr measurements of the diaphragm motion may be showing the "whole body" response with some modulation due to visceral movements with respect to the rest of the (deforming) body. In this report the latter interpretation is assumed to apply. This means that the frequency of the visceral mode must be taken from the small amplitude measurements of Coermann et al (ref. 7), and the value initially selected is

$$\omega_2 = 20.4 \text{ rads/sec} \tag{31A}$$

For an assumed visceral weight of = 15 lbs. this corresponds to a spring rate given by:

$$k_2 \quad \omega_2^2 \, m_2 = 20.4^2 \times \frac{15.0}{32.2} = 194 \text{ lb/ft} \tag{31B}$$

There is no simple and direct way to determine what damping factor to use. If the value used is too low, however, the visceral mode shows up as a peak on the impedance plot. No such peak is observed in the experimental data. Thus, the visceral damping is adjusted to the minimum value needed to surpress the visceral peak in the impedance magnitude; values of $\bar{c}$ of .125, .25 and .5 were used. Clearly, the representation of the viscera as being simply suspended from the upper torso is a gross oversimplification as there must be a considerable visceral load acting directly on the pelvic mass.

Thus, for the visceral mode the following values were adopted for this study:

Mass:	$m_2 = 15/32.2$ lb sec^2/ft	
Spring Rate:	$k_2 = 194$ lb/ft	
Undamped Natural Frequency:	$\omega_2 = 20.4$ rads/sec	(31C)
Damping Ratio:	$\bar{c}_2 = .125, .25, .5$ (-)	
Damping Rate:	$2K_2 = 2.375, 4.75, 9.5$ lb sec/ft	

THE NECK MODE

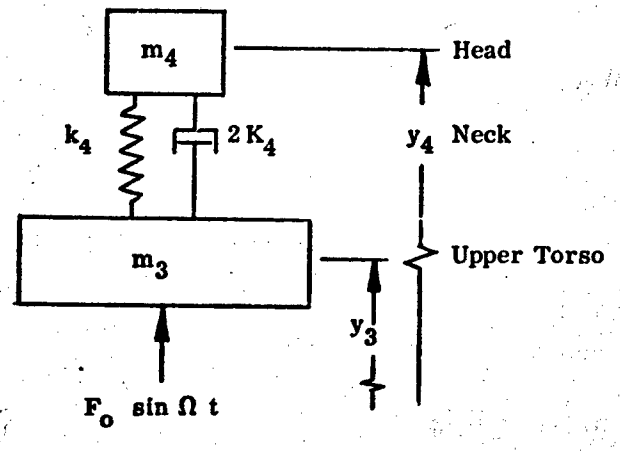

Figure 21. Idealization of the Neck Mode

The transmissability experiments of Dieckmann (ref. 13) indicate a head/shoulder resonance of 3.5 at 30 Hz, for a seated, sinusoidally excited subject,

$$\text{i.e.,} \quad \frac{(\ddot{y}_4)_{max}}{(\ddot{y}_3)_{max}} = 3.5$$

if the motion is sinusoidal. The frequency of 30 Hz is so much greater than the values derived for the visceral and spinal modes that preliminary calculations can be based upon the simplified two mass system of figure 21.

Thus

$$\left.\begin{aligned} m_3 \ddot{y}_3 &= F_o \sin \Omega t - (2K_4 \dot{\delta}_4 + k_4 \delta_4) \\ m_4 \ddot{y}_4 &= (2K_4 \dot{\delta}_4 + k_4 \delta_4) \end{aligned}\right\} \quad (3z)$$

And since $\ddot{y}_4 = \ddot{y}_3 - \ddot{\delta}_4$ the second equation becomes

$$\ddot{y}_3 = \ddot{\delta}_4 + 2c_4 \dot{\delta}_4 + \omega_4^2 \delta_4 = \ddot{y}_4 + 2\zeta_4 \omega_4 \dot{\delta}_4 + \omega_4^2 \delta_4$$

$$\therefore \ddot{\delta}_4 + 2c_4 \dot{\delta}_4 + \omega_4^2 \delta_4 = \frac{F_o}{m_3} \sin \Omega t - \frac{m_4}{m_3} (2c_4 \dot{\delta}_4 + \omega_4^2 \delta_4) \quad (33)$$

or $$\ddot{\delta}_4 + 2 c_4 \left[1 + \phi\left(\tfrac{4}{3}\right)\right] \dot{\delta}_4 + \omega_4^2 \left[1 + \phi\left(\tfrac{4}{3}\right)\right] \delta_4 = \phi\left(\tfrac{4}{3}\right) \frac{F_0}{m_4} \sin \Omega t \tag{34}$$

where $$\phi\left(\tfrac{4}{3}\right) = \frac{m_4}{m_3}$$

Thus, the apparent undamped frequency is

$$\omega_{A_4} = \omega_4 \sqrt{1 + \phi\left(\tfrac{4}{3}\right)}$$

and the apparent damping coefficient is

$$c_{A_4} = c_4 \left[1 + \phi\left(\tfrac{4}{3}\right)\right]$$

The apparent damping ratio is

$$\bar{c}_{A_4} = \frac{c_{A_4}}{\omega_{A_4}} = \bar{c}_4 \sqrt{1 + \phi\left(\tfrac{4}{3}\right)}$$

The response of equation (34) will be

$$\delta_4 = \frac{\frac{\phi(\frac{4}{3}) F_0}{m_4 \omega_{A_4}^2} \sin(\Omega t + \psi_4)}{\sqrt{\left[1 - \left(\frac{\Omega}{\omega_{A_4}}\right)^2\right]^2 + 4 \bar{c}_{A_4}^2 \left(\frac{\Omega}{\omega_{A_4}}\right)^2}} = \frac{\phi(\frac{4}{3}) F_0}{m_4 \omega_{A_4}^2} q_{A_4} \sin(\Omega t + \psi_4) \tag{35}$$

$$q_{A_4} = \left\{\left[1 - \left(\frac{\Omega}{\omega_{A_4}}\right)^2\right]^2 + 4 \bar{c}_{A_4}^2 \left(\frac{\Omega}{\omega_{A_4}}\right)^2\right\}^{-1/2}$$

$$= \frac{\phi(\frac{4}{3}) F_0}{k_4} q_{A_4} = \phi\left(\tfrac{4}{3}\right) \delta_{4_{ss}} q_{A_4}$$

where $\delta_{4_{ss}}$ is the steady state deflection of the neck spring.

This solution may be expressed in terms of $(\ddot{y}_4)_{max}$ / $(\ddot{y}_3)_{max}$ and since, from equations (33) and (35)

$$(\ddot{y}_3)_{max} = \frac{\phi(\frac{4}{3}) F_0}{m_4} q_{A_4} \frac{\omega_4^2}{\omega_{A_4}^2} \sqrt{\left[1 - \left(\frac{\Omega}{\omega_4}\right)^2\right]^2 + 4 \bar{c}_4^2 \left(\frac{\Omega}{\omega_4}\right)^2}$$

$$= \frac{\phi(\frac{4}{3}) F_0 q_{A_4}}{\left[1 + \phi(\frac{4}{3})\right] m_4 q_4} \tag{36}$$

Similarly, since $\ddot{y}_4 = 2 c_4 \dot{\delta}_4 + \omega_4^2 \delta_4$ from equation (32), and, from equation (35)

$$= \frac{\phi(\frac{\omega}{3}) F_0}{m_4} g_{n_4} \frac{\omega_4^2}{\omega_{n_4}^2} \left\{ 2 \bar{c}_4 \frac{\Omega}{\omega_4} \cos(\Omega t + \psi) + \sin(\Omega t + \psi) \right\}$$

and $$(\ddot{y}_4)_{max} = \frac{\phi(\frac{\omega}{3})}{\left[1 + \phi(\frac{\omega}{3})\right]} \frac{F_0}{m_4} g_{n_4} \sqrt{1 + 4 \bar{c}_4^2 \left(\frac{\Omega}{\omega_4}\right)^2} \qquad (37)$$

$$\frac{(\ddot{y}_4)_{max}}{(\ddot{y}_3)_{max}} = g_4 \sqrt{1 + 4 c_4^2 \left(\frac{\Omega}{\omega_4}\right)^2}$$

$$= \frac{\sqrt{1 + 4 c_4^2 \left(\frac{\Omega}{\omega_4}\right)^2}}{\sqrt{\left[1 - \left(\frac{\Omega}{\omega_4}\right)^2\right]^2 + 4 \bar{c}_4^2 \left(\frac{\Omega}{\omega_4}\right)^2}} \qquad (38)$$

This function is discussed in Appendix I, where it is thought in figure I.2 that the amplitude ratio of 3.5 corresponds to a damping coefficient ratio of

$$c_4 = 0.15 \qquad (39)$$

and to resonant frequency/natural frequency ratio of

$$\frac{\Omega_{max}}{\omega_4} = .979$$

Thus, if resonance occurs at 30 Hz the frequency ω_4 is given by:

$$\omega_4 = \frac{30.0}{0.979} = 30.6 \text{ Hz} = 192.3 \text{ rads/sec} \qquad (40)$$

and the corresponding damping force is:

$$F_{D_4} = 2 \bar{c}_4 \omega_4 m_4 \dot{\delta}_4 = \frac{2 \times .15 \times 192.3 \times 12}{32.17} = 10.75 \dot{\delta}_4 \qquad (41)$$

Taking a typical head weight of 12.0 lbs, the spring rate corresponding to ω_4 is therefore

$$k_4 = \omega_4^2 m_4 = \frac{12.0}{32.2} \times (192.3)^2 = 14,000 \text{ lb/ft} \qquad (42)$$

Thus, for the head and neck mode the following values were selected:

Mass:	m_4	=	$12/32.2$ lb sec^2/ft
Spring Rate:	k_4	=	14,000 lb/ft
Undamped Natural Frequency:	ω_4	=	192.3 rads/sec (43)
Damping Ratio:	$\bar{c}_4$	=	0.15
Damping Rate:	$2K_4$	=	10.75 lb sec/ft

These quantities were not varied in the subsequent analysis as they seem to be fairly well established (in ref. 13) and the head and neck are remote enough from the driving force for their influence on the measured impedance to be small.

IMPEDANCE CALCULATIONS FOR AN EQUIVALENT LINEAR MODEL

Having now an approximate idea of the magnitudes of most of the coefficients for the four-degree-of-freedom model, it is instructive to determine the driving point impedance of the model and compare the results with the existing experimental data. By systematically changing the model coefficients, it is then possible to obtain better agreement with experment, and to study the influence of the individual elements. This has been done, and some of the more interesting results are presented in figures 22 and 51 inclusive. The effect of the head and visceral masses on the driving point impedance could only be minor, so these masses, springs and dampers were not varied in this analysis, except for the visceral damping discussed earlier. Neither was the mass distribution varied as this was considered to be well enough established.

The fixed values were the following

Masses:	Pelvic	m_1	=	64.0/32.2 lb sec^2/ft
	Viscera	m_2	=	15.0/32.2 lb sec^2/ft
	Upper Torso	m_3	=	48.0/32.2 lb sec^2/ft
	Head	m_4	=	12.0/32.2 lb sec^2/ft
Springs:	Viscera/Upper Torso	ω_2	=	20.4 rads/sec (see eq. 31A)
	Head/Upper Torso	ω_4	=	192.3 rads/sec
		k_4	=	14,000 lb/ft (see eq. 41)
Dampers:	Head/Upper Torso	$\bar{c}_4$	=	.15 (see eq. 39)

and the variable values were varied according to table 5.

Figures 22 to 51 are plotted to the same scale as the experimentally measured values shown in figures 11 and 12. The closer that the analytical curve simulate the measured values of figures 11 and 12, the more representative the analytical model may be assumed to be.

The curves plotted were calculated using an analog simulation routine on a digital computer.

TABLE V

Variables Used in Linear Four-Degree-of-Freedom Model

Mode	2. Viscera	3. Spine		1. Buttocks	
Link	Damper	Spring	Damper	Spring	Damper
Parameter	$\bar{c}_2$	ω_3	$\bar{c}_3$	ω_1	$\bar{c}_1$
Units	--	rad/sec	--	rad/sec	--
Case No. 2 Fig 22	.25	59.1	.15	--	--
Case No. 3 Fig 23	.125	59.1	.075	39.55	.125
Case No. 4 Fig 24	.25	59.1	.15	39.55	.25
Case No. 5 Fig 24	.25	59.1	.15	47.5	.25
Case No. 6 Fig 25	.25	59.1	.15	55.5	.25
Case No. 7 Fig 25	.25	59.1	.15	63.2	.25
Case No. 8 Fig 26	.25	59.1	.15	198.0	.05
Case No. 9 Fig 27	.25	50.6	.15	39.55	.25
Case No. 10 Fig 28	.25	50.6	.15	39.55	.5
Case No. 11 Fig 29	.5	59.1	.15	39.55	.25
Case No. 12 Fig 30	.25	59.1	.3	39.55	.25
Case No. 13 Fig 31	.5	59.1	.3	39.55	.25
Case No. 14 Fig 32	.25	59.1	.15	47.5	.5
Case No. 15 Fig 33	.25	50.0	.15	47.5	.5
Case No. 16 Fig 34	.25	40.0	.15	47.5	.5
Case No. 17 Fig 35	.5	59.1	.15	47.5	.5
Case No. 18 Fig 36	.5	59.1	.15	44.0	.25
Case No. 19 Fig 37	.5	59.1	.15	44.0	.5
Case No. 20 Fig 38	.5	59.1	.15	47.5	.5
Case No. 21 Fig 39	.5	59.1	.15	51.0	.5
Case No. 22 Fig 40	.5	59.1	.15	47.5	.25
Case No. 23 Fig 41	.5	59.1	.15	47.5	.125
Case No. 24 Fig 42	.5	59.1	.15	--	--
Case No. 27 Fig 43	.5	65.0	.15	--	--
Case No. 28 Fig 44	.5	65.0	.125	--	--
Case No. 29 Fig 45	.5	65.0	.1	--	--
Case No. 30 Fig 46	.5	59.1	.11	47.5	.25
Case No. 31 Fig 47	.5	59.1	.15	108.0	.25
Case No. 32 Fig 48	.5	59.1	.15	80.0	.25
Case No. 33 Fig 49	.5	59.1	.15	120.0	.25
Case No. 34 Fig 50	.5	59.1	.15	140.0	.25
Case No. 35 Fig 51	.5	59.1	.15	160.0	.25

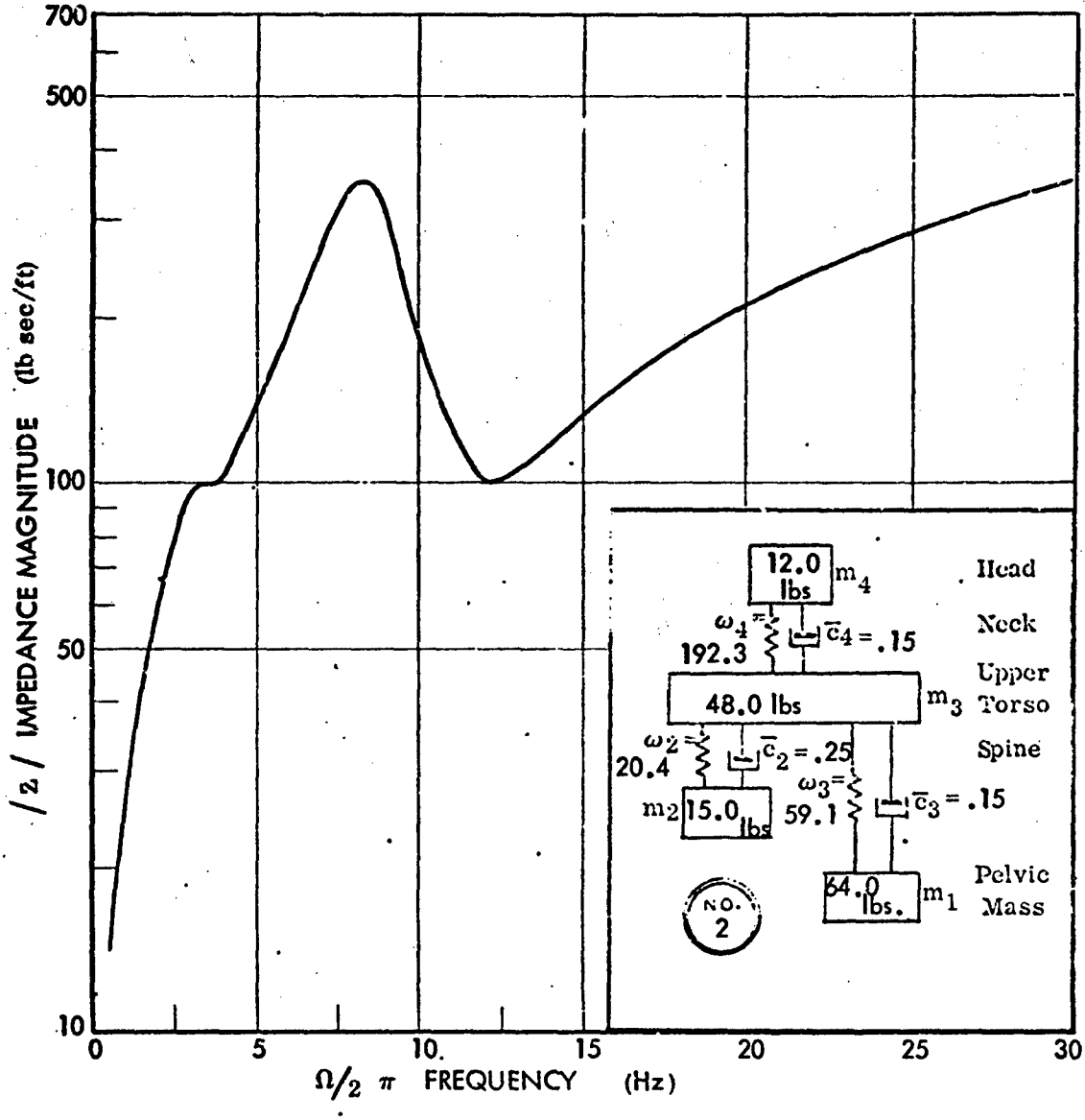

Figure 22. Four Mass System Without Buttock Damper and Spring, Case No. 2.

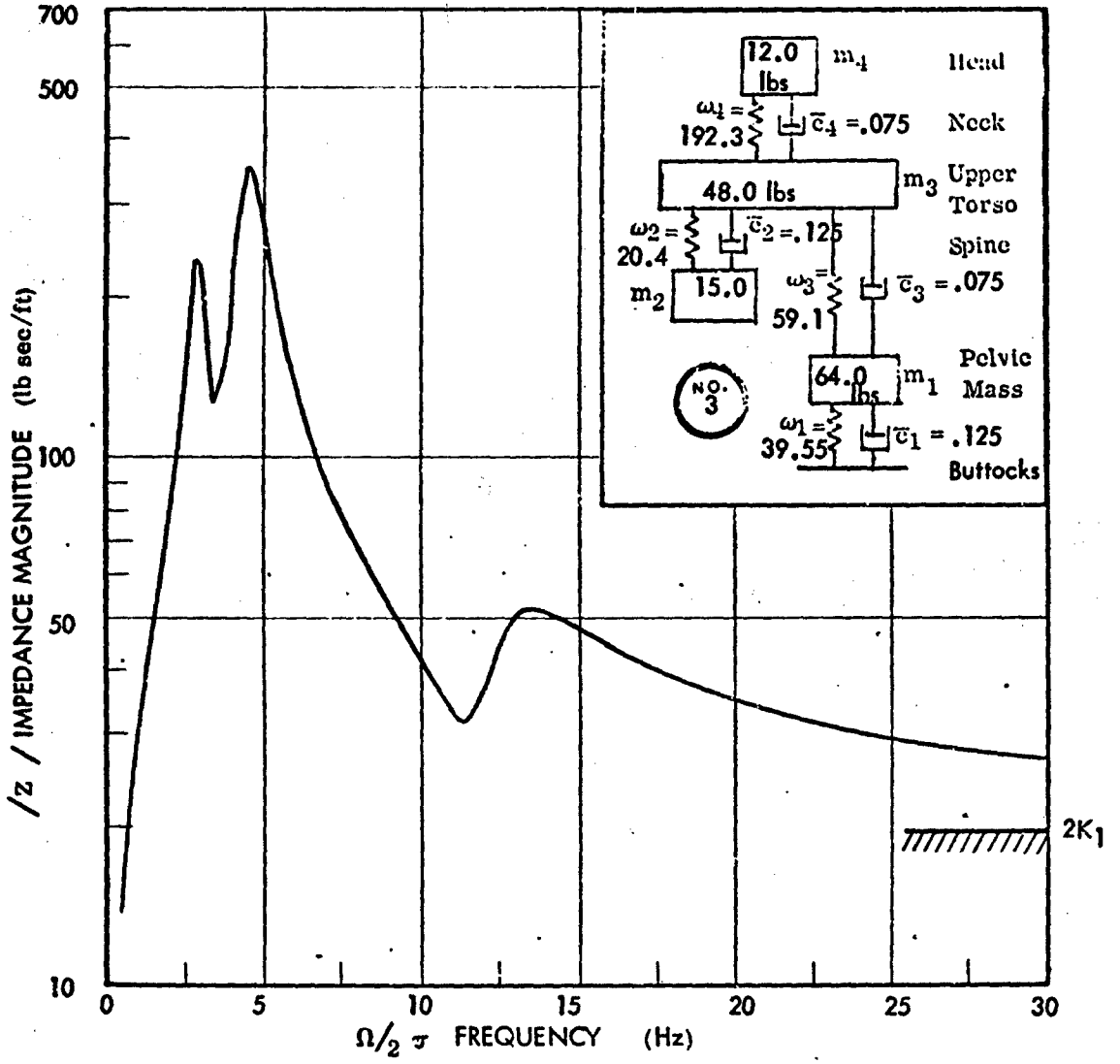

Figure 23. Four Mass System Case No. 3

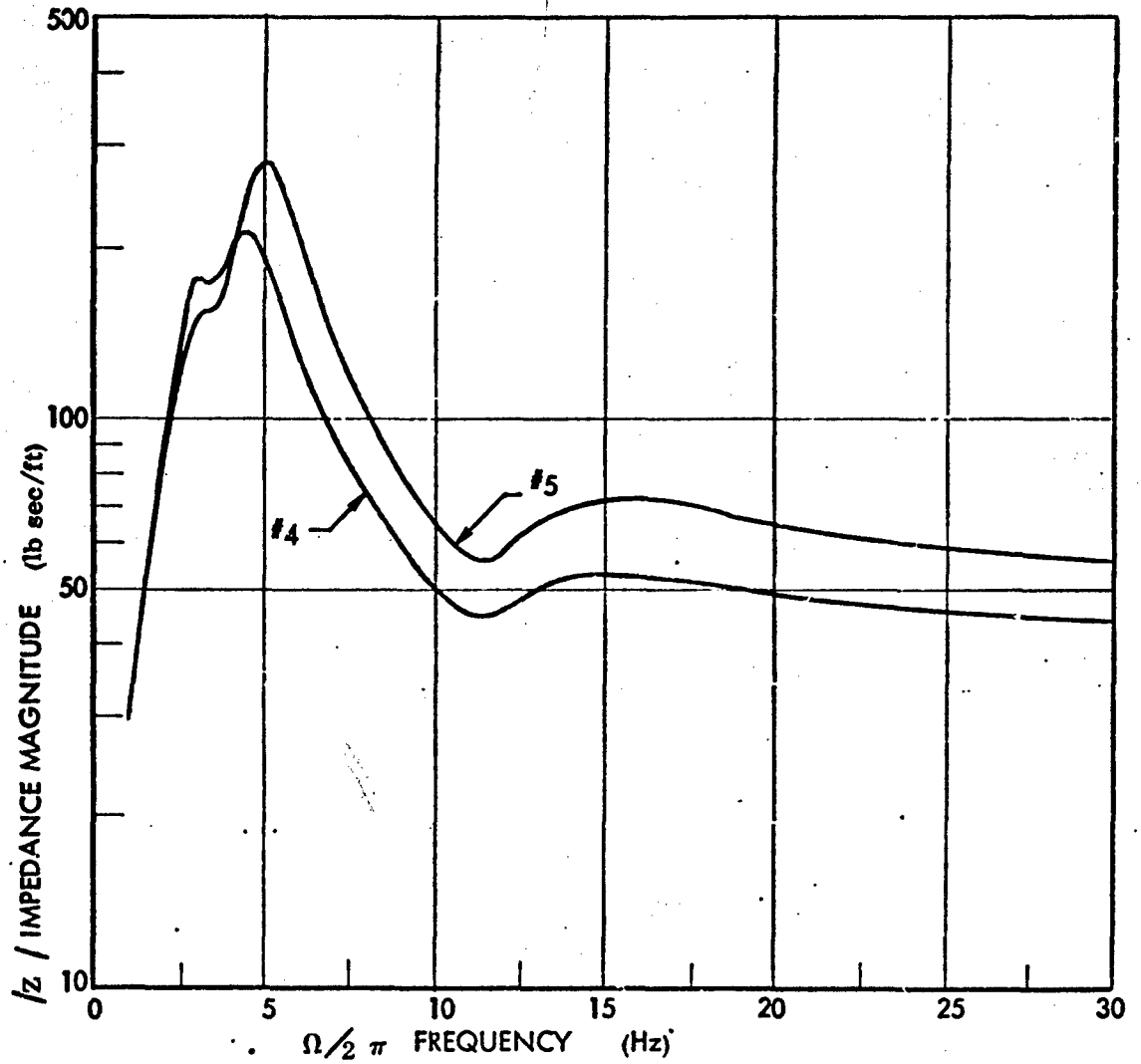

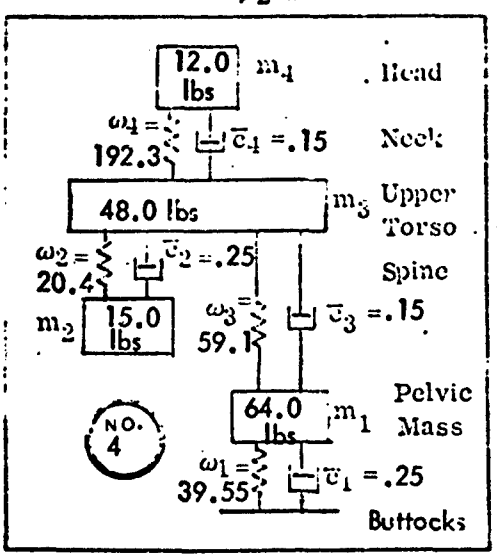

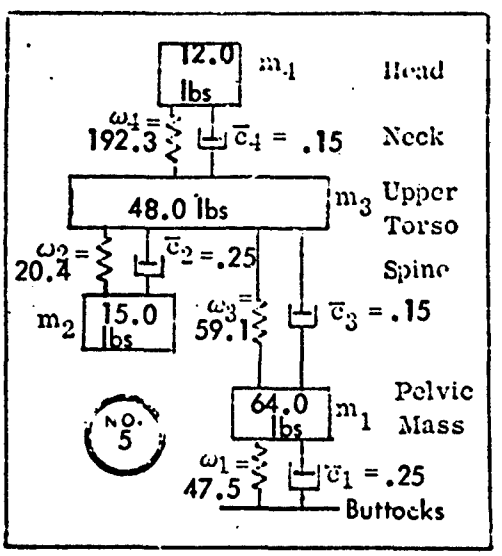

Figure 24. Four Mass Systems Cases Nos. 4 and 5

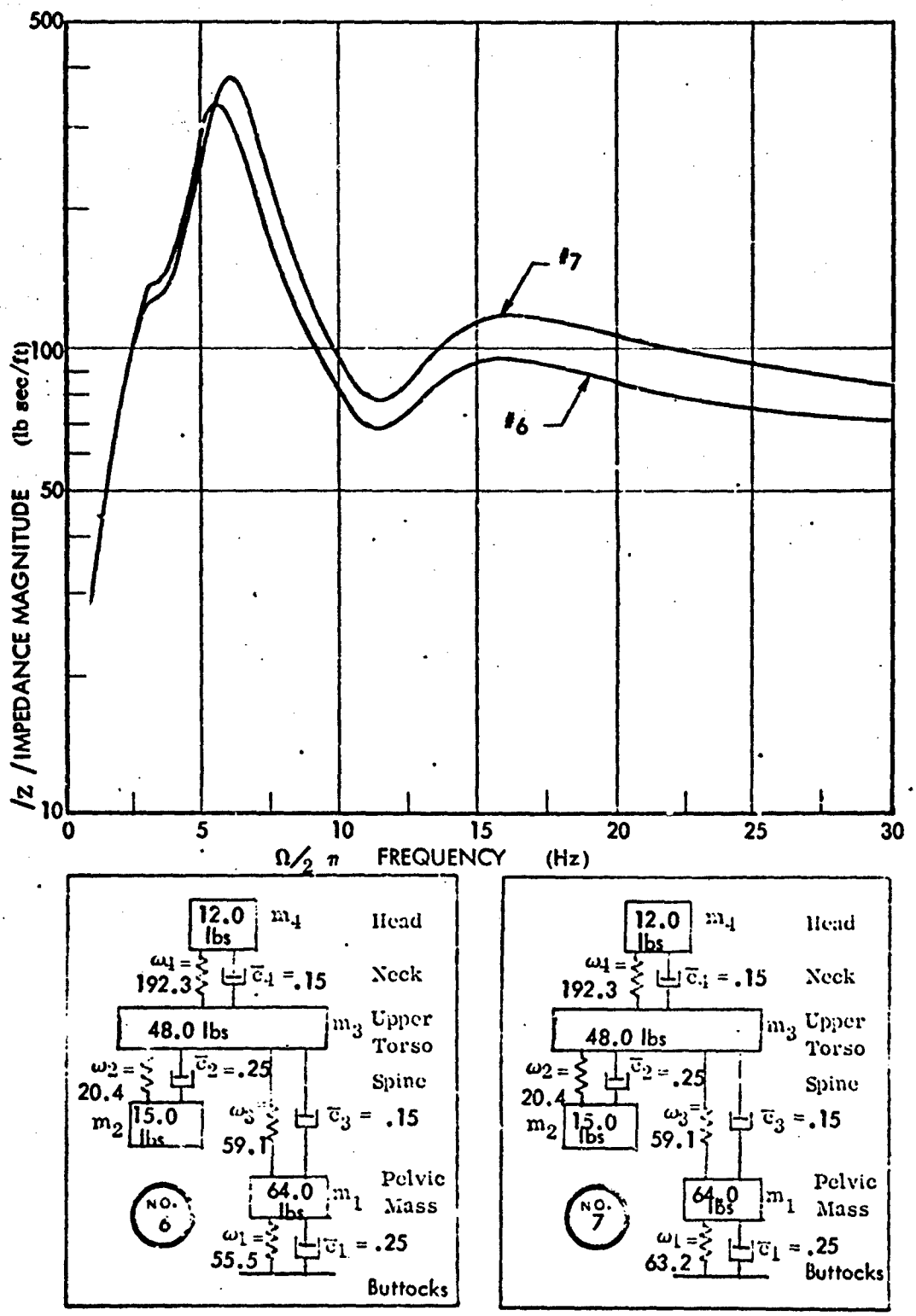

Figure 25. Four Mass Systems Cases Nos. 6 and 7

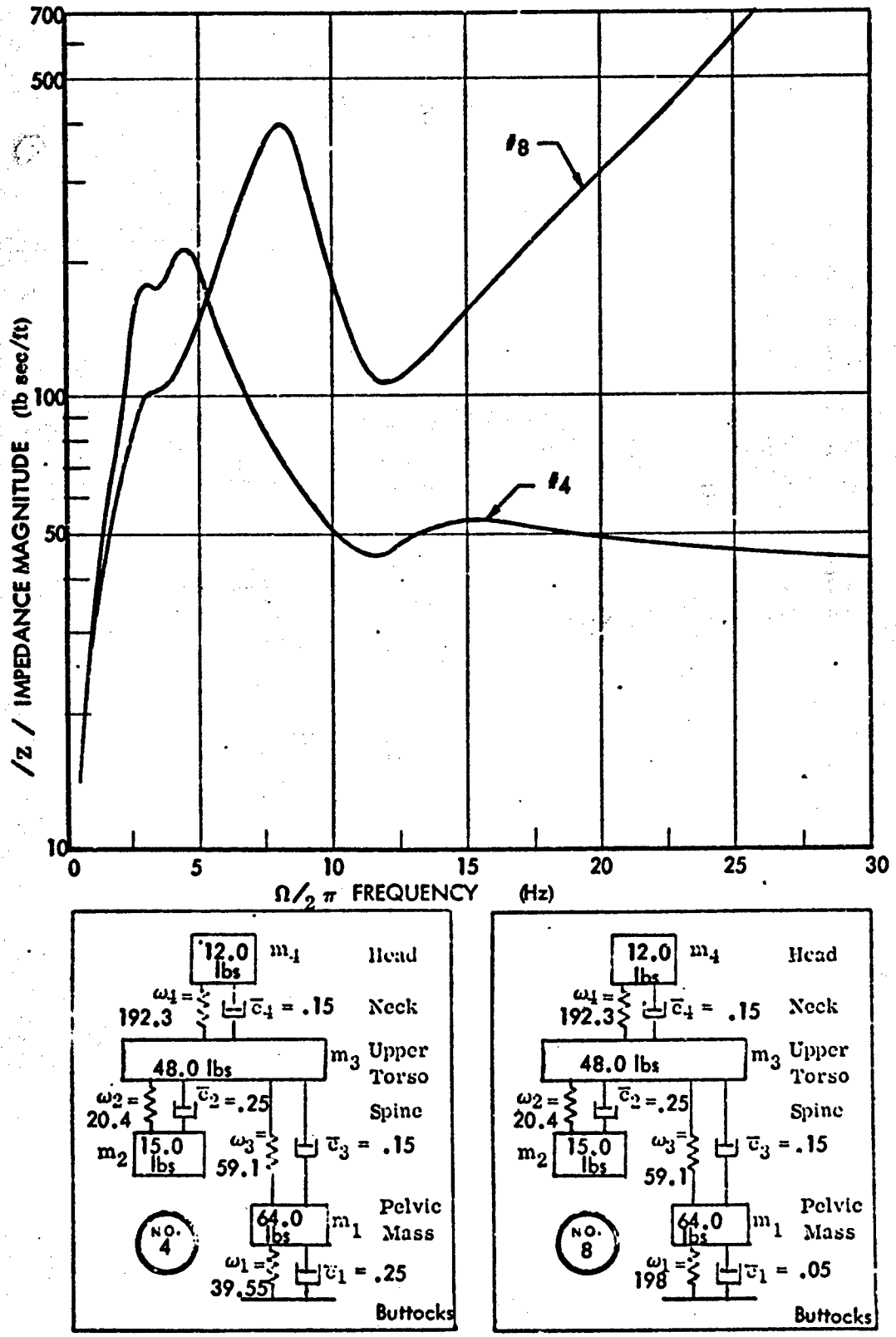

Figure 26. Four Mass Systems Case Nos. 4 and 8

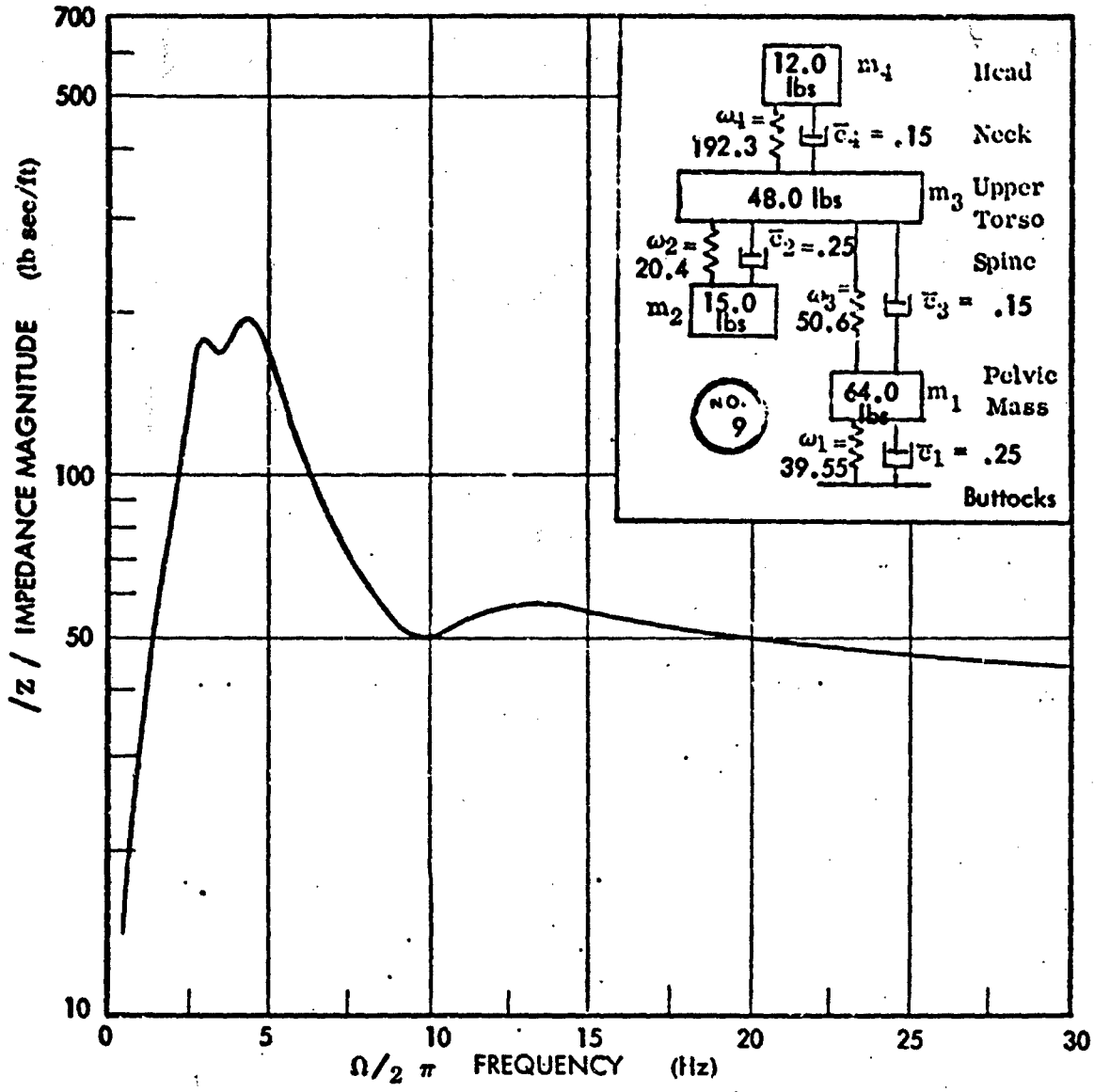

Figure 27. Four Mass Systems Case No. 9

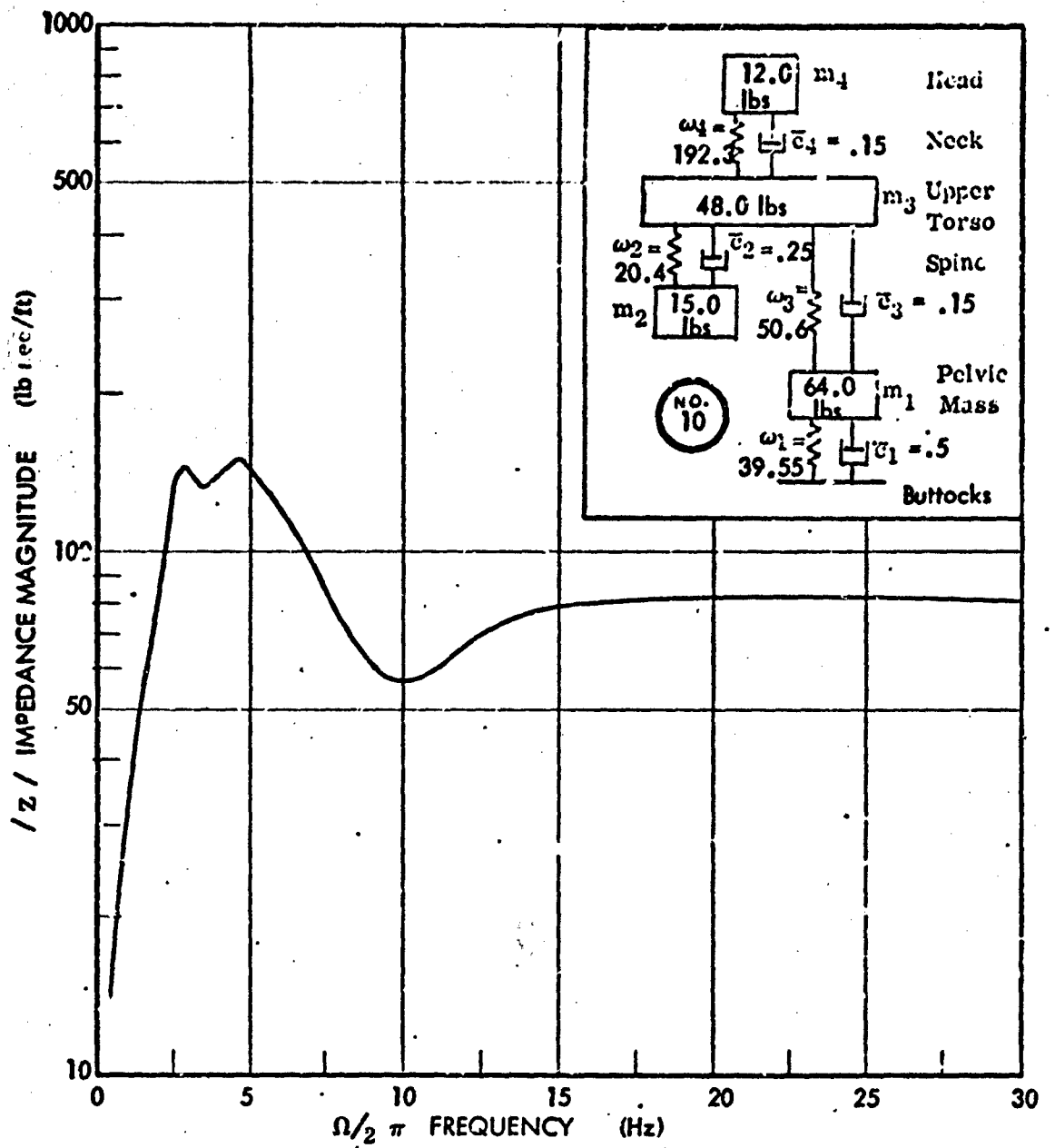

Figure 28. Four Mass System Case No. 10

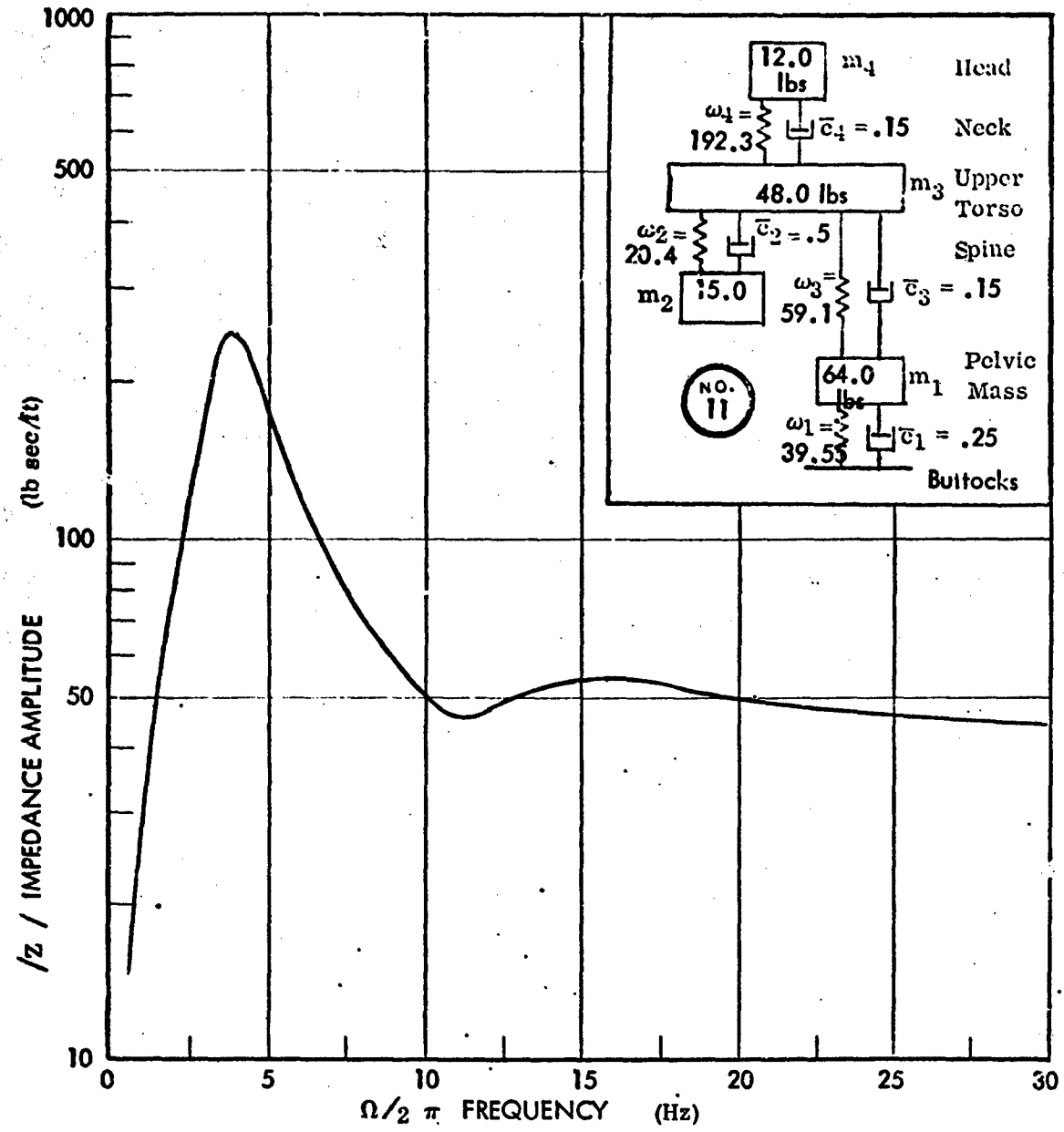

Figure 29. Four Mass Systems Case No. 11

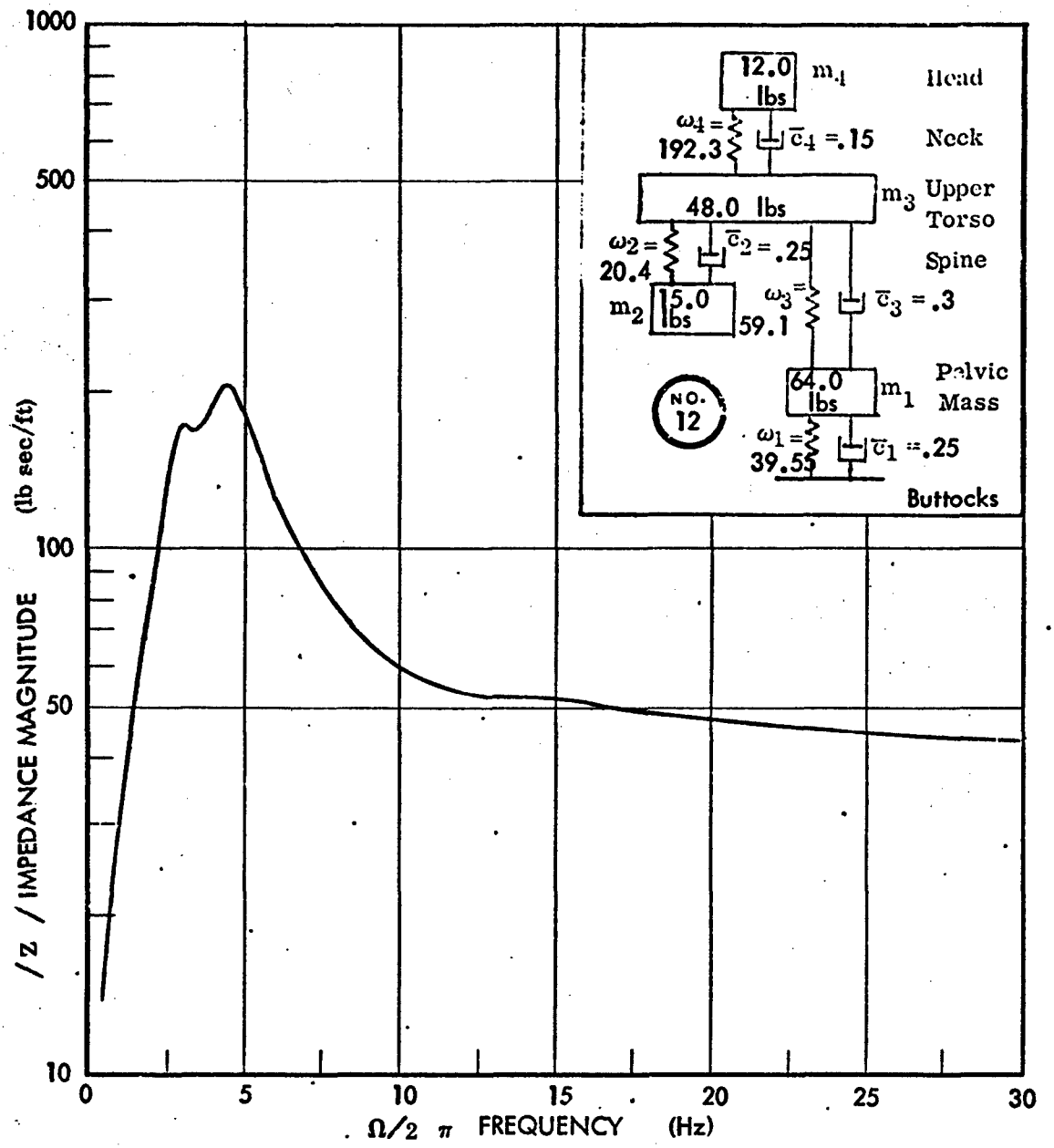

Figure 30. Four Mass Systems Case No. 12

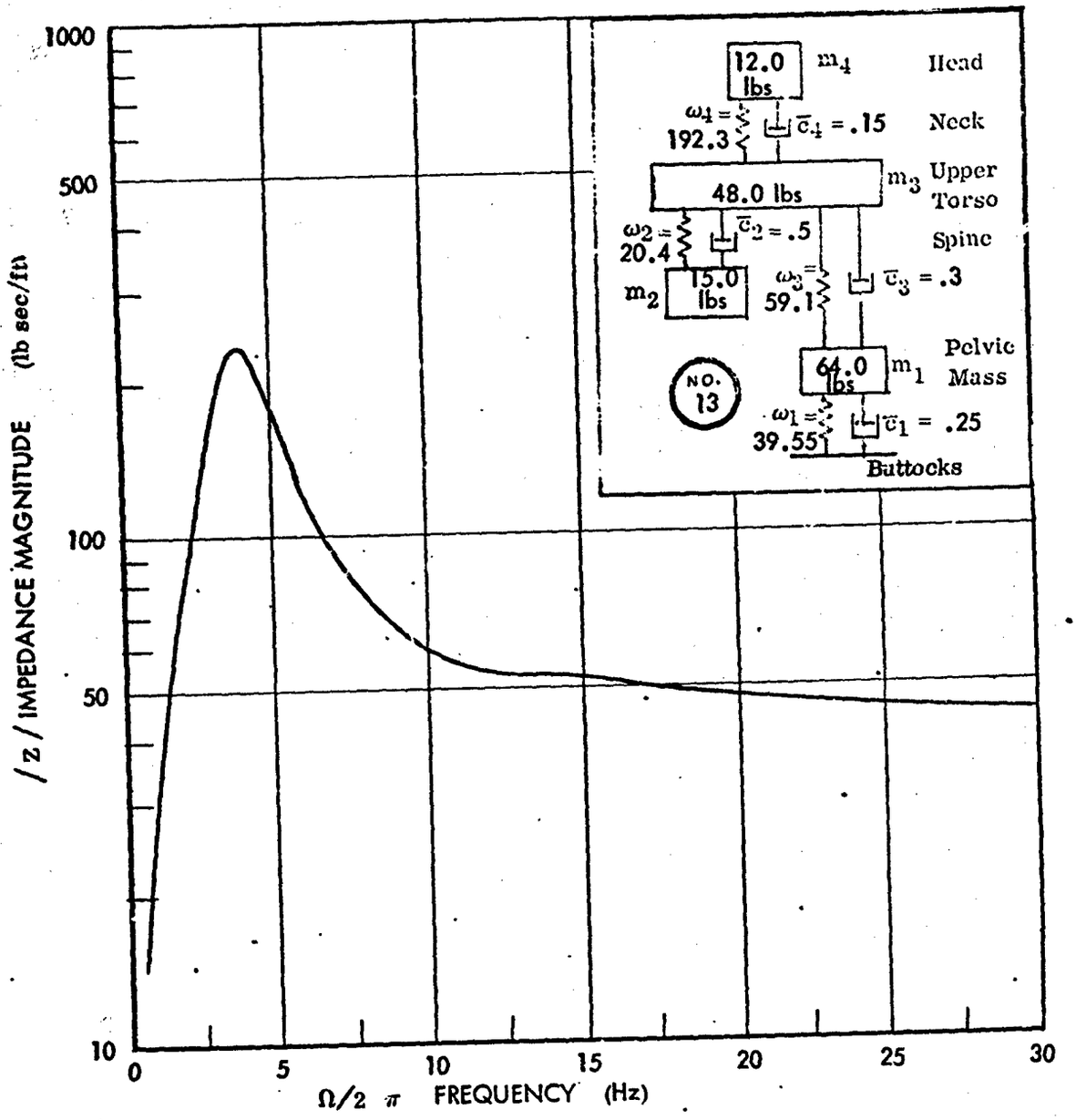

Figure 31. Four Mass Systems Case No. 13

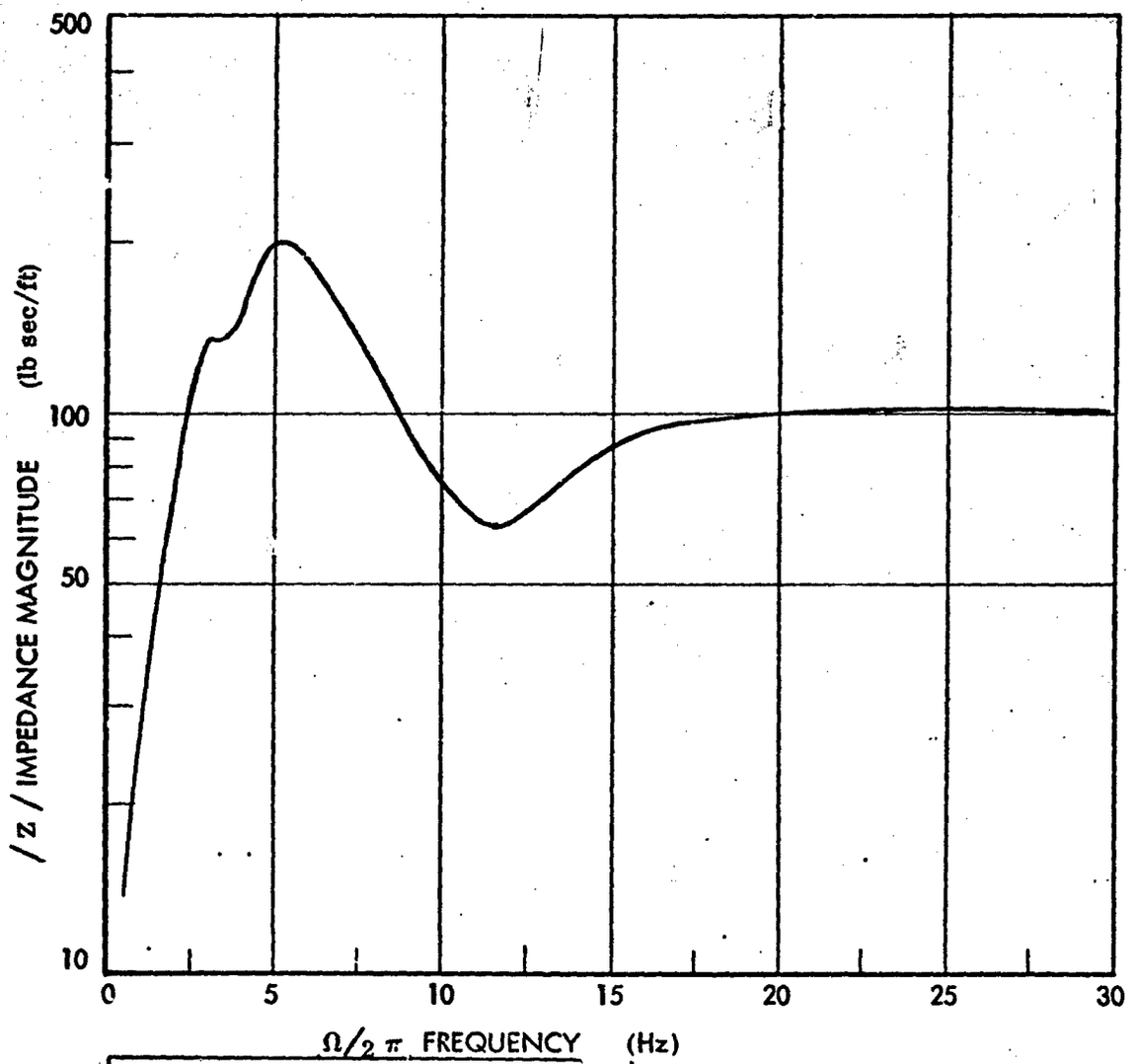

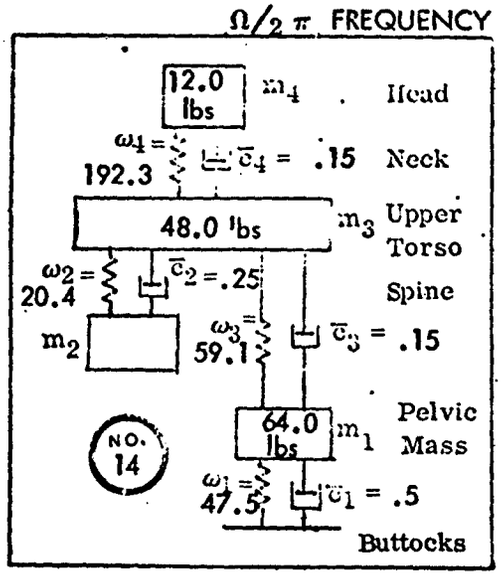

Figure 32. Four Mass Systems Case No. 14

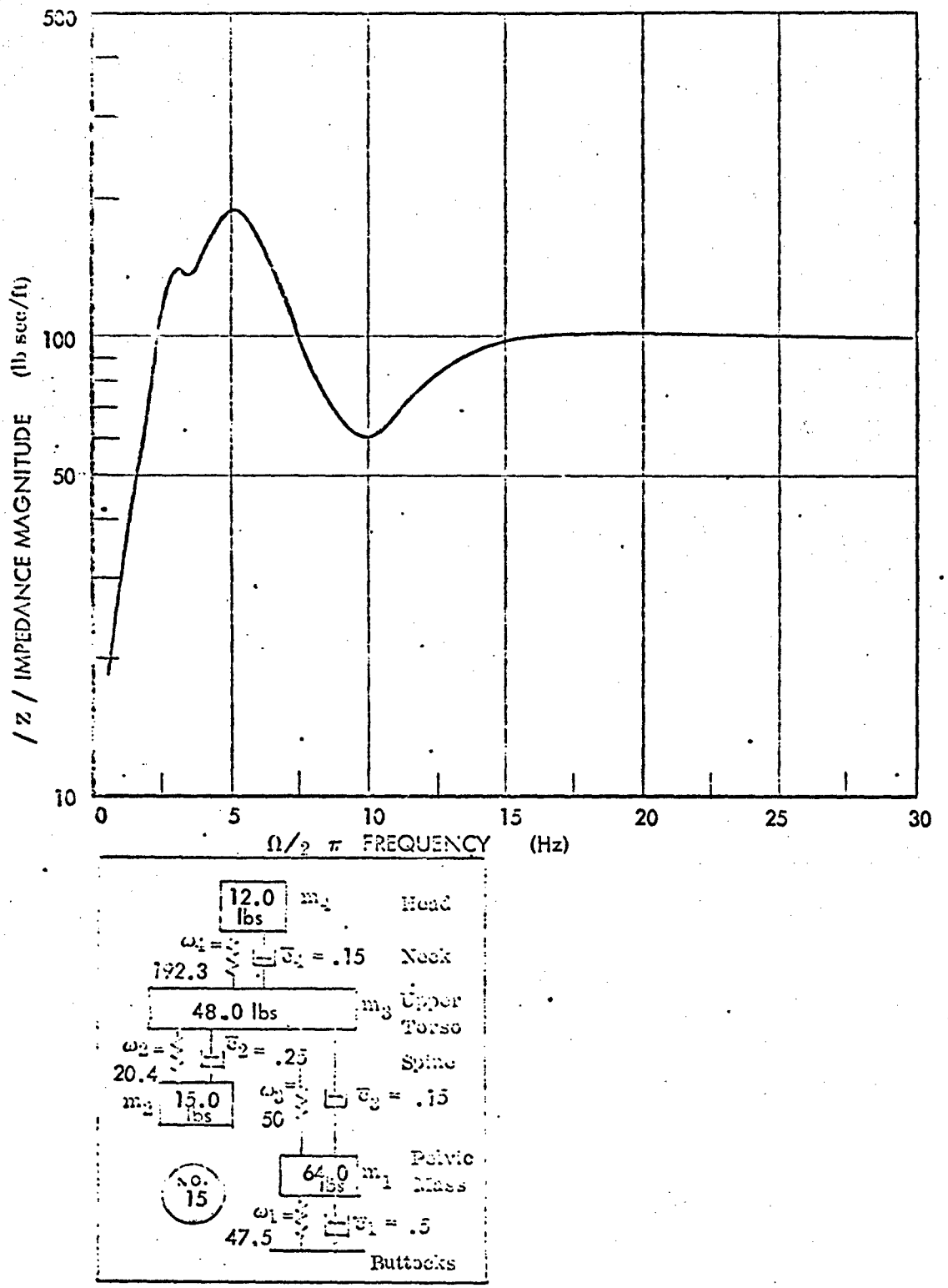

Figure 33. Four Mass Systems Case No. 15

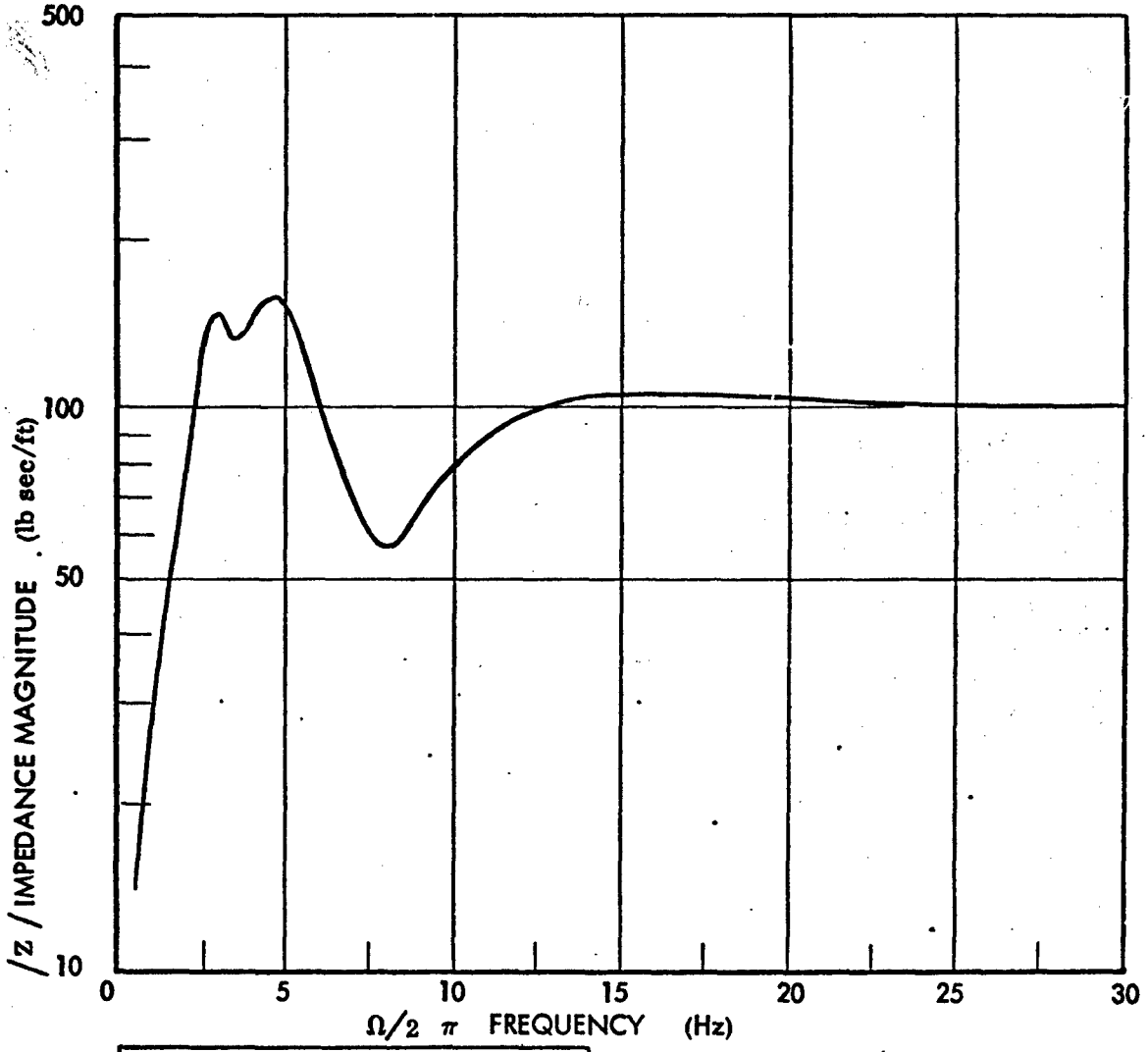

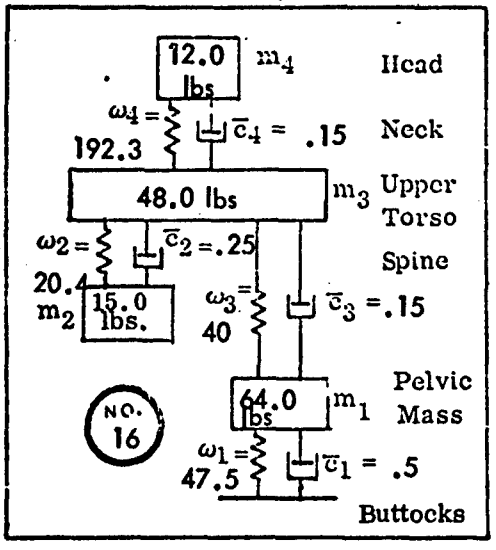

Figure 34. Four Mass Systems Case No. 16

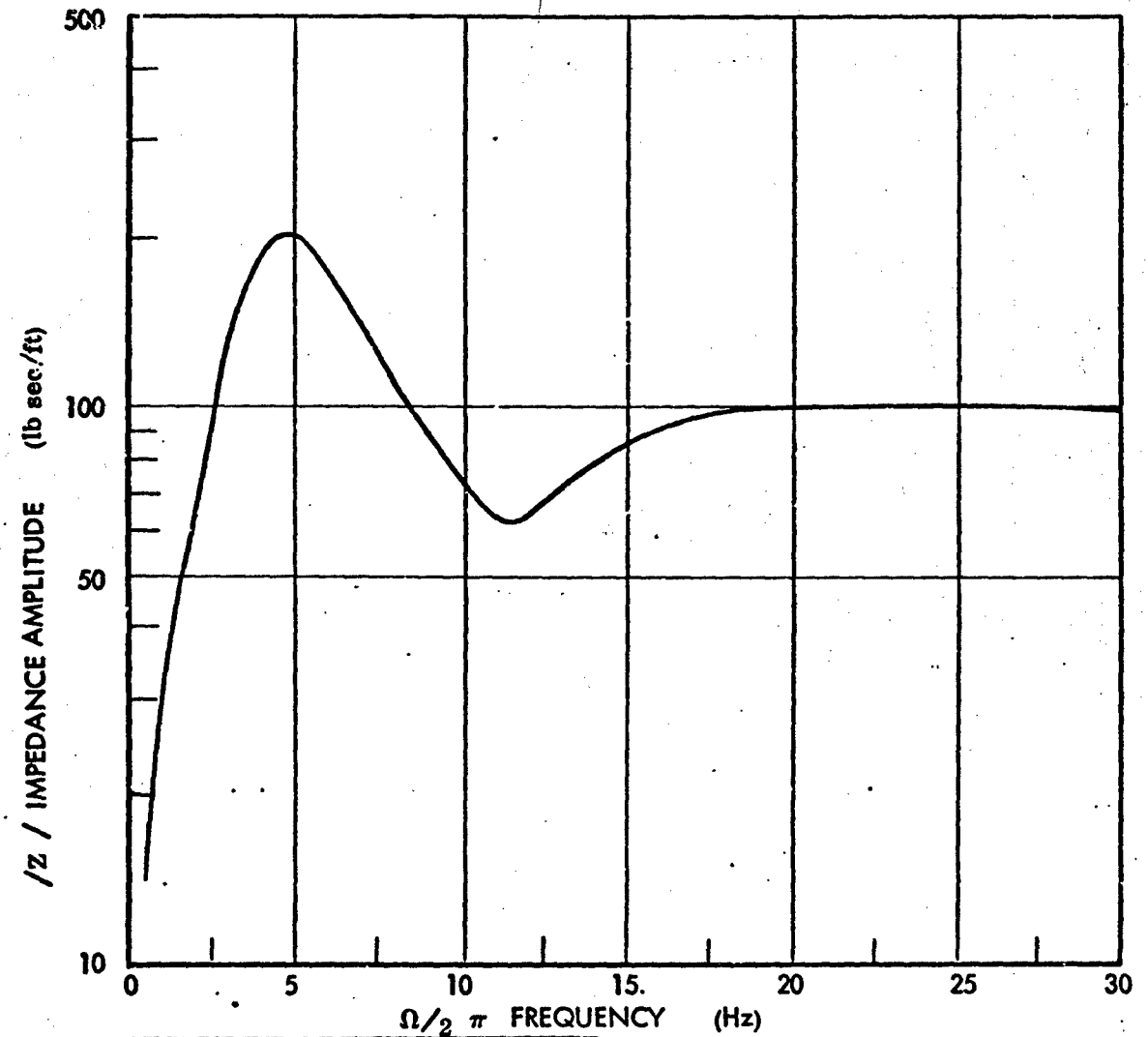

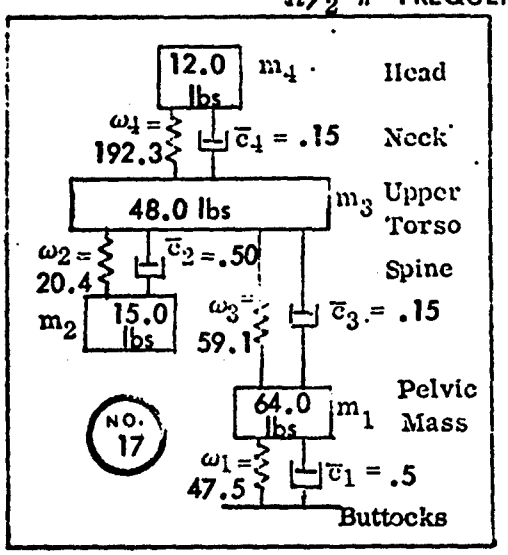

Figure 35. Four Mass Systems Case No. 17

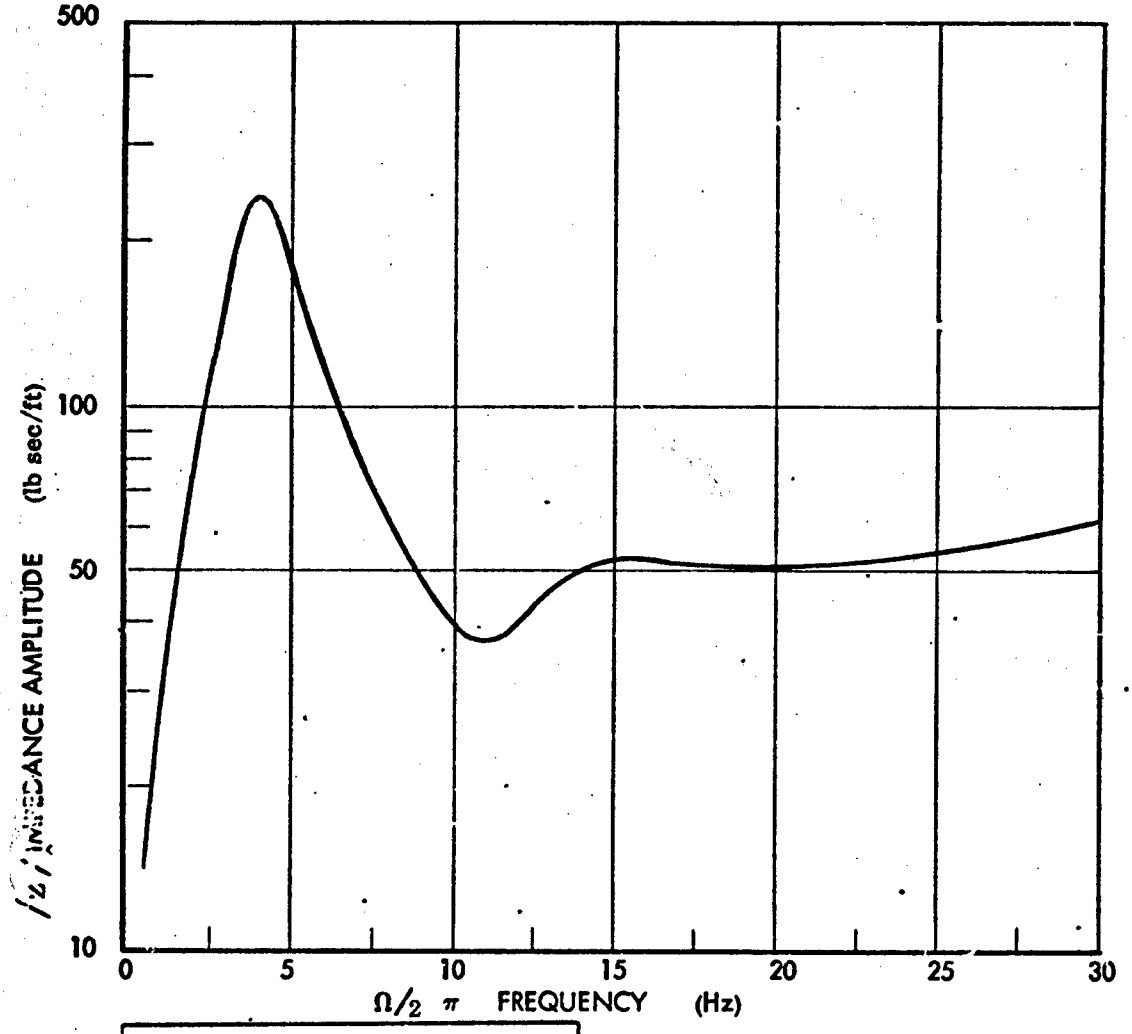

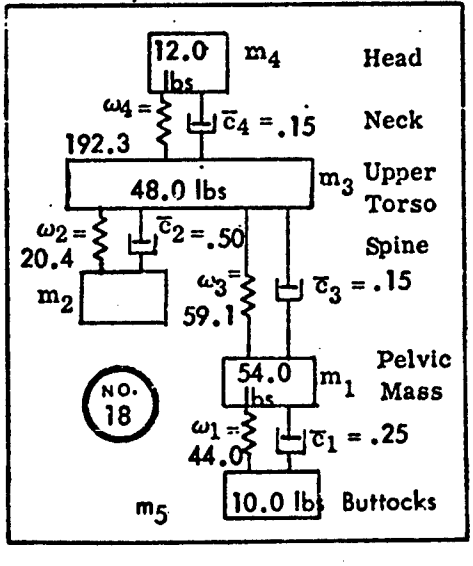

Figure 36. Four Mass Systems Case No. 18

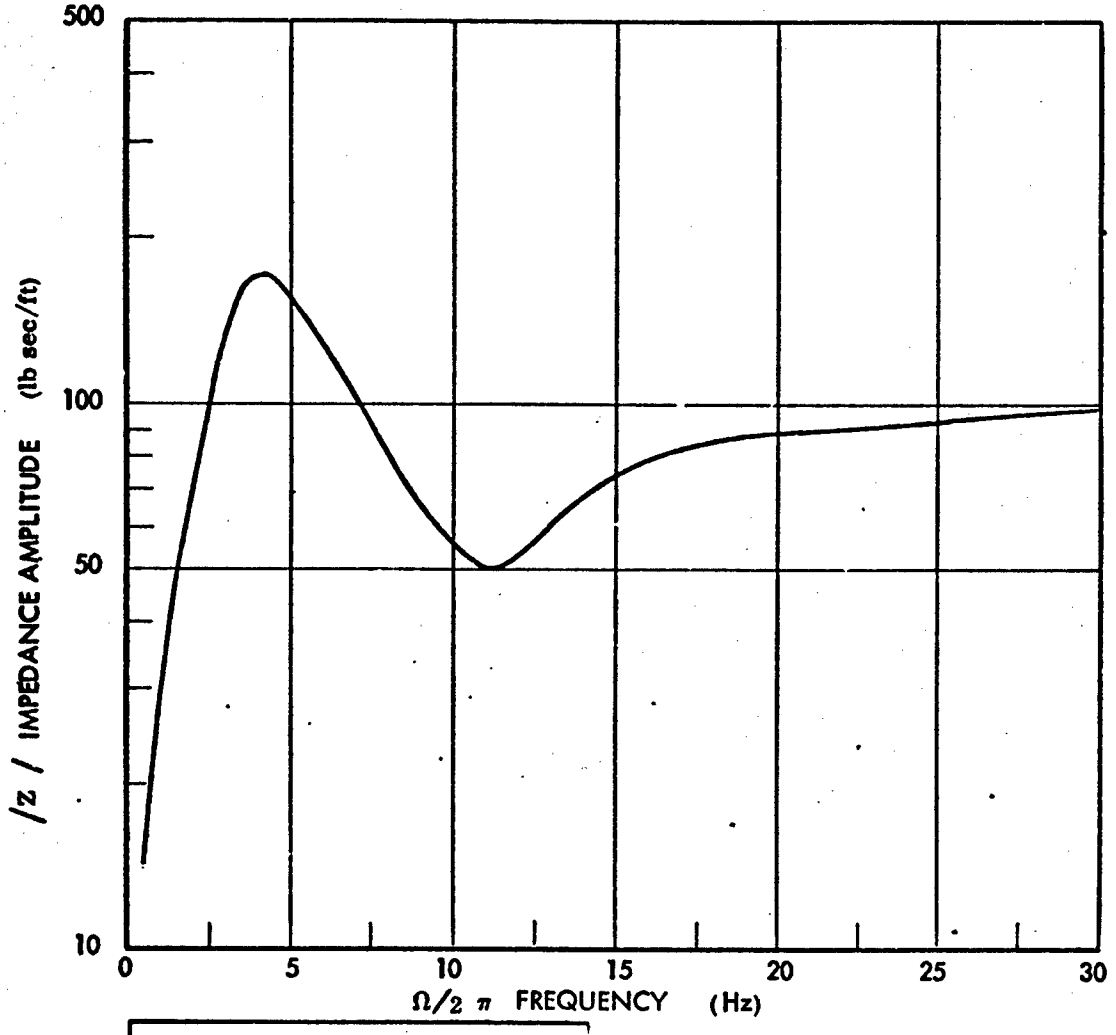

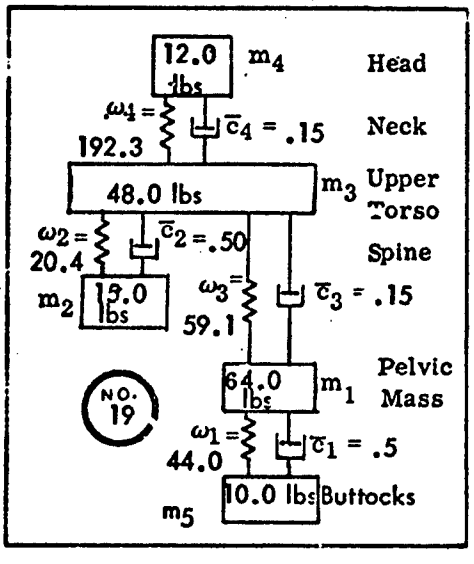

Figure 37. Four Mass Systems Case No. 19

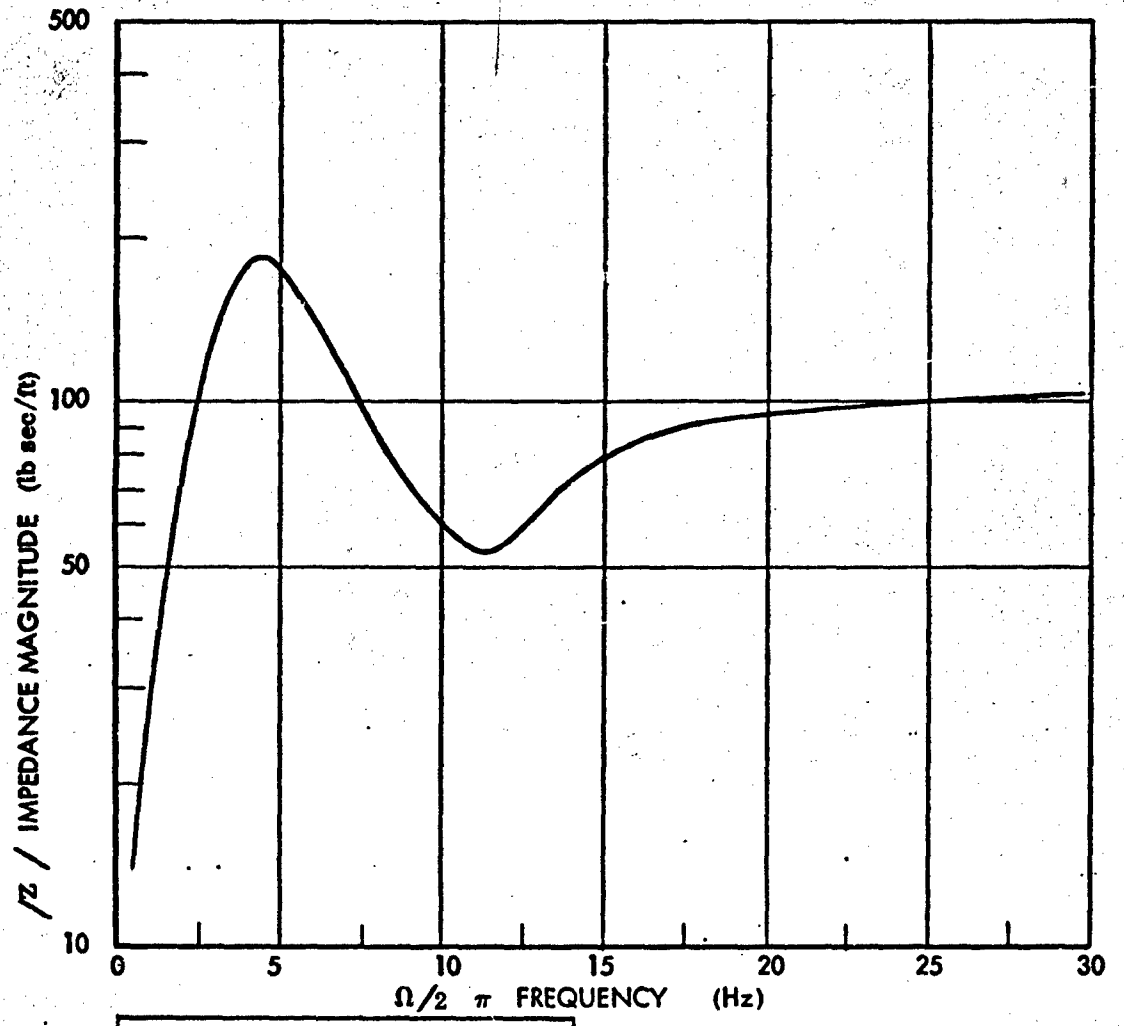

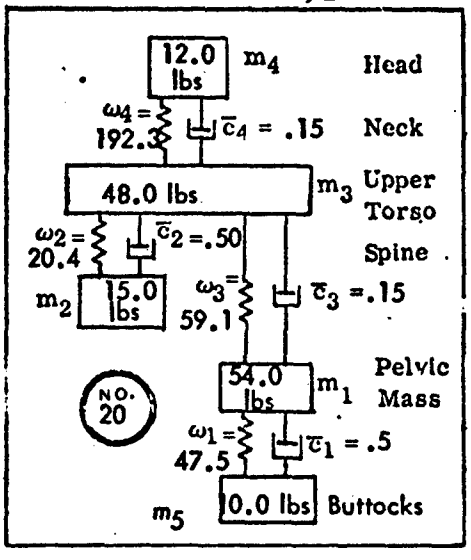

Figure 38. Four Mass Systems Case No. 20

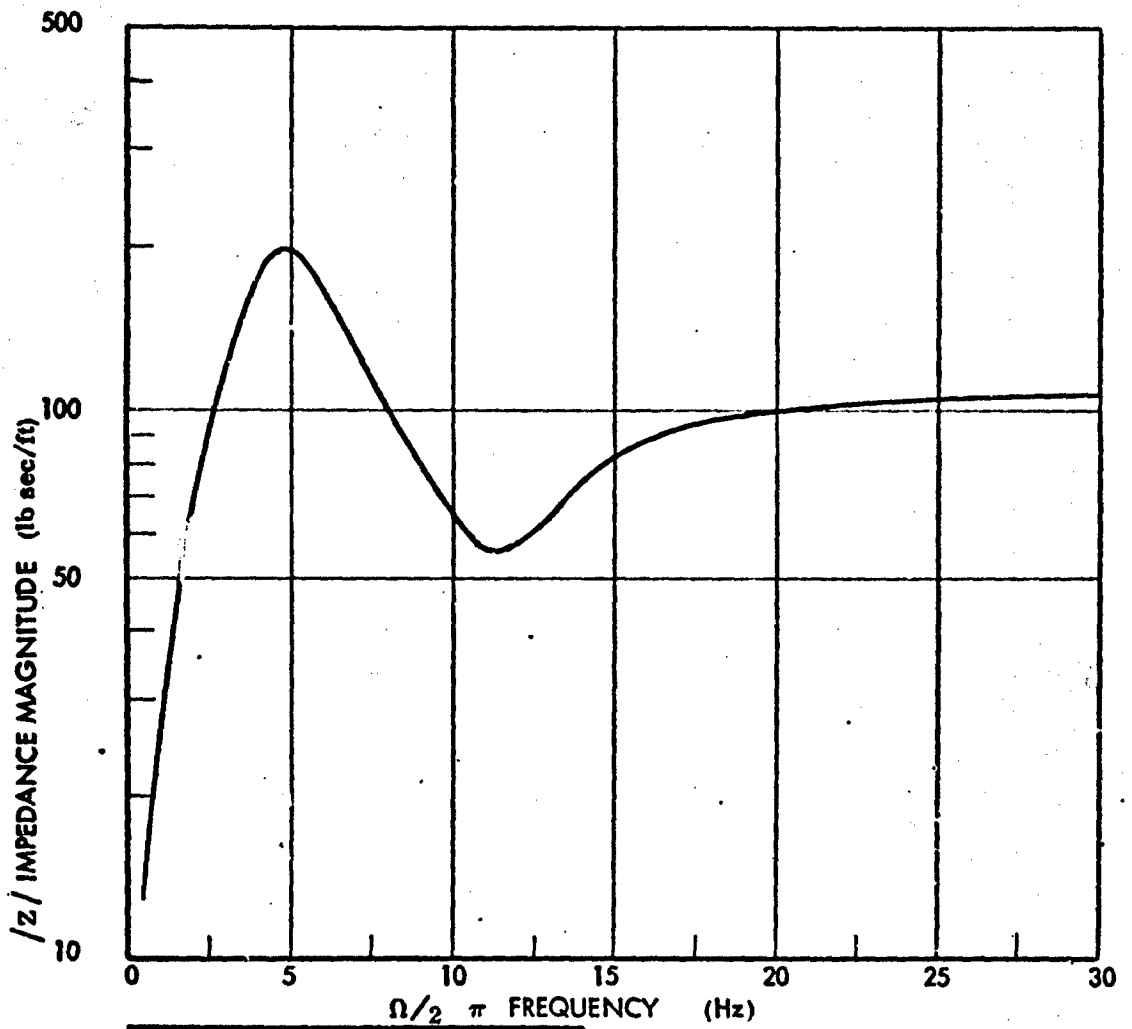

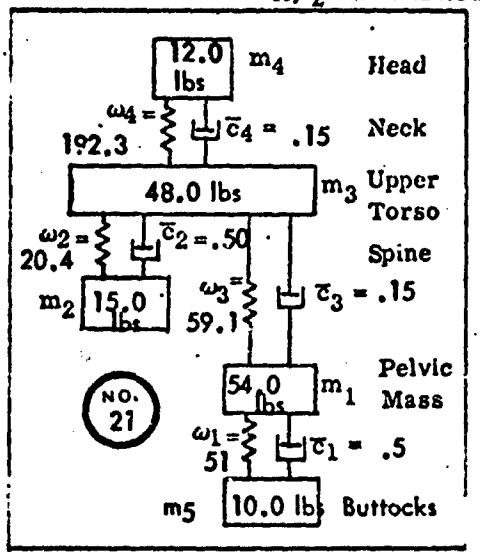

Figure 39. Four Mass Systems Case No. 21

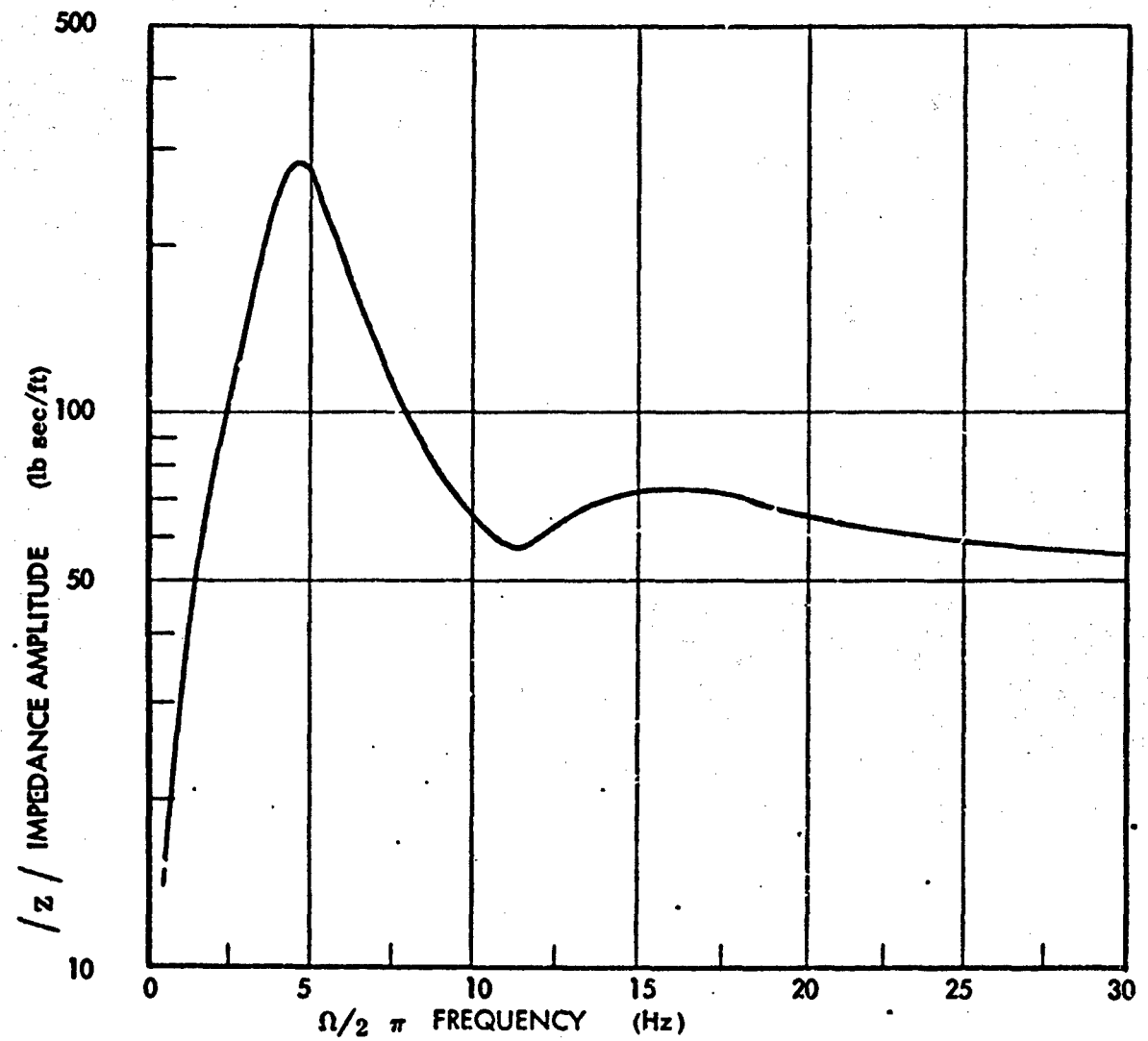

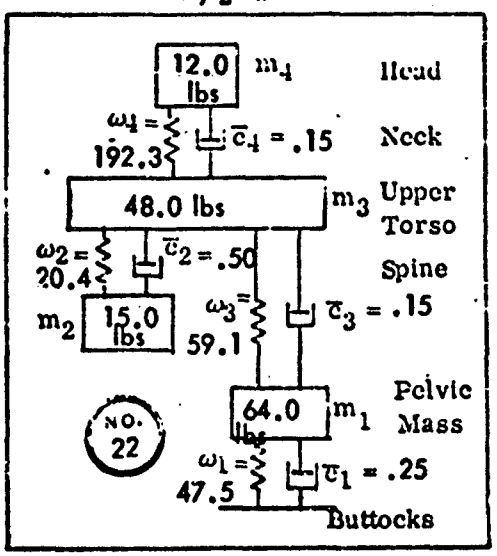

Figure 40. Four Mass Systems Case No. 22

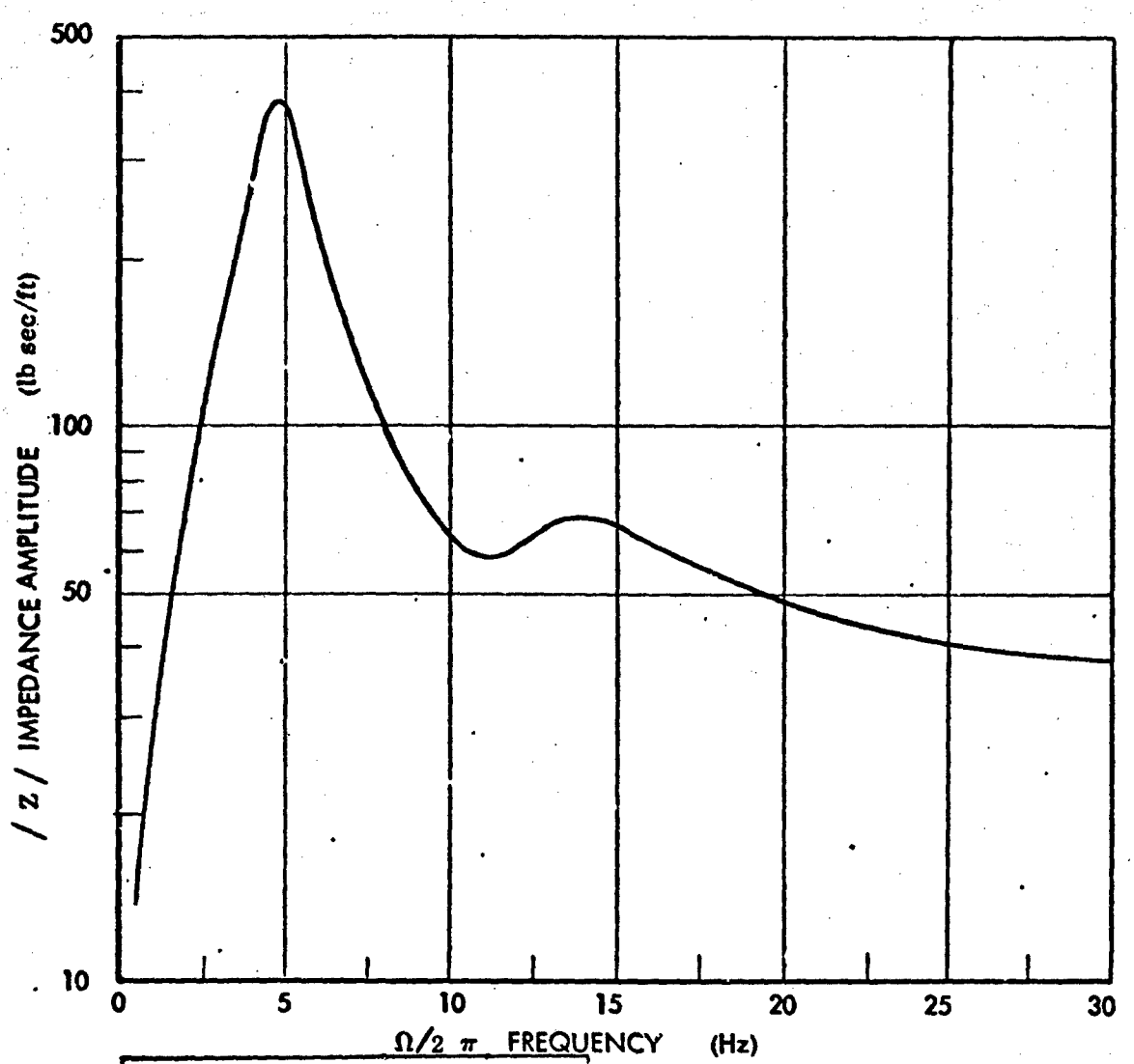

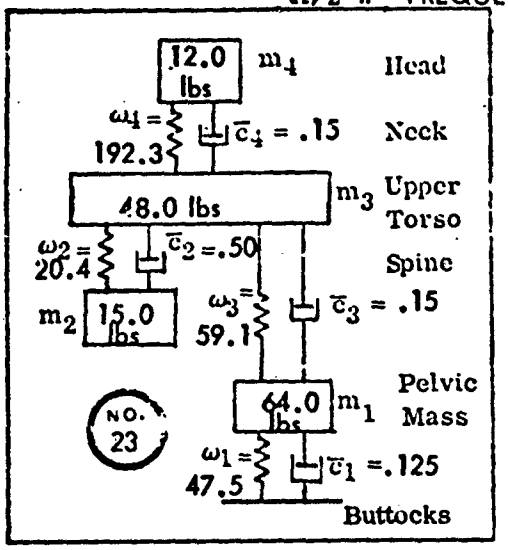

Figure 41. Four Mass Systems Case No. 23

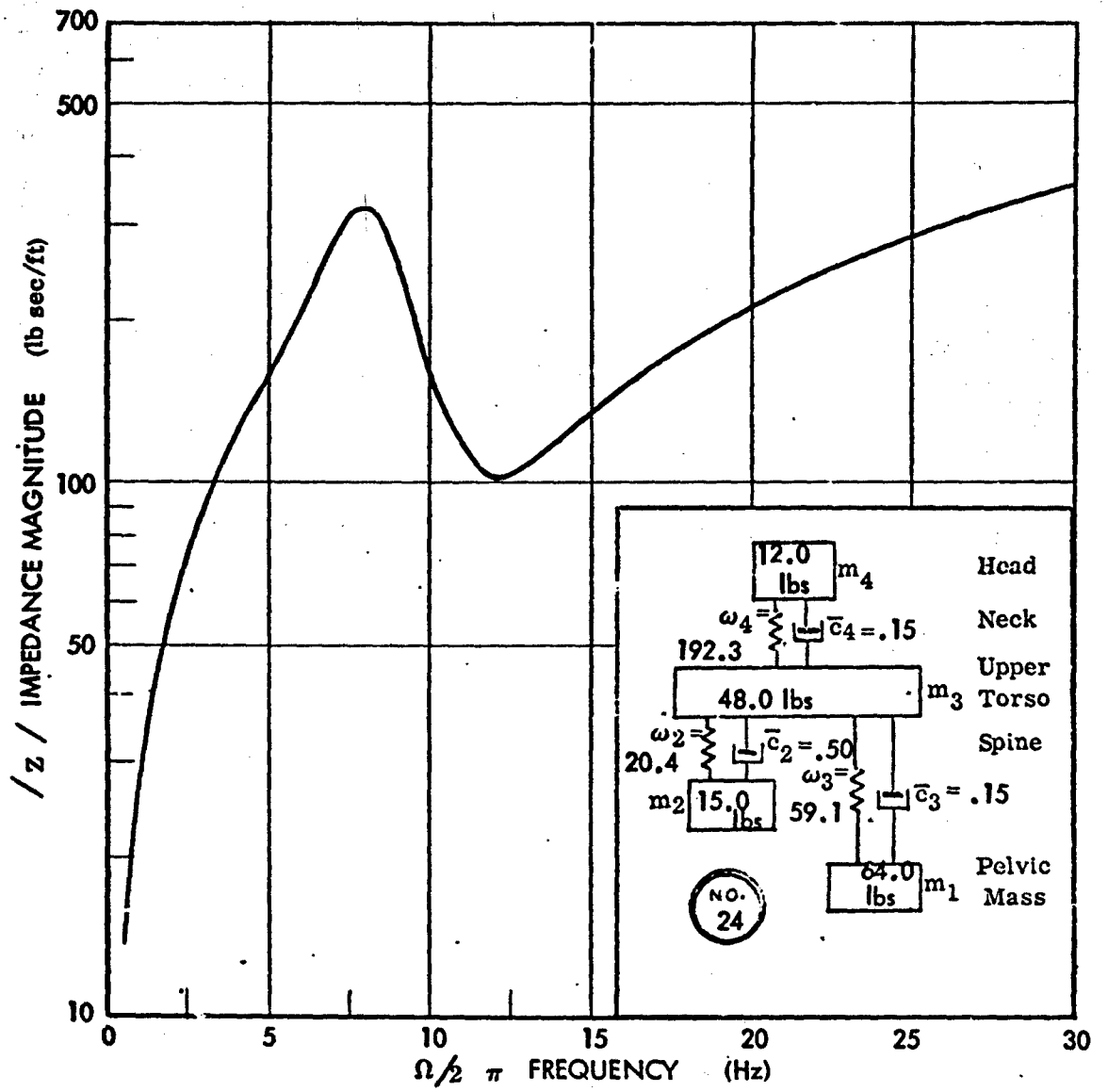

Figure 42. Four Mass Systems Case No. 24

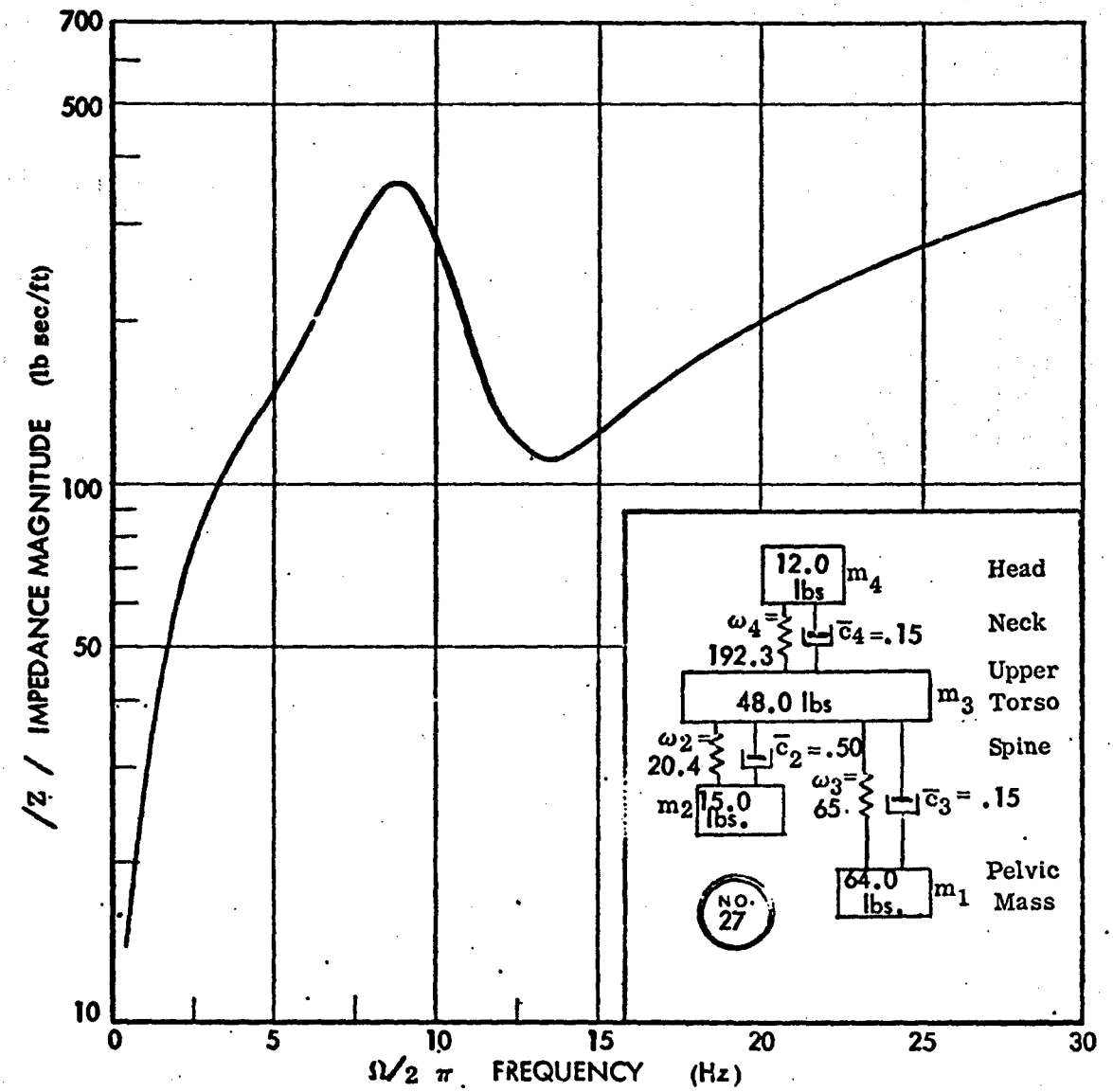

Figure 43. Four Mass Systems Case No. 27

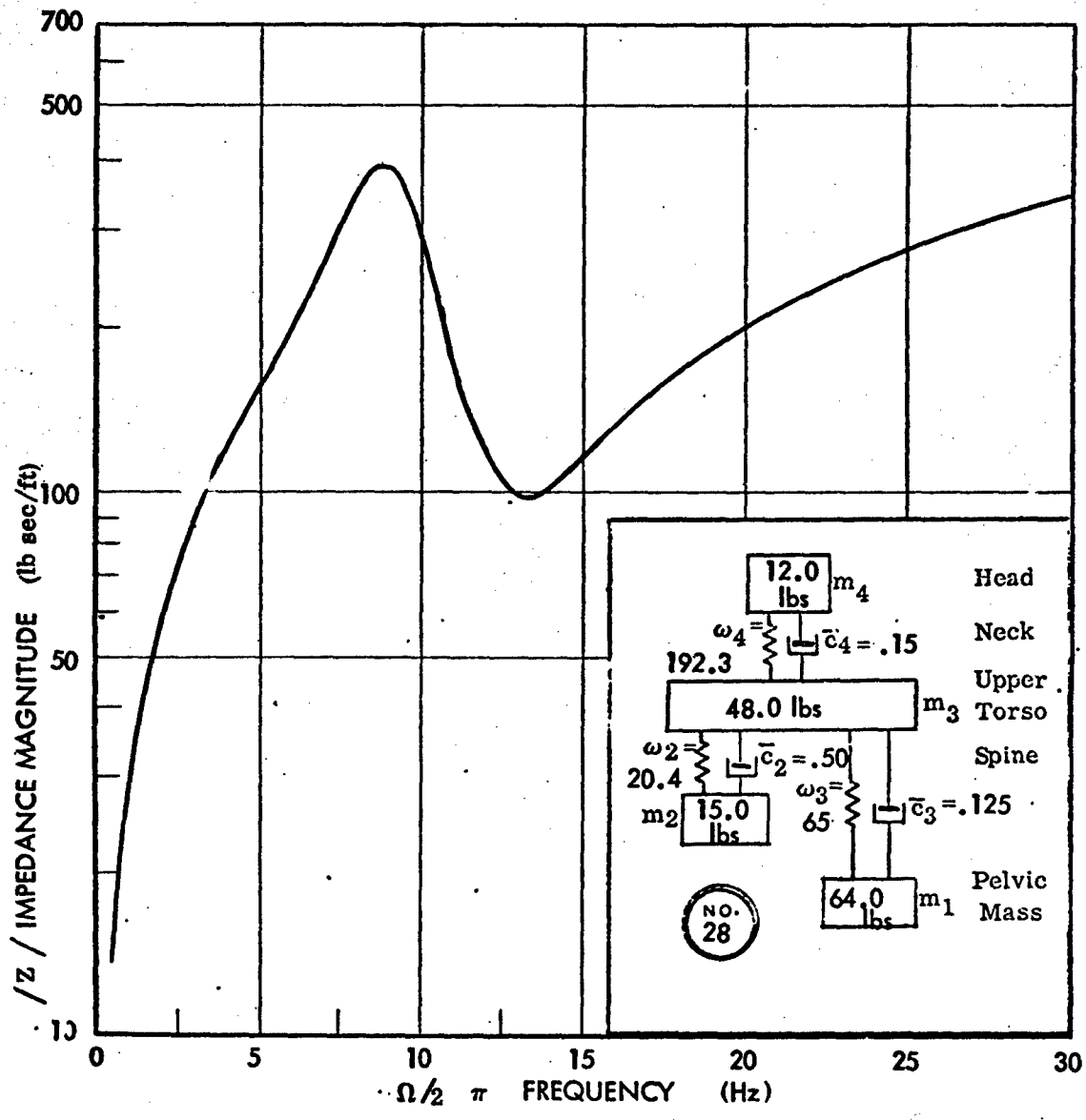

Figure 44. Four Mass Systems Case No. 28

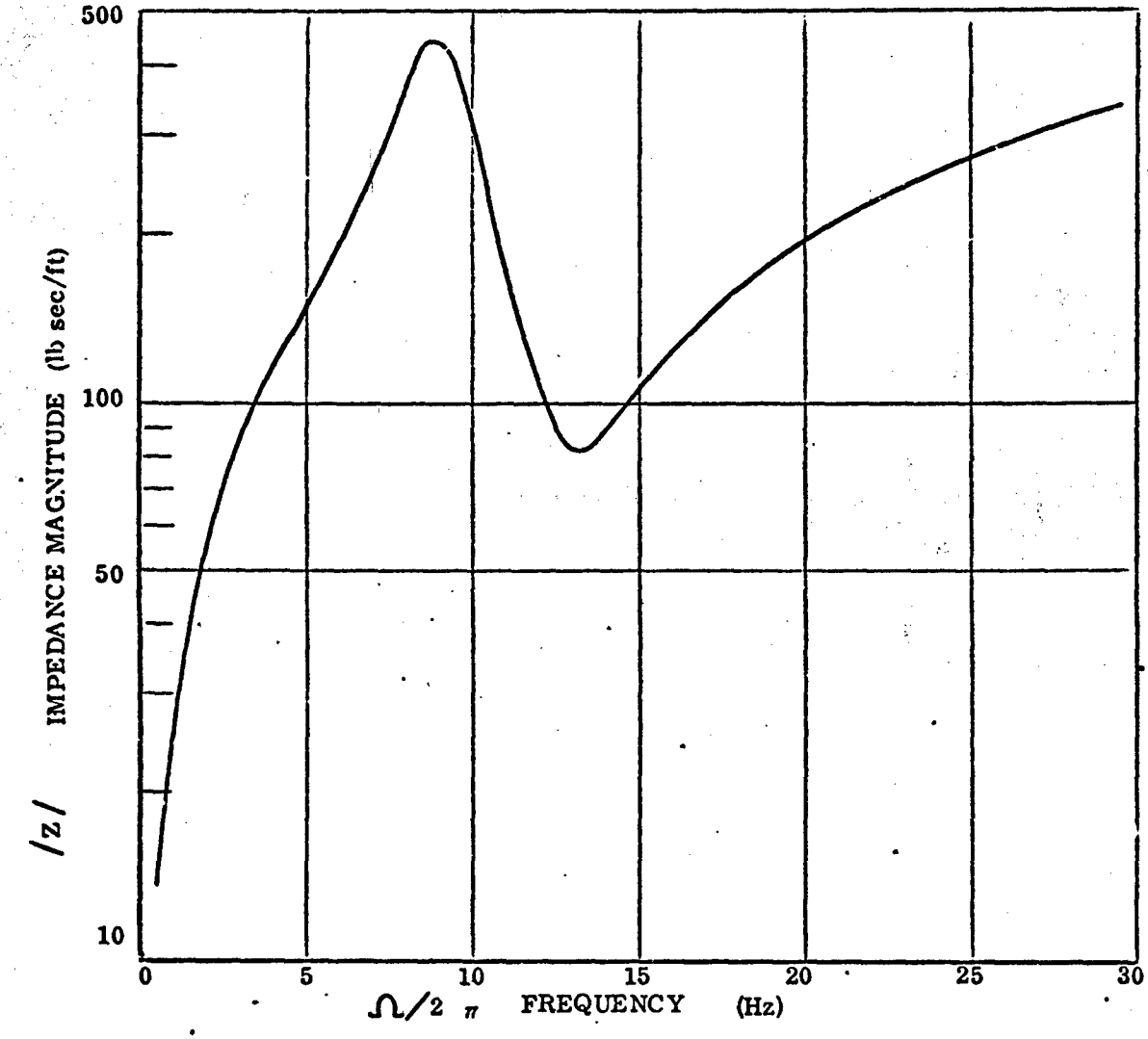

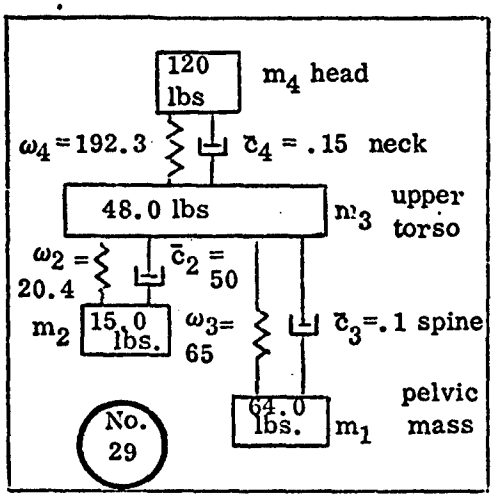

Figure 45. Four Mass Systems Case No. 29

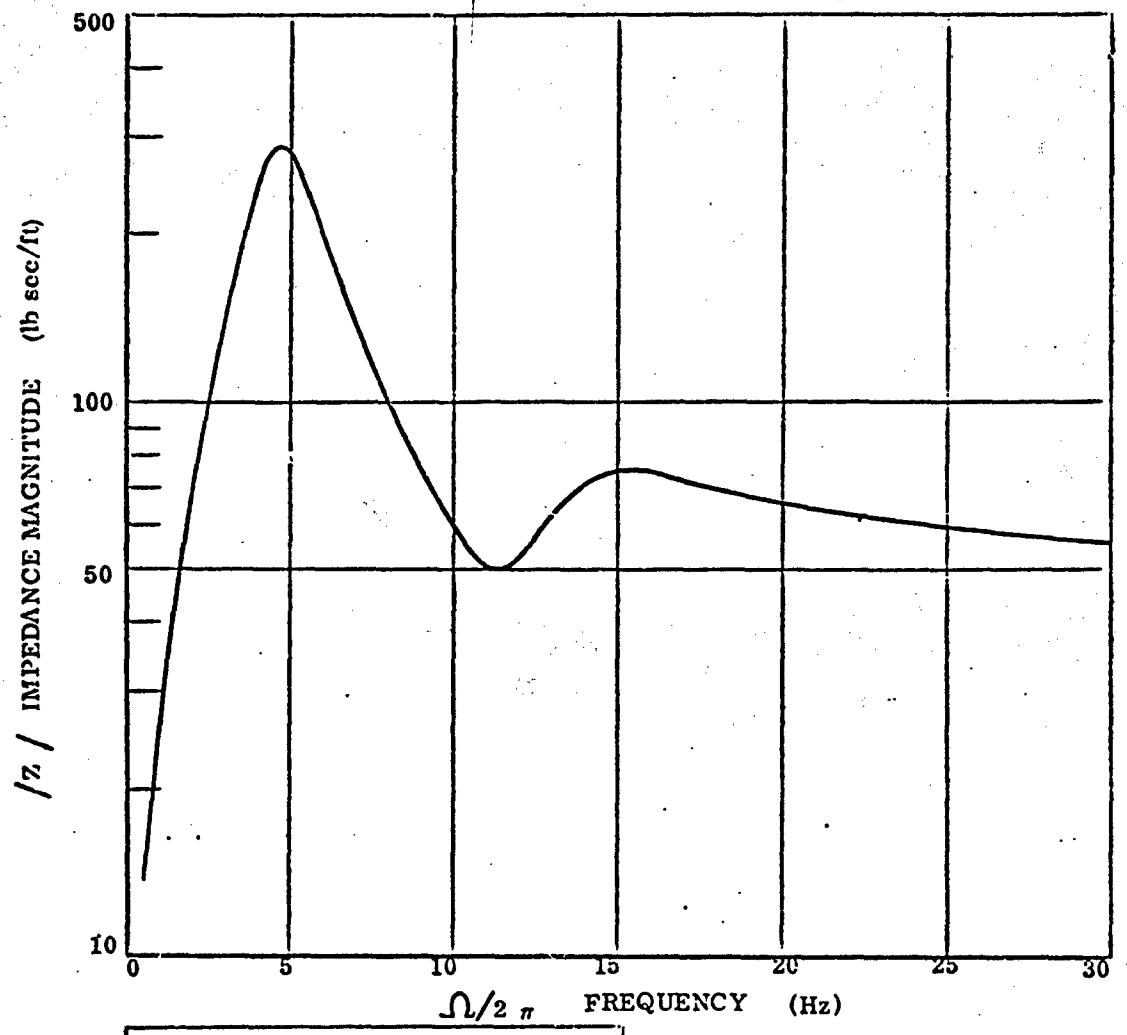

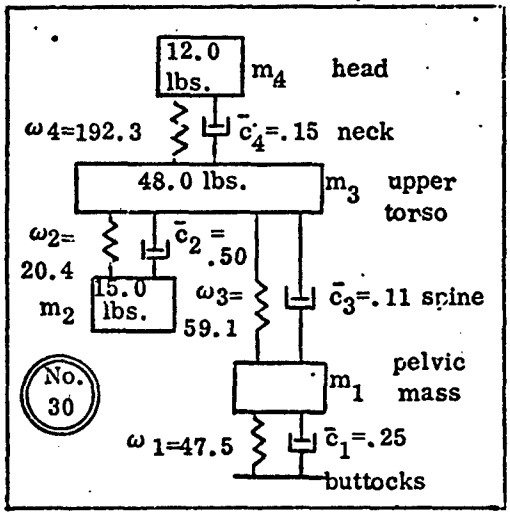

Figure 46. Four Mass Systems Case No. 30

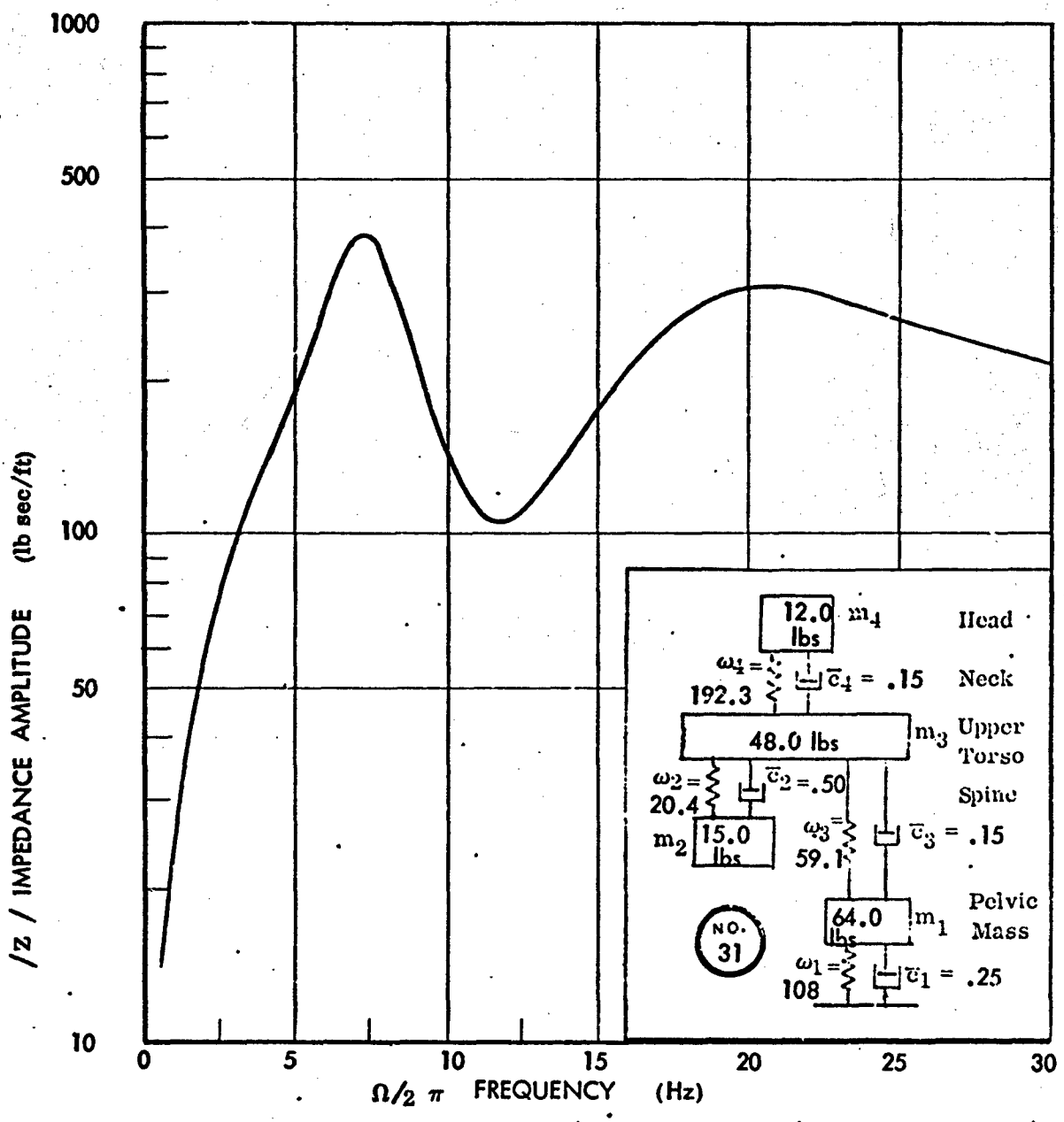

Figure 47. Four Mass Systems Case No. 31

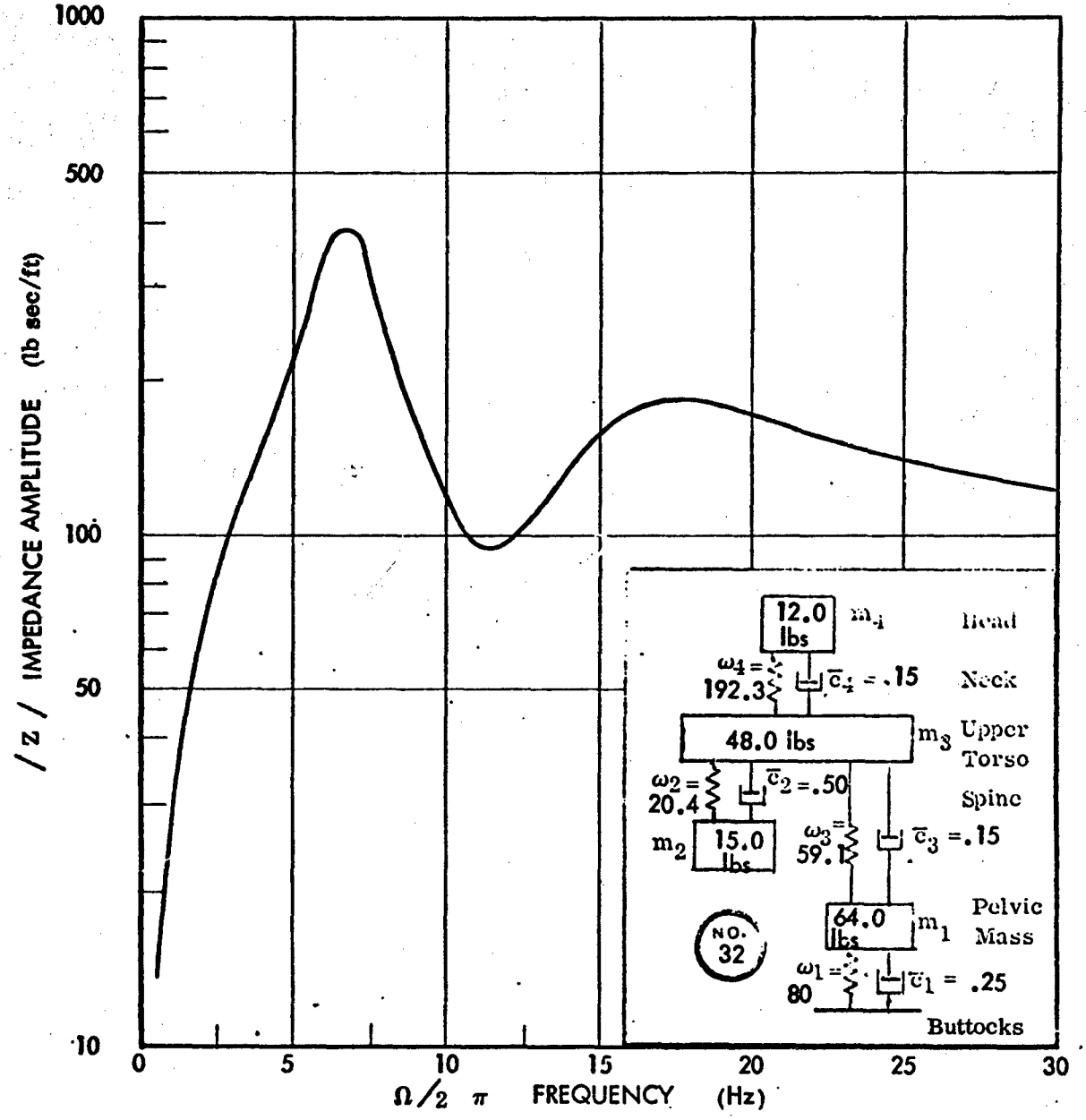

Figure 48. Four Mass Systems Case No. 32

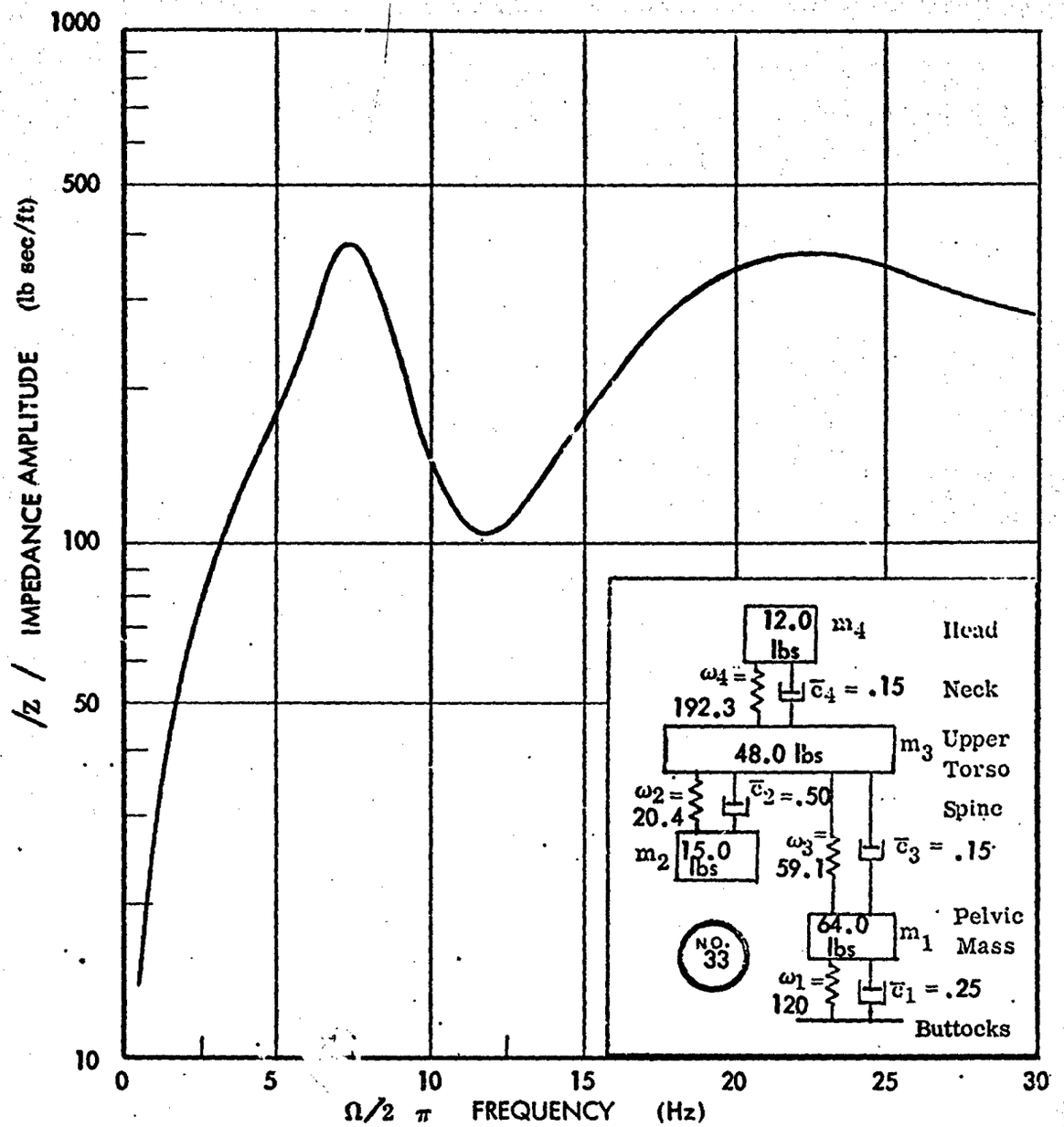

Figure 49. Four Mass Systems Case No. 33

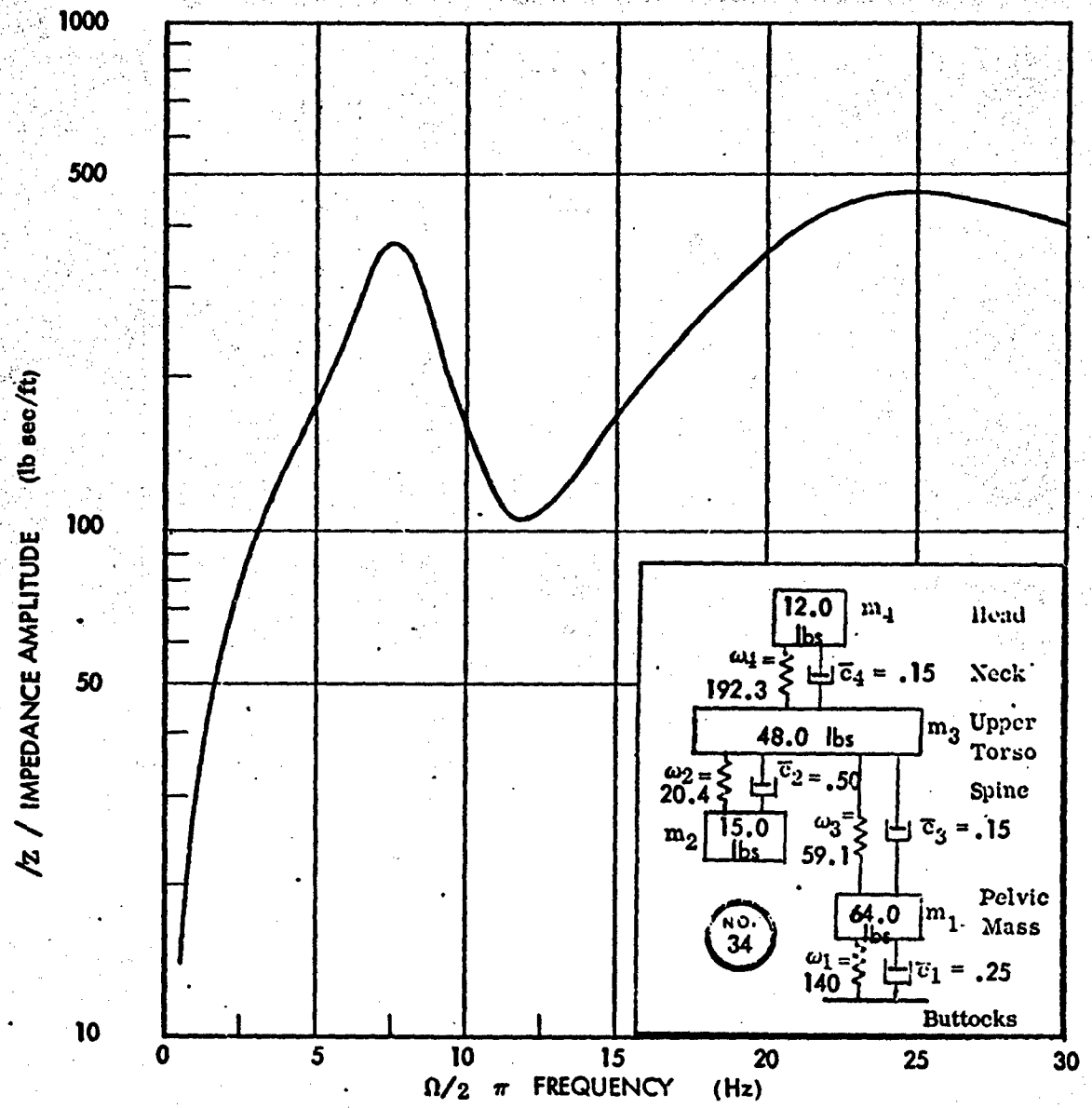

Figure 50. Four Mass Systems Case No. 34

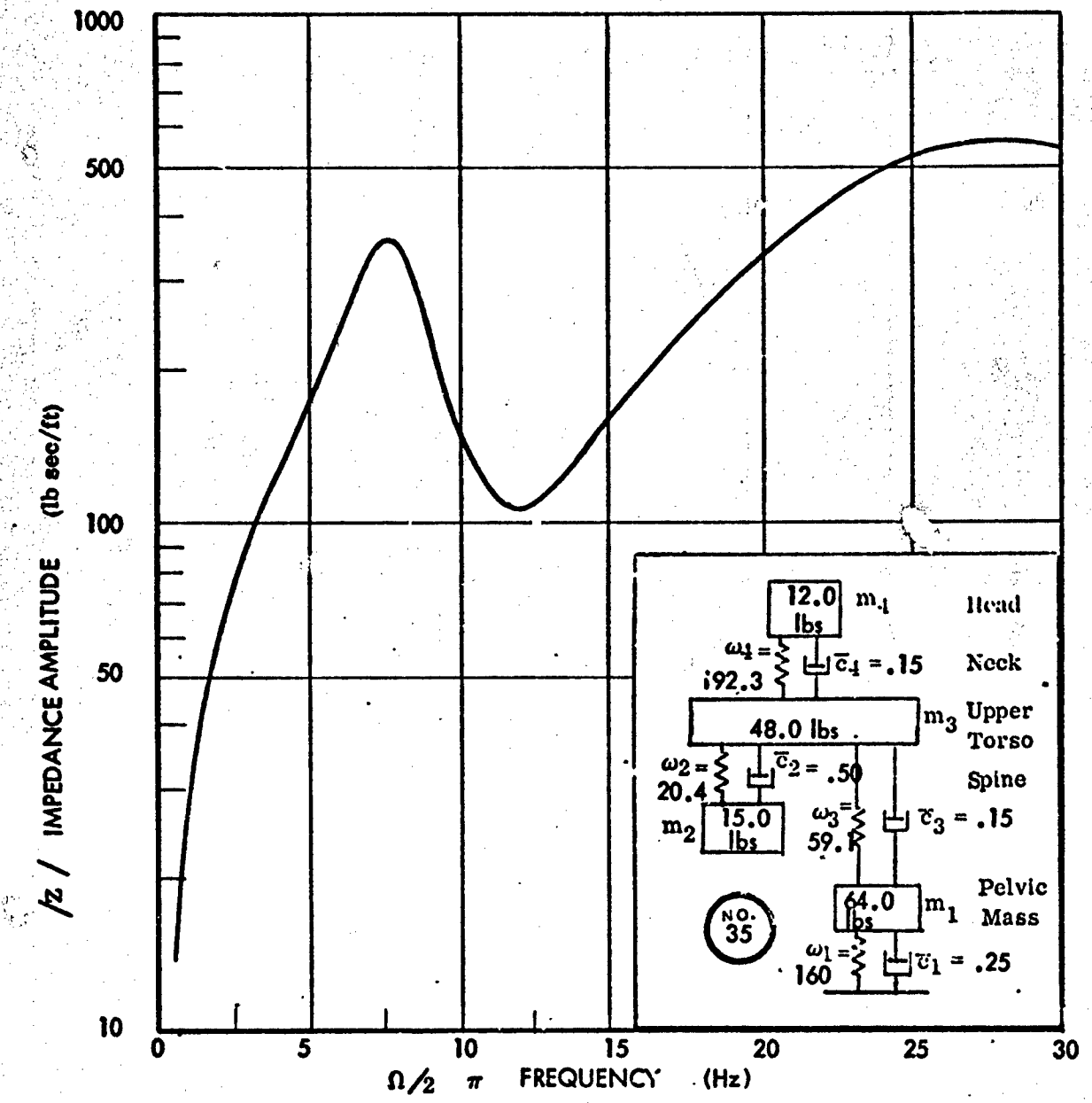

Figure 51. Four Mass Systems Case No. 35

SECTION IV

DEVELOPMENT OF THE NON-LINEAR FOUR-DEGREE-OF-FREEDOM MODEL

The linear model described in the preceeding pages had some evident shortcomings, particularly in the attempt to force the spinal and buttock modes into a linear representation, when both are clearly highly nonlinear. The next stage in the development was to expand the computer model to accept nonlinear representations of at least the spinal and buttock spring and damping rates. This analysis is discussed in the following pages.

CORRECTIONS TO SPINE STIFFNESS AND DAMPING BASED ON IMPEDANCE DATA

Steady state mechanical impedance measurements of seated subjects have been made under 1 g conditions by several investigators. As indicated in figure 11, the results are very variable.

Vogt, Coermann and Fust (ref. 5) also measured impedance in a centrifuge, with steady state acceleration biases of 2 and 3 g. Their results are plotted as experimental points in figure 12, because there seems to be no justification for drawing lines from point-to-point when the 1 g data has already demonstrated rather extreme variability, and therefore, presumably, considerable experimental scatter.

The most reliable 1 g data is presumably the most recent (shown as curve 3 in figure 11). Figure 46 shows a linear dynamic model which gives good agreement with measured data, up to a frequency of about 8 Hz. In this case the location and magnitude of the first peak is largely dependent upon the stiffness and damping of the buttock mode. At the present time the poor agreement above 8 Hz is not felt to be significant, because, as already shown, this is characteristic of nonlinear systems, and the buttock spring is known to be very nonlinear.

It is also known that the buttocks tend to vary, from subject to subject, more than any other part of the human anatomy. Thus, the primary dependence of the first peak on the buttock mode elegantly explains the wide variability in the 1 g measurements.

It might be thought that the larger impedance peak, at a higher frequency (about 8.5 Hz) which is measured under 2 and 3 g bias, is caused by the stiffening of the buttocks under the higher loading. As indicated in figure 52, this turns out not to be so. Increasing buttock stiffness beyond a value corresponding to about $\omega_1 = 60$ rads/sec causes the spinal resonance mode to increase in amplitude, and the first peak becomes asymptotic to about 8.8 Hz as $\omega_1 \to \infty$. For large values of ω_1 the motion is almost entirely in the spinal mode, and the buttock mode can be considered to be "shorted out".

With "shorted-out" buttocks the model shown in figure 45 gives good agreement with impedance measurements, below about 11 Hz. Note that in figures 45 and 46

$$\omega_3 = 59.1 \text{ rads/sec for 1 g,} \quad (k_3 = (59.1)^2 \times \frac{48.0}{32.2} = 5200 \text{ lb/ft}) \tag{44}$$

$$\omega_3 = 65.0 \text{ rads/sec for 2-3 g,} \quad (k_3 = (65.0)^2 \times \frac{48.0}{32.2} = 6300 \text{ lb/ft}) \tag{45}$$

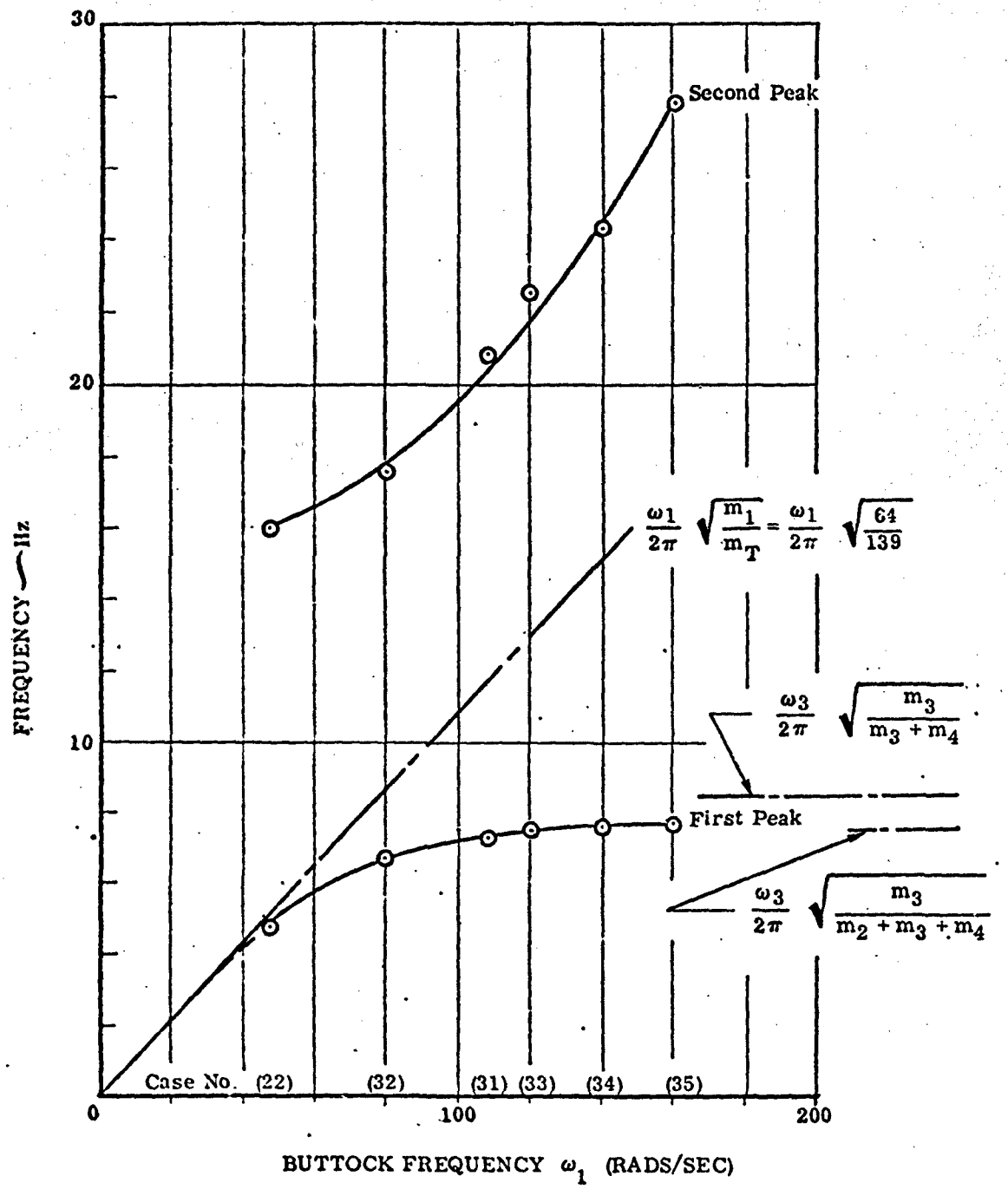

Figure 52. Influence of Buttock Stiffness on Location of the First and Second Impedance Peaks

The 1 g stiffness given above is 83% of the spinal model, and the 2-3 g local stiffness is 79% of the spinal model, corrected to age 27.9 years. An average stiffness reduction to 81% of the age 27.9 years value is seen from figure 19 to correspond to a test subject age of about 44 years, which is not impossible, but is unlikely. (Unfortunately, subject age is not usually documented in such test reports.) On balance, it seems best to provisionally assume that the live human spinal stiffness is 80% of the value determined from cadaver data.

In order to estimate the total spine force deflection characteristics, using the data shown in figure 16 for the L4 vertebra, the deflection scale was assumed to be inversely proportional to the stiffness. Thus, a deflection of .1 inches of the L4 vertebra was assumed to correspond to

$$\frac{.1}{12} \times \frac{108.5}{7.56} = .1196 \text{ feet}$$

of the whole spine between the L5 and T4 vertebrae. [108.5×10^3 lb/ft is the local 1 g stiffness for the L4 vertebra from figure 16, 7.56×10^3 is the total local 1 g stiffness for the spine of a 27.9 year old man, from equation (26).] Reducing the force scale by a factor of .80, as suggested above, allows the force deflection curve for the whole spine of a live 27.9 year old man to be given by making the appropriate corrections to the coefficients of equation (23).

$$\begin{aligned} F_{\delta_3} &= 3.88 \times 10^3 \left(.8 \times \frac{.1}{.1196}\right) \delta_3 + 2.032 \times 10^5 \left(.8 \times \frac{1}{.1196}\right)^2 \delta_3^2 \\ &\quad - 1.22 \times 10^6 \left(.8 \times \frac{.1}{.1196}\right)^3 \delta_3^3 \\ &= 2.59 \times 10^3 \delta_3 + 1.138 \times 10^5 \delta_3^2 - 5.7 \times 10^5 \delta_3^3 \quad (\text{for } \delta_3 < .12) \end{aligned} \tag{46}$$

In practice this curve is found to produce sensible values of F_{δ_3} for $\delta_3 < .12$ ft. For $\delta_3 > .12$ ft the tangent to the curve at that point was used in numerical calculations:

$$F_{\delta_3} = 331.2 + 527.8 \ \delta_3 \quad (\text{for } \delta_3 \geq .12) \tag{47}$$

This revised curve of force F_3 versus deflection for the whole spine is shown in figure 53.

So far as spinal damping is concerned, a value of $\bar{c} = 0.1$ (associated with $\omega_3 = 65$ rads/sec) seems to give best agreement with the centrifuge impedance data. Thus, the damping force is given by:

$$F_{D_3} = 2 \times 0.1 \times 65.0 \times \frac{48.0}{32.2} \dot{\delta}_3 = 19.4 \dot{\delta}_3 \text{ lb.} \tag{48}$$

In the absence of any other data, this damping is assumed to be linear and thus applies to the spinal model for all deflections and deflection rates.

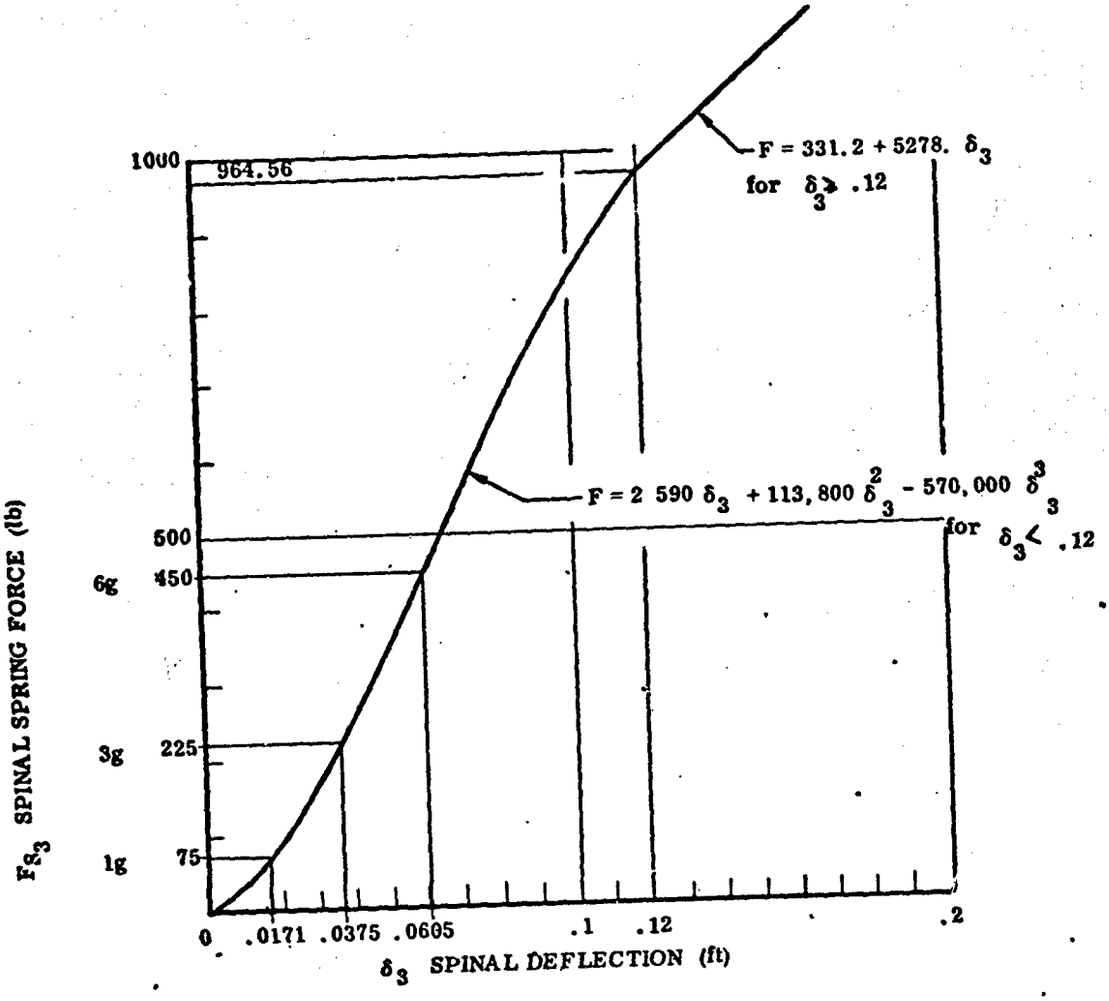

Figure 53. Spinal Spring Force Deflection Curve Assumed for 27.9 Year Old Live Male Subject

BUTTOCK STIFFNESS

As shown by Phillips,* as indeed, would be intuitively supposed, buttock stiffness is nonlinear, at least up to 1g loading. The Phillips data, plotted in figure 54 is very scattered, and does not go above the 1g loading case. One might suspect that creep (primarily displacement of blood) and muscle tension variation would both contribute to this scatter.

An average value of Phillips' data is

$$F_{\delta_1} = 77.0 \quad \delta_1 \text{ (inches)}^{2.44}$$

$$= 3.3 \quad \delta_1^{2.44} \times 10^4 \tag{49}$$

when δ_1 is in feet.

The local slope is

$$\frac{dF_{\delta_1}}{d} = 8.05 \quad \delta_1^{1.44} \times 10^4$$

$$= 172.0 \quad F_{\delta_1}^{0.59} \text{ (lb/ft)} \tag{50}$$

If all the subject above the buttock cushion, including thighs, were rigid, the small pertubation natural frequency for a 172-lb subject, with 150 lbs supported on the buttocks and 68-lb pelvic mass would be given by:

$$\omega_o^2 = \frac{dF_{\delta_1}}{d\delta_1} \Big/ \left(\frac{W}{g}\right) = \frac{172.0\ (N.W)^{0.59}}{\left(\frac{W}{g}\right)}$$

$$= \frac{172.0 \times N^{.59} \times (150)^{.59}}{\left(\frac{150}{32.2}\right)}$$

$$\omega_o = 26.63\ N^{.295} \text{ (radians/sec)} \tag{51}$$

where $N = \dfrac{\text{steady state acceleration}}{g}$ (-)

The natural frequency of the buttock spring at the corresponding steady state acceleration, when associated only with the pelvic mass is given by:

$$\omega_1 = \omega_o \sqrt{\frac{150}{68}} = 1.485\ \omega_o \tag{52}$$

*Unpublished trial report by Norman J. Phillips on Contract No. AF 33(657)-1894, Aerospace Medical Research Laboratory, Wright-Patterson Air Force Base (Nov 1967) entitled "Research on Human Responses to Complex Vibrations and Design Principles for Body Support, Restraint and Vibration Isolation Systems"

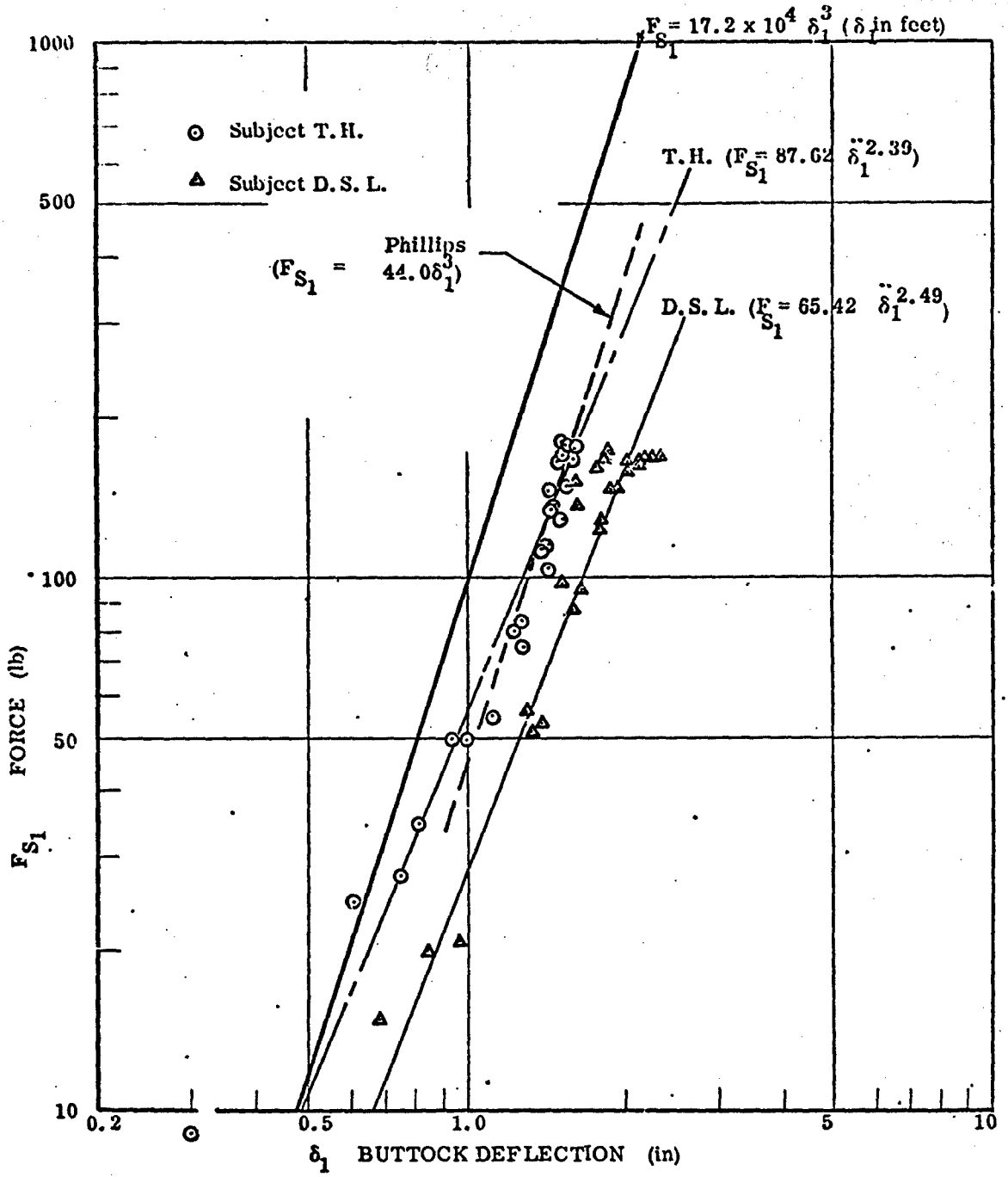

Figure 54. Measurements of Buttock Deflection Data Reported by Phillips

For	N	=	1	2	3	
	$N^{.295}$	=	1.0	1.227	1.383	
	ω_o	=	26.63	32.65	36.8	rads/sec
		=	4.24	5.2	5.86	Hz
	ω_1		39.6	48.5	54.7	rads/sec

In order to obtain agreement with impedance measurements, it is necessary to assume $\omega_1 = 47.5$ rads/sec (1 g) and $\omega_1 \geq 160$ rads/sec (2-3 g). (Compare figures 42 and 51, for example.) The 1 g value of 47.5 rads/sec is 120% of the value indicated by Phillips' data, a difference which is not at all surprising when it is recalled that buttock size and muscle tone are very variable. Because of the poorness of this data, therefore, it is convenient to adopt Phillips' assumption that the buttock spring is a cubic up to 1 g.

Rough measurements made by loading up a subject seated on a hard chair, indicate that the buttocks "bottom out" at 1.5 g, so that above this force value the buttock frequency is arbitrarily assumed to be $\omega_1 = 160$ rads/sec corresponding to a "stiffness" k_1 given by:

$$k_1 = \frac{160^2 \times 64}{32.2}$$

$$= 50,100 \ \frac{lb}{ft} \qquad (53)$$

Below 1.5 g, if $F_{\delta_1} = b_1 \delta_1^3$

$$\frac{dF_{\delta_1}}{d\delta_1} = 3b_1\delta_1^2$$

At 1 g, assuming a subject with 139 lb supported on the buttocks and a 64.0 lb pelvic mass:

$$\delta_1 = \left(F_{\delta_1}/b_1\right)^{\frac{1}{3}}$$

$$\omega_1 = \sqrt{\frac{dF_{\delta_1}}{d\delta_1}\frac{1}{m_1}} = \sqrt{\frac{3b_1}{m_1}\left(F_{\delta_1}/b_1\right)^{2/3}} = b_1^{\frac{1}{6}}\sqrt{\frac{3\times(139)^{2/3}}{64/32.2}}$$

For the 1 g case where $F_{\delta_1} = 139.0$ lb

$$\omega_1 = 6.36\, b_1^{1/6} = 47.5 \text{ rads/sec} \tag{54}$$

$$\therefore\ b_1 = \left(\frac{47.5}{6.36}\right)^6 = 1.72 \times 10^5 \tag{55}$$

and the general expression for F_{δ_1} for less than a 1.5 g load, which corresponds to a deflection of 0.1066 ft is:

$$F_{S_1} = 1.72 \times 10^5 \quad \delta_1^3 \tag{56}$$

Thus the buttock spring is assumed to be as shown in figure 55.

The buttock damping is assumed to be constant, so that

$$2K = 2cm = 2\bar{c}\omega_1 m = 2 \times 0.25 \times 47.5 \times \frac{64.0}{32.2} = 47.2 \text{ lb sec/ft} \tag{57}$$

and the buttock damping force is therefore given by:

$$F_{D_1} = 47.2\, \dot{\delta}_1 \quad \text{(lb)} \tag{58}$$

FINAL MAN MODEL

The final form mass analog of a seated man used in subsequent computations is shown in figure 56. The total weight of the man is assumed to be 160 lb, distributed as follows:

Head	12 lbs	
Upper Torso	48 lbs	
Viscera	15 lbs	
Lower Pelvic Mass	64 lbs	
	139 lbs	(supported by buttocks)
Legs and Feet	21 lbs	(assumed to move with seat)
	160 lbs	

The values used for the spring and damping forces for the four modes are shown in figure 56. The spring and damping constants are shown in table 6.

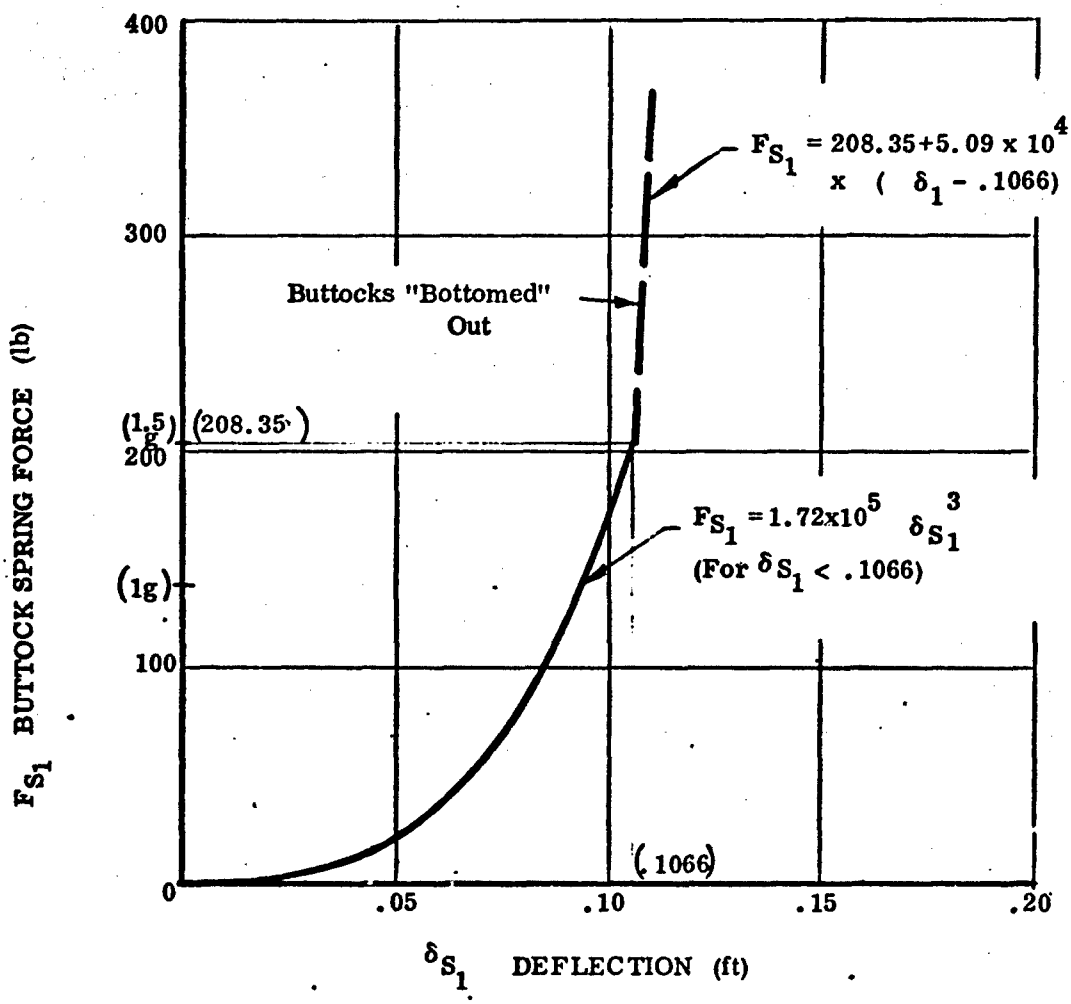

Figure 55. Buttock Spring Force/Deflection Curves Assumed for a 27.9 Year Old Live Male Subject

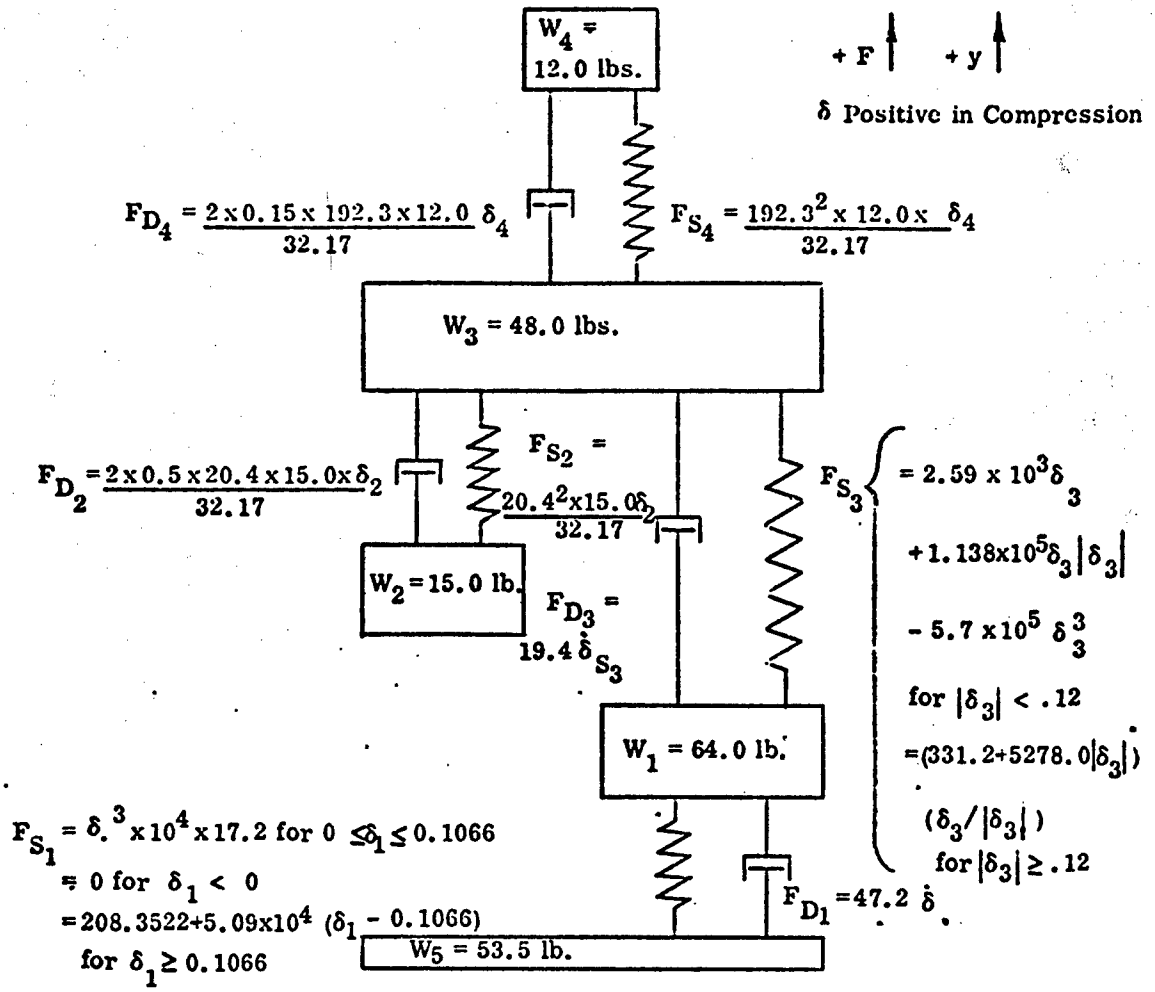

Figure 56. Mass, Spring and Damping Force Equation for Final Man Model

TABLE VI

Mass Spring and Damping Constants Used In Final Non-Linear Four-Degree-Of-Freedom Model

Mode	0 Legs/Feet	1 Buttocks	2 Visceral	3 Spinal	4 Head/Neck
Weight Distribution (lb) (Total Weight =160 lb 139 lb supported by buttocks	21 (Assumed to move with feet)	(Lower Pelvic Mass) 64	15	(Upper Torso Mass) 48	12
Spring Constant k (lb/ft)	--	Variable (eq.56)	194 (eq.31B)	Variable (eq.46)	14,000 (eq.42)
Undamped natural frequency ω (rad/sec)	--	47.5(1 g load) variable (eq.54)	20.4 (eq.31.A)	65.0 for 2-3 g load (eq.45)	192.3 (eq.41)
Spring Force F_S (lb)	--	See fig 55 (eq.56)	$194\ ^{2}$ (eq.31B)	See fig 53 (eq.46,47)	$14,000\ ^{4}$ (eq.42)
Damping Ratio $\bar{c}$ (-)		.25 (for ω_1=47.5) (eq.57)	0.5 (eq.31.C)	0.1(for ω_3 =65 rad/sec) (eq.48)	0.15 (eq.39)
Damping Coefficient 2K (lb/ft/sec)		47.2 (eq.57)	9.5 (eq.31.C)	19.4 (eq.48)	10.75 (eq.40)
Damping Force F_D (lb)		$47.2\ ^{1}$ (eq.57)	$9.5\ ^{2}$ (eq.31.C)	$19.4\ ^{3}$ (eq.48)	$10.75\ ^{4}$ (eq.40)

SECTION V

COMPARISON BETWEEN MODEL OUTPUTS AND EXPERIMENT

As can be seen from figure 46, linear impedance model number 30 gives good agreement with experiment up to a frequency of about 8 Hz. Since the model coefficients were adjusted with this end in view, such agreement is meaningless by itself, of course. The lack of agreement at the higher frequencies is also to be expected because of the importance of damping at the higher frequencies. As indicated by figure 10, for the simple case of a single-degree-of-freedom cubic model, the presence of nonlinear damping can markedly change the apparent impedance.

If impedance model number 30 (figure 46) is driven by a sinusoidal imput, the relative amplitudes of the various masses are as indicated in figure 57. These results are very similar to the experimental measurements of Dieckmann (ref. 13) and Latham (ref. 14). Since these experiments are quite different to impedance measurements, the qualitative agreement of the model is very encouraging.

Moving now to the final model configuration, with the nonlinear spine and buttock springs, we should expect similar results for both input impedance and amplitude ratio. Unfortunately, there was insufficient time available to carry out such a comparison during the present study.

The nonlinear model was compared with an AMRL drop test tower experiment, however. As indicated in figure 58, the input acceleration was approximated by two polynomials, and the resulting force-time history is given in figure 59. Except for the fact that the model appears to be slightly under-damped, the agreement with experiment is considered to be excellent.

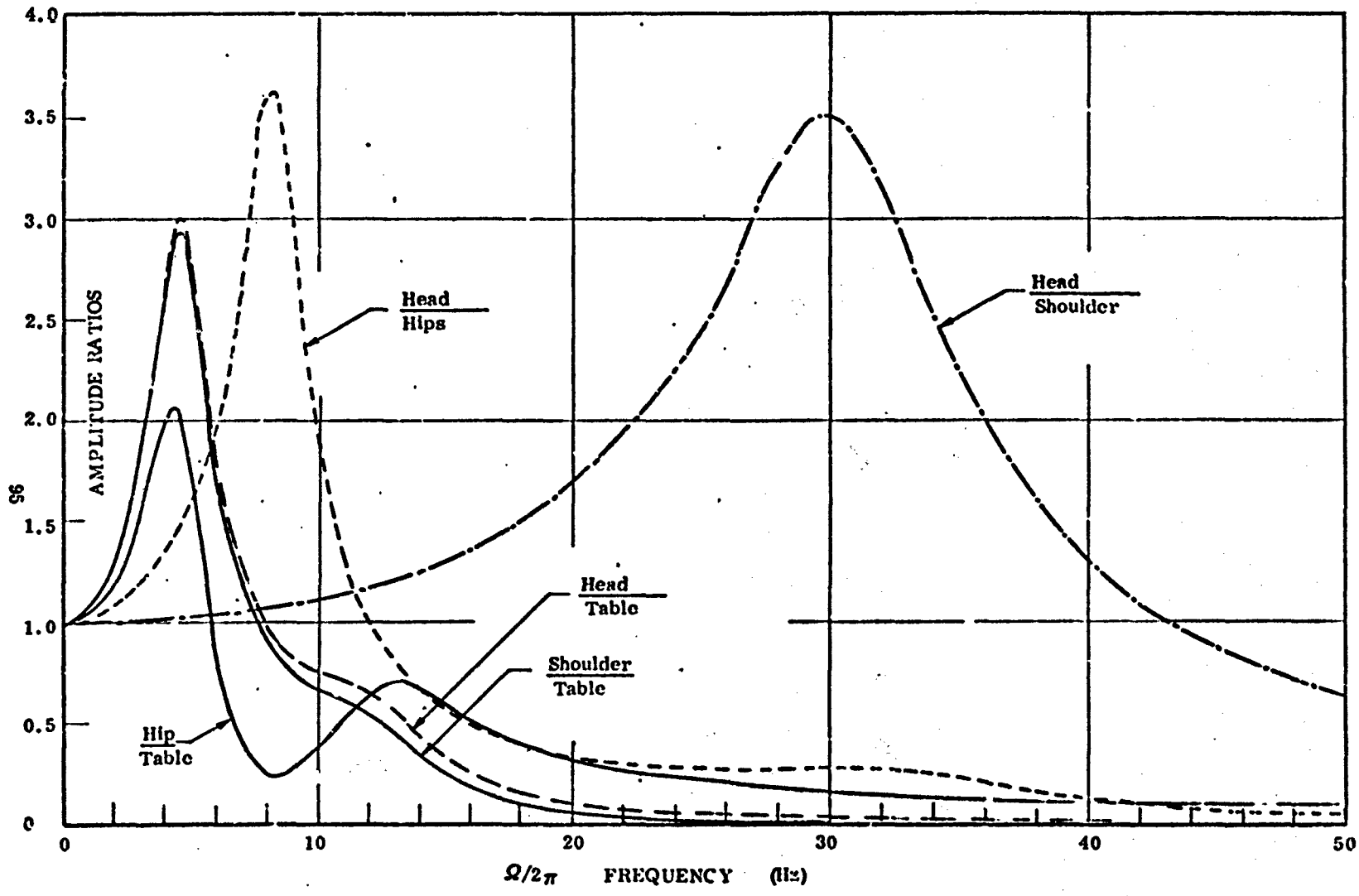

Figure 57. Response of Model #30 at 1 g.

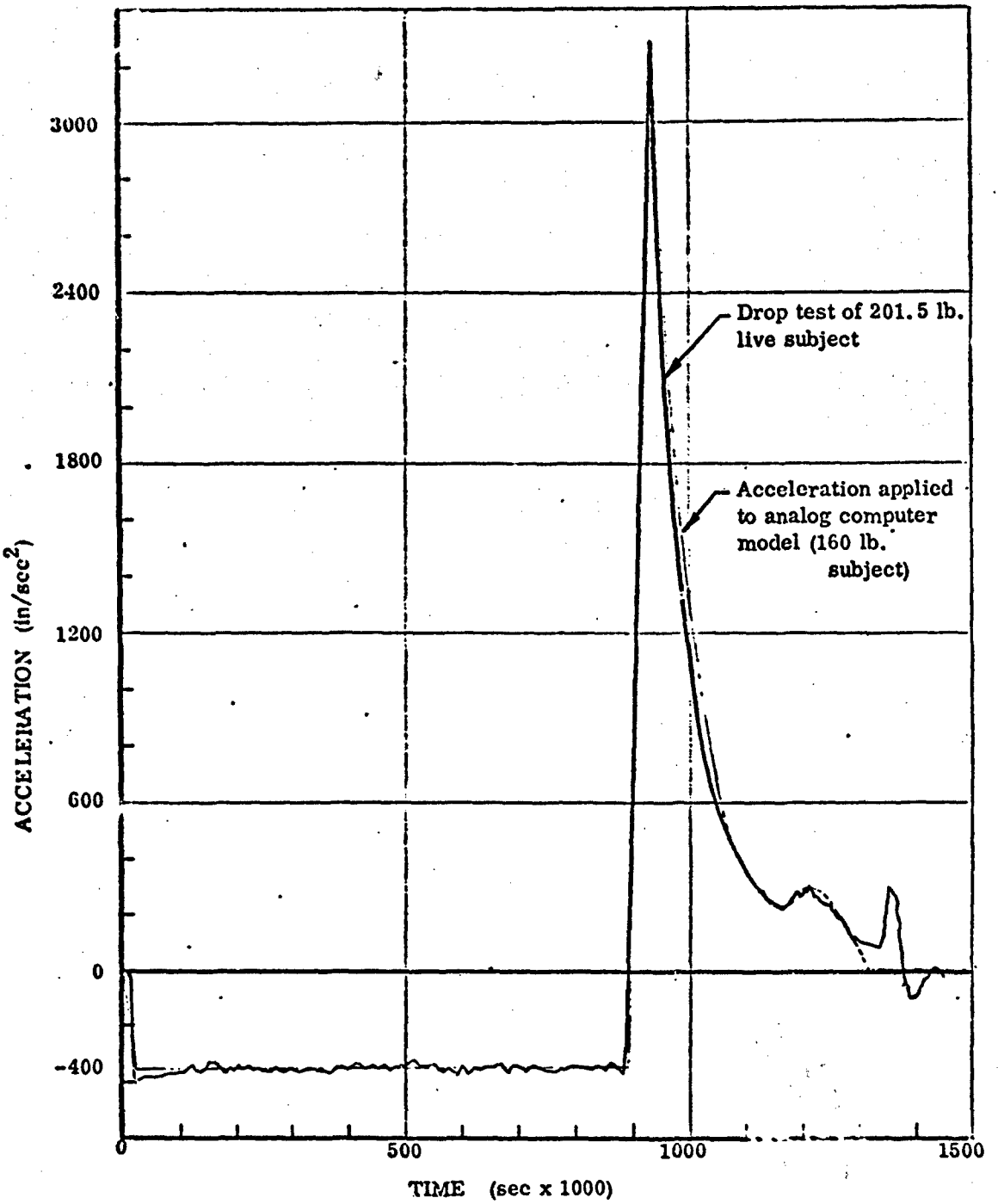

Figure 58. Acceleration Measured During Drop Test of Live Subject in an Ejection Seat

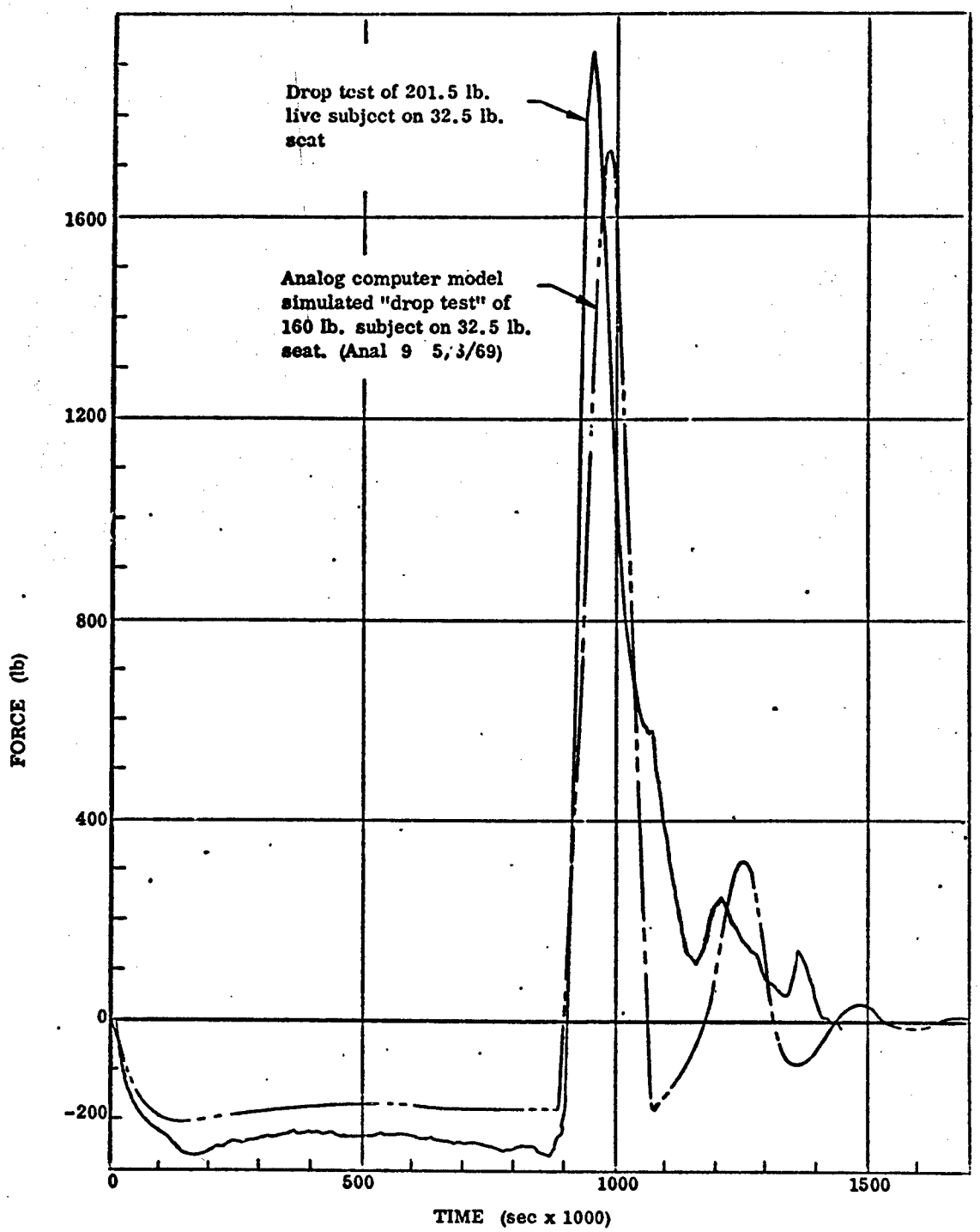

Figure 59. Comparison of Measured and Theoretically Calculated Force on Live Subject During a Drop Test

SECTION VI

SUGGESTED FUTURE WORK

BUTTOCK DYNAMICS

The stiffness and damping of the buttock mode should be investigated experimentally. Some preliminary work in this area has been carried out by Phillips, * but much more extensive testing is needed. It should be possible to establish meaningful methods of defining buttock size and muscle tone and to correlate the dynamic measurements with these parameters. This opens the way to determining the buttock dynamic characteristics of a particular air crew member by simple measurements during routine physicals, if further work indicates that buttock dynamics have a significant influence on injury potential.

SPINAL DYNAMICS

It should be relatively easy to determine spinal stiffness from cadaver material, using complete spines from subjects of different ages, and there seems no good reason why this important data should not be obtained at once. Spinal mode damping is more difficult, since it must be obtained with live subjects. At the moment, and excepting the work of Kazarian** with monkeys, even the mechanism of spinal damping is unknown. It should be possible to build a fixture which will oscillate the upper torso with respect to the pelvic girdle, and in this way obtain damping data for small and moderate spine deflections. If the mechanism for this damping can then be discovered, it may be possible to extrapolate the damping data throughout the range of operational interest.

GENERAL RESEARCH ON DAMPING MECHANISMS

It has generally been assumed that damping of the human body is linear; mostly, one suspects, because only linear damping can be handled analytically. Kazarian's work with monkeys implies that "orifice" or "hydraulic" damping may be significant in the spinal model. There may also be a substantial amount of quasi-coulomb (constant force) damping in other parts of the body, however, and as has been shown, this can have a substantial effect on the apparent impedance at the higher frequencies.

It is therefore essential to obtain a better understanding of the mechanism of damping in the various parts of the human body, so that more realistic damping relationships can be used in future dynamic models. Some new possibilities in this area are pointed out in some earlier work done by Payne and Anthony. ***

---

* See footnote on p. 88.

** Verbal communication from L. Kazarian of AMRL.

*** Unpublished Wyle Laboratory working paper No. 140-1 (13 November 1969) entitled "Notes on a Simple Model of a Spinal Vertebra" by P. R. Payne and A. Anthony.

RELATIVE MOTION OF BODY COMPONENTS

Dieckmann (ref. 13), Latham (ref. 14), and Woods (ref. 15) (among others) have all contributed to the investigation of transmissibility, and the relative motion of body components (head, shoulder, hips, etc.) under steady state sinusoidal excitation. Unfortunately their data is rather fragmentary, and a more ambitious program needs to be undertaken, using at least ten different subjects, with very carefully designed instrumentation. It might be helpful to use both accelerometers and optical techniques at the same time, for example. In addition, excitation of the subject should be applied at different locations and bias, as suggested below.

(a) Excitation at zero g bias, (with the subject supported horizontally on air jets). Excitation should be at various locations (feet, shoulders, head, for the "standing" position, and buttocks, shoulders and head for the "seated" position).

(b) Similar experiments under normal 1 g bias.

(c) Similar experiments (excluding head excitation) in a centrifuge, to obtain higher bias values.

(d) Experiments where "intermediate" positions (such as the hips) are driven after being cast in plaster.

APPENDIX I

DISCUSSION OF AN AMPLITUDE RATIO FUNCTION

APPENDIX I

DISCUSSION OF AN AMPLITUDE RATIO FUNCTION

In the analysis of a two mass problem we obtain the amplitude ratio function

$$f = \frac{\sqrt{1+q^2p^2}}{\sqrt{[1-p^2]^2+q^2p^2}}$$

where

$$p = \frac{\Omega}{\omega_n} \qquad q = 2\zeta_n$$

Let $u = \sqrt{1+q^2p^2}$

so that $\frac{du}{dp} = \frac{q^2p}{\sqrt{1+q^2p^2}}$

Let $w = \sqrt{1-(2-q^2)p^2+p^4}$

so that $\frac{dw}{dp} = \frac{2p^3-(2-q^2)p}{\sqrt{1-(2-q^2)p^2+p^4}}$

Then $$\frac{df}{dp} = \frac{q^2p\sqrt{1-(2-q^2)p^2+p^4} - [2p^3-(2-q^2)p]\sqrt{1+q^2p^2}}{\sqrt{1+q^2p^2}\sqrt{1-(2-q^2)p^2+p^4}}$$

$$\frac{}{[1-(2-q^2)p^2+p^4]}$$

Equating to zero and solving for p at $\frac{df}{dt} = 0$, we obtain

$$q^2 p^4 + 2p^2 - 2 = 0$$

whence

$$p^2\Big|_{f_{max}} = \frac{1}{q^2}\left[\sqrt{1+2q^2} - 1\right]$$

Substituting back into the equation for f we obtain, after some manipulation

$$f_{max} = \frac{q^2}{\sqrt{2\sqrt{1+2q^2} - (2+2q^2-q^4)}}$$

Note that as $q \to 0$ (corresponding to zero damping)

$p\big|_{f_{max}} \to 1$ (corresponds to $\Omega_{res} \to \omega_n$)

Note: $p\big|_{f_{max}} = \frac{\Omega_{res}}{\omega_n}$ (where Ω_{res} is resonant frequency for maximum amplitude ratio)

$f_{max} \to \frac{1}{q} \to \infty$ (corresponds to amplitude ratio $\to \infty$)

Thus for low damping the function tends to behave like the dynamic magnifier analyzed in Appendix II, near the point of resonance.

A typical plot of the function f is given in figure I.1. The maximum value of f, the corresponding value of the frequency ratio parameter p, is plotted in figure I.2.

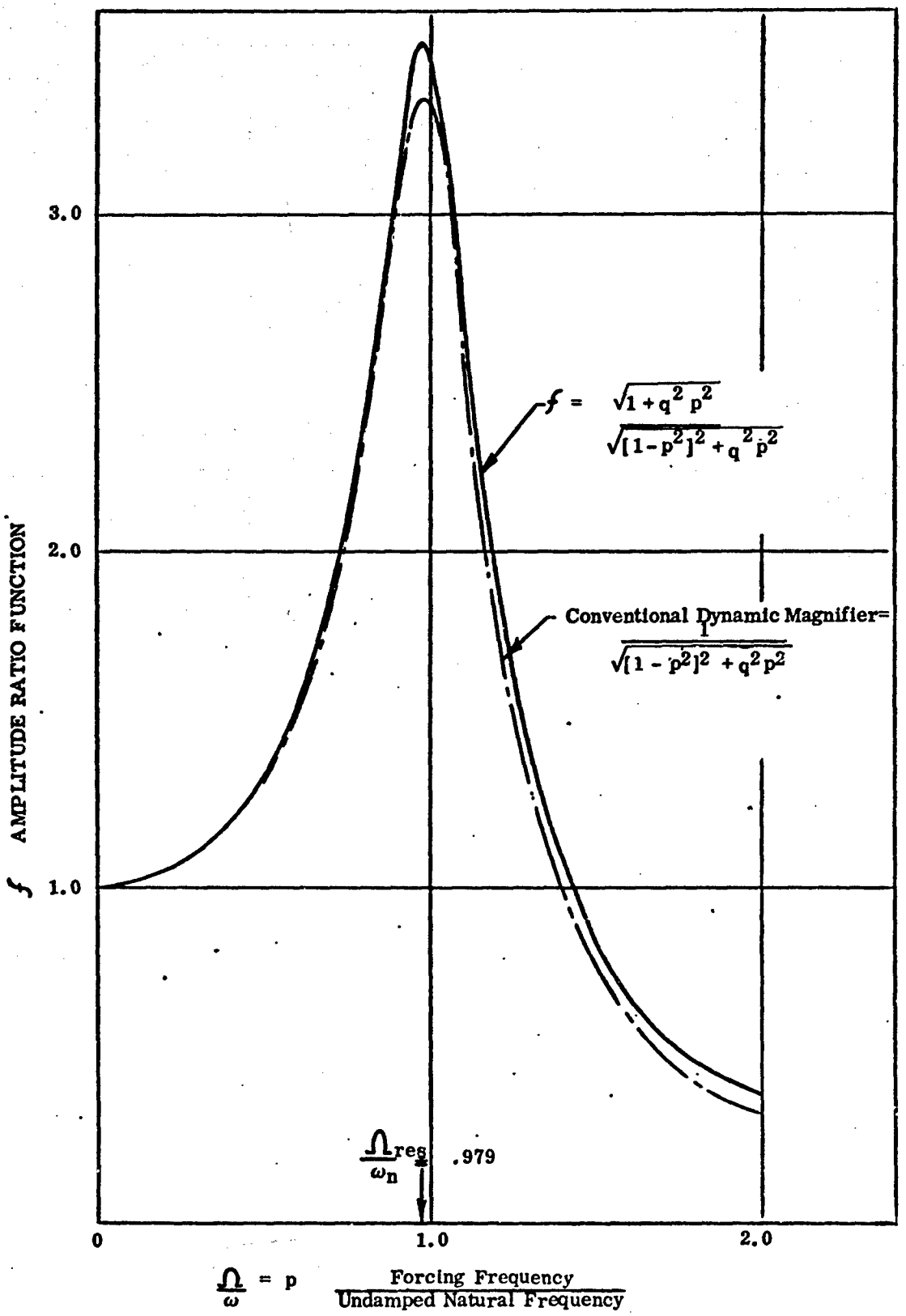

Figure I.1. The Functions f for $\bar{c} = 0.15$

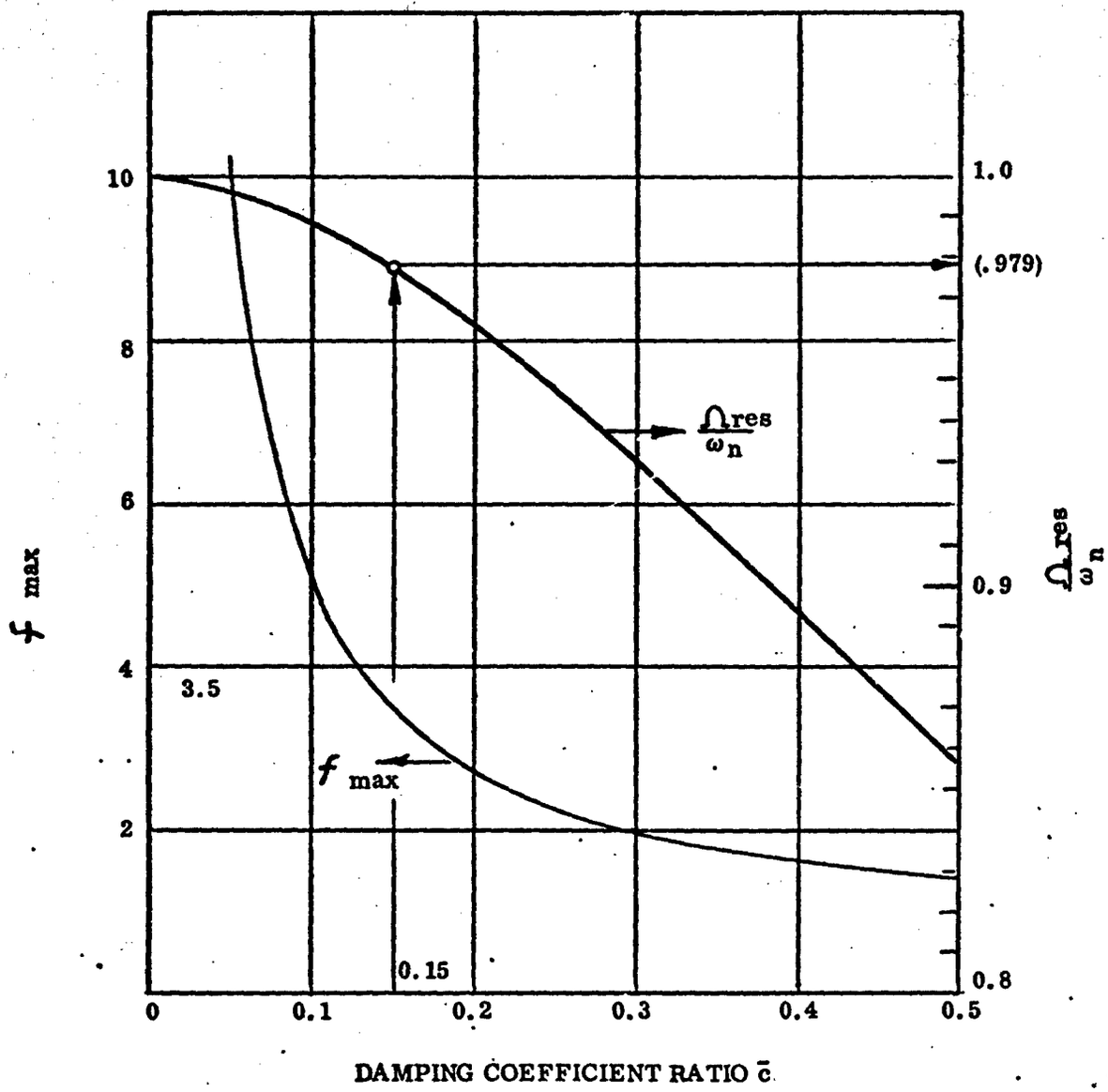

Figure I.2. Variation of f max and $\frac{\Omega}{\omega}$ with damping coefficient.

APPENDIX II

THE DYNAMIC MAGNIFIER FOR A SINGLE-DEGREE-OF-FREEDOM SYSTEM

APPENDIX II

THE DYNAMIC MAGNIFIER FOR A SINGLE-DEGREE-OF-FREEDOM SYSTEM

A standard result for the equation

$$\ddot{\delta} + 2c\dot{\delta} + \omega^2\delta = \frac{F_0}{m}\sin\Omega t \qquad \text{(II. 1)}$$

is $$\frac{\delta_{DYN}}{\delta_{STATIC}} = \frac{\delta_{MAX}}{F_0/k} = q$$

where $$q = \left[(1-p^2)^2 + 4\bar{c}^2p^2\right]^{-\frac{1}{2}} \qquad \text{(II.2)}$$

$$p = \frac{\Omega}{\omega} \qquad \bar{c} = \frac{c}{\omega}$$

Note that when $p = 1$, $q = 1/2\bar{c}$

The maximum value of q is obtained by differentiating the Equation (II. 2) and equating to zero in order to determine

$$p\Big|_{q_{MAX}} = \sqrt{1-2\bar{c}^2}$$

Substitution in equation II. 2 yields

$$q_{MAX} = \frac{1}{2\bar{c}\sqrt{1-\bar{c}^2}}$$

when q_{max} is known

$$\bar{c}^4 - \bar{c}^2 + \left(\frac{1}{2q_{MAX}}\right)^2 = 0$$

so that

$$\bar{c}^2 = \frac{1}{2}\left[1 - \sqrt{1 - \frac{1}{q^2_{MAX}}}\right]$$

APPENDIX III

NOTE ON COMPUTER TECHNIQUES EMPLOYED IN LUMPED PARAMETER SYSTEM ANALYSIS

APPENDIX III

NOTE ON COMPUTER TECHNIQUES EMPLOYED IN LUMPED PARAMETER SYSTEM ANALYSIS

During the analysis described in this report a number of computational techniques were employed.

LINEAR MODELS

The simplest method of treating the linear models was found to be by use of a simple electric analog as shown in figure III.1. The one-to-one correspondence between electrical and mechanical impedance and between, respectively, inductance and mass, capacitance and elasticity, and resistance and damping coefficient coupled with the existence of electric circuit analysis routines made the analysis of these cases extremely easy. This method was used for developing the frequency impedance curves shown in figures 22 to 51. This method is currently not flexible enough to accept arbitrary transient inputs.

NONLINEAR SPRING MODELS

The cases illustrated in figures 53 through 59 in which the buttock and spinal spring forces were represented by nonlinear discontinuous functions could not be treated by the simple electric analog method used for the linear model.

In the nonlinear cases a digital simulation of a 75 block analog program was used. This program was sufficiently flexible to allow the introduction of a transient input acceleration such as that shown in figure 58.

MODELS WITH NONLINEAR DAMPING AND SPRINGING

The case (illustrated in figure 10) in which nonlinear damping and springing was used was programmed in a conventional digital program. A Runge-Kutta step-by-step integration routine was used and sufficient cycles were calculated to ensure a steady-state response had been reached. This digital program could readily be adapted to the constant friction force case or to transient inputs although the latter were not actually used.

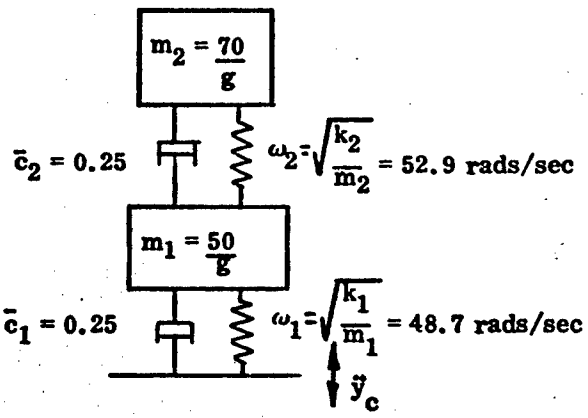

MECHANICAL SYSTEM

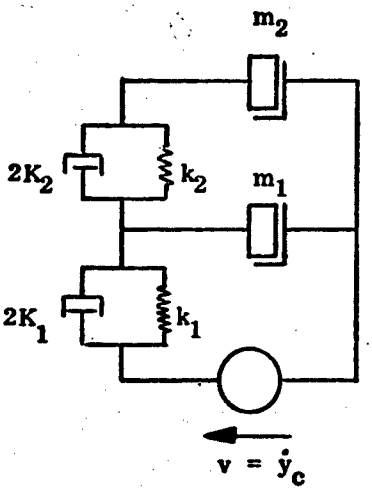

MECHANICAL CIRCUIT

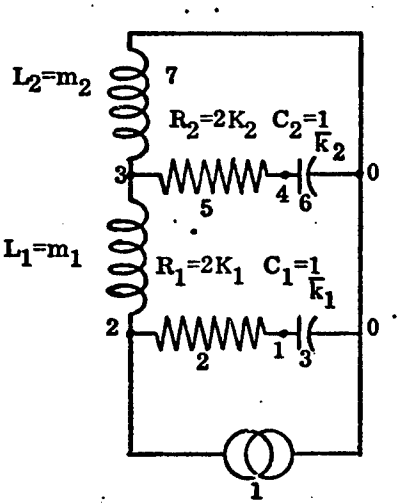

VOLTAGE FORCE
ELECTRIC ANALOG

	1	2
W(lb)	50	70
m(lb sec^2/ft)	$\frac{50}{32.172}$ = 1.554	$\frac{70}{32.172}$ = 2.176
L(Henry's)=m=	1.554	2.176
ω(rads/sec)	48.7	52.9
$k=m\omega^2$(lb/ft)	3685.61	6089.34
C (Farad)=1/k=	.000271	.000164
$\bar{c}$ (-)	0.25	0.25
$2K=2m\omega\bar{c}$ (lb sec/ft)	37.84	57.555
R (ohms) = 2K =	37.84	57.555

Figure III.1. The Electric Analog of a Mechanical Two Degree of Freedom System

REFERENCES

1. Goldman, David W. and Henning Von Gierke, "Effects of Shock and Vibration of Man," Shock and Vibration Handbook, Harris and Crede, Vol. 3, pp. 44-1 through 44-51, McGraw-Hill Book Co., New York, 1961.

2. Ruff, Sigmund, "Brief Acceleration: Less than One Second," German Aviation Medicine in World War II, Vol. 1, U. S. Government Printing Office, Washington, D. C., 1950.

3. Hixson, Elmer L., "Mechanical Impedance and Mobility," Shock and Vibration Handbook, Harris and Crede, Vol. 1, Chapter 10, McGraw-Hill Book Co., New York, 1961.

4. Wittmann, Thomas J. and Norman S. Phillips, "Human Body Nonlinearity and Mechanical Impedance Analyses," Journal of Biomechanics, Vol. 2, No. 3, July, 1969.

5. Vogt, H. L., R. R. Coermann, and H. D. Fust, "Mechanical Impedance of the Sitting Human Under Sustained Acceleration," Aerospace Medicine, Vol. 39, No. 7, July, 1968.

6. Vykukal, Hubert C., "Dynamic Response of the Human Body to Vibration When Combined with Various Magnitudes of Linear Acceleration," Aerospace Medicine, Vol. 39, No. 11, November, 1968.

7. Coermann, R. R., Gerd H. Zeigerruecker, Albert L. Wittwer and Henning Von Gierke, "The Passive Dynamic Mechanical Properties of the Human Thorax-Abdomen System and of the Whole Body System," Aerospace Medicine, Vol. 31, No. 6, June, 1960.

8. Payne, P. R., Personnel Restraint and Support Systems Dynamics, AMRL-TR-65-127, Aerospace Medical Reserach Laboratory, Wright-Patterson Air Force Base, Ohio, October, 1965.

9. U. S. Air Force, Seat System: Upward Ejection, Aircraft, General Specification for, MIL-S-9479A, USAF, June 16, 1967.

10. Stech, E. L., and P. R. Payne, Dynamic Models of the Human Body, AMRL-TR-66-157. Aerospace Medical Research Laboratory, Wright-Patterson Air Force Base, Ohio, February, 1966.

11. Yorra, Alvin J., The Investigation of the Structural Behavior of the Intervertebral Disc, Masters Thesis, Massachusetts Institute of Technology, May, 1956.

12. Weis, Edmund B., Jr., and George C. Mohr, "Cineradiographic Analysis of Human Visceral Responses to Short Duration Impact," Aerospace Medicine, Vol. 38, No. 10, October, 1967.

13. Dieckmann, D., Intern. Z. angew. Physiol. einschl. Arbeitsphysiol., 16:519, 1957.

14. Latham, F., "A Study in Body Ballistics; Seat Ejection," Proceedings of the Royal Society, B, Vol. 147, pp. 121-139, 1957.

15. Woods, A. G., "Human Response to Low Frequency Sinusoidal and Random Vibration," Aircraft Engineering, Vol. 39, July, 1967.

Security Classification

DOCUMENT CONTROL DATA - R & D

(Security classification of title, body of abstract and indexing annotation must be entered when the overall report is classified)

1. ORIGINATING ACTIVITY (Corporate author)	2a. REPORT SECURITY CLASSIFICATION
Wyle Laboratories, Payne Division 12221 Parklawn Drive Rockville, Maryland 20852	UNCLASSIFIED
	2b. GROUP N/A

3. REPORT TITLE

A FOUR-DEGREE-OF-FREEDOM LUMPED PARAMETER MODEL OF THE SEATED HUMAN BODY

4. DESCRIPTIVE NOTES (Type of report and inclusive dates)

Final Report, June 15, 1967 - June 15, 1970

5. AUTHOR(S) (First name, middle initial, last name)

Peter R. Payne
Edward G. U. Band

6. REPORT DATE	7a. TOTAL NO. OF PAGES	7b. NO. OF REFS
January 1971	118	15

8a. CONTRACT OR GRANT NO. F33615-67-C-1807 b. PROJECT NO. 7231 c. Task No. 723101 d. Unit No. 723101050	9a. ORIGINATOR'S REPORT NUMBER(S) WP No. 59101-6 9b. OTHER REPORT NO(S) (Any other numbers that may be assigned this report) AMRL-TR-70-35

10. DISTRIBUTION STATEMENT

This document has been approved for public release and sale; its distribution is unlimited.

11. SUPPLEMENTARY NOTES	12. SPONSORING MILITARY ACTIVITY
	Aerospace Medical Research Laboratory Aerospace Medical Div., Air Force Systems Command, Wright-Patterson AFB, OH 45433

13. ABSTRACT

A four-degree-of-freedom lumped parameter model is tentatively proposed to study the problem of the vertical accelerations of the seated human body such as may be imposed by aircraft ejection systems. The coefficients defining the mass distribution and the spring and damping rates of the connecting links are obtained from experimental data. The way in which these coefficients are derived is described in the report. Development of the model is preceded by a study of the driving point impedance of generalized multi-degree of freedom systems. This study was carried out to determine how much reliance should be placed on experimental impedance measurements in the construction of the model. It is concluded that a reasonable representation of the dynamics of a seated human subject can be obtained by the four-degree-of-freedom lumped parameter model, but that there exists a surprisingly small amount of usable data, indicating that a sophisticated experimental program should be initiated to examine in detail particular aspects of body dynamics.

DD FORM 1 NOV 65 1473

Security Classification

Security Classification

14. KEY WORDS	LINK A		LINK B		LINK C	
	ROLE	WT	ROLE	WT	ROLE	WT
Biomechanics Impact Acceleration Impedance						

Security Classification

END

DATE

FILMED

5-4-71